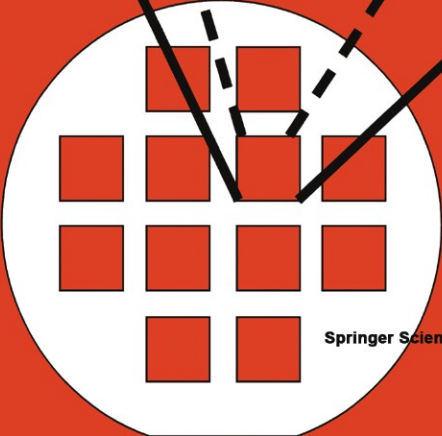


Sangeeta Bhatia

**MICROFABRICATION IN  
TISSUE ENGINEERING  
AND BIOARTIFICIAL  
ORGANS**



Springer Science+Business Media, LLC

---

**MICROFABRICATION IN TISSUE  
ENGINEERING AND BIOARTIFICIAL ORGANS**

---

---

# MICROSYSTEMS

*Series Editor*

**Stephen D. Senturia**

*Massachusetts Institute of Technology*

## ***Editorial Board***

Roger T. Howe, *University of California, Berkeley*

D. Jed Harrison, *University of Alberta*

Hiroyuki Fujita, *University of Tokyo*

Jan-Åke Schweitz, *Uppsala University*

## ***Books in the Series***

### **MICROMACHINED ULTRASOUND-BASED PROXIMITY SENSORS**

M.R. Hornung, O. Brand

ISBN: 0-7923-8508

### **BRINGING SCANNING PROBE MICROSCOPY UP TO SPEED**

S.C. Minne, S.R. Manalis, C.F. Quate

ISBN: 0-7923-8466-0

### **MICROCANTILEVERS FOR ATOMIC FORCE MICROSCOPE DATA STORAGE**

B.W. Chui

ISBN: 0-7923-8358-3

### **METHODOLOGY FOR THE MODELING AND SIMULATION OF MICROSYSTEMS**

B. Romanowicz

ISBN: 0-7923-8306-0

---

**MICROFABRICATION IN TISSUE  
ENGINEERING AND BIOARTIFICIAL ORGANS**

**Sangeeta Bhatia, M.D., Ph.D.**



**SPRINGER SCIENCE+BUSINESS MEDIA, LLC**

**Library of Congress Cataloging-in-Publication Data**

Bhatia, Sangeeta, 1968 -

Microfabrication in tissue engineering and bioartificial organs /  
Sangeeta Bhatia

p. cm. -- (Microsystems ; mict 5)

Includes bibliographical references and index.

ISBN 978-1-4613-7386-5 ISBN 978-1-4615-5235-2 (eBook)

DOI 10.1007/978-1-4615-5235-2

1. Animal cell biotechnology. 2. Microfabrication. 3. Artificial organs.  
4. Tissue culture. I. Title. II Series: Microsystems (series) ; 5.  
[DNLM: 1. Tissue Culture--methods. 2. Artificial Organs.  
3. Biocompatible Materials. 4. Biomedical Engineering. 5. Cell  
Communication. QS 525 B575m 1999]

TP248.27 . A53B47 1999

660.6--dc21

DNLM/DLC

for Library of Congress

99-35715

CIP

---

**Copyright** © 1999 by Springer Science+Business Media New York

Originally published by Kluwer Academic Publishers in 1999

Softcover reprint of the hardcover 1st edition 1999

All rights reserved. No part of this publication may be reproduced, stored in a retrieval system or transmitted in any form or by any means, mechanical, photocopying, recording, or otherwise, without the prior written permission of the publisher, Springer Science+Business Media, LLC.

*Printed on acid-free paper.*

## Editor's Preface

The Microsystems Series has as its goal the creation of an outstanding set of textbooks, references, and monographs on subjects that span the broad field of microsystems. Exceptional PhD dissertations provide a good starting point for such a series, because, unlike monographs by more senior authors, which must compete with other professional duties for attention, the dissertation becomes the sole focus of the author until it is completed. Conversion to book form is then a streamlined process, with final editing and book production completed within a few months. Thus we are able to bring important and timely material into book form at a pace which tracks this rapidly developing field. Our first four books in the series were drawn from the more physics-oriented side of the microsystems field, including such diverse subjects as computer-aided design, atomic-force microscopy, and ultrasonic motion detection. Now, with Sangeeta Bhatia's work, we enter the realm of biology. Her use of artificially structured substrates to encourage the liver cells to form orderly assemblies is a fine example of how microfabrication technology can contribute to cell biology and medicine. I am pleased to be able to add this very new and very interesting work to the Microsystems Series.

Stephen D. Senturia  
Cambridge MA

## **Foreword**

One of the emerging applications of microsystems technology in biology and medicine is in the field of tissue engineering and artificial organs. In order to function, cells need to receive proper signals from their environment. Among these signals are the chemistry and geometry of the extracellular matrix to which cells adhere, and the intercellular communication between homotypic and heterotypic cells. The mechanisms by which various signals mediate their effect on cells is an active area of research in cell biology, and are of utmost importance to tissue engineers who are faced to develop functional tissue substitutes. Microsystems technology provides an unmatched opportunity to scientists and engineers to create complex cellular structures by controlling cell-matrix and cell-cell interactions at a micrometer scale.

The Ph.D. thesis presented in this volume by Dr. Sangeeta Bhatia investigates at a fundamental level the role of heterotypic cell-cell interactions toward the development of a functional liver tissue. The use of microfabrication and surface chemistry techniques enabled Dr. Bhatia to precisely control the heterotypic interactions between hepatocytes and fibroblasts. The results from this study showed, for the first time, that the extent of heterotypic cell-cell interactions determine the level of liver-specific function, and thus, the engineered liver tissue. Furthermore, Dr. Bhatia was able to show that hepatocytes closer to the heterotypic interface differentiated and functioned; whereas, hepatocytes more than several hundred micrometers (i.e., 3 to 4 cell layer) away from the interface lost their functional capacity. The importance of these findings and their utility in the development of a bioartificial liver assist system is described in detail in this thesis.

Dr. Bhatia's work represents a cutting-edge, innovative example of the use of microsystems technology in biology and medicine. Although her work was targeted toward the development of an engineered hepatic tissue, the implications of her work are far-reaching and include many other living systems where the interaction between multiple cell types is important, such as developmental biology, wound healing, and cancer.

Mehmet Toner, Ph.D.  
Associate Professor  
Center for Engineering in Medicine  
Massachusetts General Hospital  
Harvard Medical School



## Abstract

The repair or replacement of damaged tissues using in vitro strategies has focused on manipulation of the cell environment by modulation of cell-extracellular matrix interactions, cell-cell interactions, or soluble stimuli. Development of functional tissue substitutes through 'tissue engineering' has been facilitated by the ability to control each of these environmental influences; however, in co-culture systems with two or more cell types, cell-cell interactions have been difficult to manipulate precisely. These interactions are important in normal physiology of many organ systems, in embryogenesis where differentiation cues are determined by the local cellular microenvironment, and implicated in the pathophysiology of certain diseases. The ability to spatially control cells at the single cell level using micropatterning would allow the precise manipulation of cell-cell interactions of interest.

We have developed an adaptable method for generating two-dimensional, anisotropic model surfaces capable of organizing two different cell types in discrete spatial locations. We have chosen a primary rat hepatocyte/3T3 fibroblast cell system due to its potential clinical significance in bioartificial liver design and also based on widely reported interactions observed in this co-culture model. We have used photolithography to pattern biomolecules (collagen I) on glass which mediates cell adhesion of the first cell type, hepatocytes, followed by non-specific, serum-mediated attachment of fibroblasts to the remaining unmodified areas. This co-culture technique allowed the manipulation of the initial cellular microenvironment without variation of cell number. Specifically, we were able to control the level of homotypic and heterotypic interactions in co-cultures over a wide range.

Modulation of initial cell-cell interactions was found to have significant effects on liver-specific markers of metabolic, synthetic, and excretory function. In particular, 2 to 3-fold variations in steady-state levels of representative hepatocellular functions were achieved from identical numbers of cells. Furthermore, our results indicated that the use of microfabrication to control cell-cell interactions may allow modulation over the kinetics of functional up-regulation; in fact, micropatterned co-cultures displayed increased levels urea synthesis up to 1 week earlier than randomly distributed, unpatterned co-cultures with the same cellular constituents. Our data indicate that control over cell-cell interactions will allow the control of bulk tissue function based on the local microenvironments.

The mechanisms by which hepatocytes and fibroblasts interact to produce a differentiated hepatocyte phenotype were also investigated. Variations in bulk tissue function were due to spatial heterogeneity in the pattern of induction of hepatocyte differentiation within a hepatocyte population due to interaction with mesenchymal cells. We found that hepatocytes adjacent to the heterotypic expressed increased levels of intracellular albumin (a marker of hepatic synthetic function); whereas, hepatocytes far from the heterotypic interface contained undetectable levels of albumin. Although the actual molecular basis of this signaling was not identified, our experimental results indicated that the source of the observed induction pattern was a tightly cell-associated fibroblast product.

Clinical implementation of a co-culture based, bioartificial liver requires optimization of hepatic function based on fibroblast number and various bioreactor design constraints. To this end, we utilized microfabrication to achieve a reduction in fibroblast number while preserving the heterotypic interface. We determined that fibroblast number could be reduced by twelve-fold with only a modest reduction in hepatic tissue function. These data were combined with a simple model of oxygen transport and viscous energy losses in a hypothetical multi-unit bioreactor, to determine design criteria for a microfabricated, co-culture based bioartificial liver. This general approach has potential applications in many areas of tissue engineering, implantation biology, and developmental biology, both in the arena of basic science and in the development of cellular therapeutics.

## Acknowledgements

I've been lucky to have such an amazing group of people carry me through my graduate school years. One of the only problems with having been so fortunate, is that I'm bound to forget someone- for that, I apologize in advance...

The center of my training has been Mehmet Toner. I have watched him think and tried to follow his example for almost 6 years. He has continuously shared his time, intellect, creativity, and enthusiasm with me. I thank him for many, many hours of advising (scientific and 'life'), editing, brain-storming, and shaping of our work together. He is a truly generous and talented mentor.

Martin Yarmush and Ron Tompkins are to be thanked most for creating such an interdisciplinary team of talented scientists. Maish, in particular, infused his vision in our surroundings and is to be credited with the creation of such a unique and dynamic atmosphere. It has been an honor to work with Dr. Elizabeth Hay as she served on my thesis committee. I thank her for taking such an active interest in this project and for bringing dimension to this work. I am also grateful to Dr. Marty Schmidt who helped to expose me to the richness of microfabrication and endured an (over?)exposure to world of cell biology.

Everyone in the lab (the "LSSE") has helped me in some way. Anne Leeds, Pat Meara, and Lynne Stubblefield, with a thousand annoying details. Drs. Jeff Morgan and Livingston Van De Water with their biological perspective. Past and present post-docs and MD fellows with their knowledge and insight- Albert Folch, Brent Foy, Howard Matthews, Fatima Merchant, Prabhas Moghe, Maura Paveo, George Pins, S.B. Rajur, Avi Rotem, Charlie Roth, Steve Reiken, Peter Stefanovich, and Craig Zupke.

Thanks go to Inne Borel Rinkes for keeping me going in the early years, Francois Berthiaume (a.k.a. “Frenchie”) for always knowing the answer or where to get it, Bob Ezzell for his help at East, Greg Russo for image-processing nightmares, Joe LeDoux for being a graduate student role model, and Pat Walton, Howard Davis, and Kyong Lee for their influx of energy into the lab. Special HUGE thanks to Ulysses Balis, Kamelia Behnia, Octavio Hurtado, Rob Schoen, and Annie Tsong whose work lies in this document - without their help, I wouldn’t be done now. Thanks also go to Kristin Hendricks, Kristin O’Neil, Kealy Ham, Annette MacDonald and Rick Snow for technical and computer support. And, of course, the three musketeers - Will Holmes, Jens Karlsson (or should I say, Professor Jens Karlsson), and Mike Russo, for all of the above and more.

On to MIT. All the faculty, staff and students of Health Sciences and Technology (HST) helped make this experience so valuable. A special thank you to Keiko Oh for making sure my education was paid for, to Ron Smith for making sure I had credit for everything, and to everyone behind the scenes who keep it running smoothly. Also, my heartfelt thank you to Chris Chen, my ‘academic twin’ who has so enriched this experience every step of the way- grad school, med school, academia... In Mechanical Engineering, thanks go to Leslie Regan for helping with everything from qualifiers to MEGAwomen. At the Microsystems Technology Lab, thanks go to Pat Burkhart and Vicki Diadiuk for helping to coordinate my project, and to Joe DiMaria and Kurt Broderick for their reliability and availability. And at the Public Service Center- my heartfelt thanks to everyone involved with KEYS- Emily Sandberg whose unshakable support has kept KEYS going, Corrie Lathan, Lynn Nelson, Tracy Purinton, Mike Halle, the interns past and present, and all the volunteers- you are an incredible group of people. I have treasured our common passion, have truly enjoyed our work/play together, and learned from each of you.

My family and friends have been my foundation. I’ll have to thank each of you in person for enduring graduate school with me. My Dad, the first one to introduce me to bioengineering, has taken an active interest in every experimental detail along the way- has marveled at the frustrating pace of experimental research- and so reveled in every new finding. My Mom and sister, Sujata, have been my glue, my caretakers, and my playmates. Jagesh, has been, at once my scientific peer, my partner, and my very best friend. I’m lucky to have all of you.

*Financial support came from the Department of Defense, the American Association of University Women, Harvard-MIT Division of Health Sciences and Technology, and the Bank of Mom and Dad.*

## Contents

<b>Editor's Preface</b>	<b>v</b>
<b>Foreword</b>	<b>vii</b>
<b>Abstract</b>	<b>ix</b>
<b>Acknowledgements</b>	<b>xi</b>
<b>Contents</b>	<b>xiii</b>
<b>List Of Figures</b>	<b>xvii</b>
<b>Introduction</b>	<b>1</b>
<b>1. Tissue Engineering</b>	<b>1</b>
<b>2. What Does The Liver Do?</b>	<b>2</b>
<b>3. What Happens When The Liver Fails?</b>	<b>5</b>
<b>4. Hepatic Tissue Engineering</b>	<b>7</b>
<b>5. How Can Hepatocytes Be Stabilized <i>In Vitro</i>?</b>	<b>9</b>
<b>6. How Are Cell-Cell Interactions Important <i>In Vivo</i>?</b>	<b>10</b>
<b>7. Co-Culture</b>	<b>11</b>
7.1 Effects Of Co-Culture On Hepatocyte Morphology And Function	13
7.2 Mechanisms Of Induction Of Liver Function In Hepatocytes	16
<b>8. Previous Attempts To Control Cell-Cell Interactions</b>	<b>19</b>
<b>9. Micropatterning Of Cells</b>	<b>21</b>

<b>10.Scope Of This Study</b>	<b>25</b>
<b><i>Methodology For Fabrication, Characterization, And Analysis Of Micropatterned Co-Cultures</i></b>	<b>29</b>
<b>1.Overview</b>	<b>29</b>
<b>2.Fabrication Of Micropatterned Co-Cultures</b>	<b>30</b>
2.1Microfabrication Of Substrates	30
2.2Surface Modification Of Substrates	31
2.3Cell Culture	31
2.4Cell Culture On Modified Surfaces	32
<b>3.Surface Characterization Of Substrates</b>	<b>33</b>
3.1Autofluorescence	33
3.2Profilometry	33
3.3Atomic Force Microscopy (AFM)	33
3.4Indirect Immunofluorescence Of Collagen I	34
3.5Immunofluorescent Staining	34
3.6Image Analysis	34
<b>4.Functional Analysis Of Micropatterned Co-Cultures</b>	<b>35</b>
4.1Experimental Design	35
4.2Analytical Assays	35
4.3Immunohistochemistry	37
4.4Functional Bile Duct Staining	37
4.5Image Acquisition And Analysis	37
4.6Statistics And Data Analysis	38
<b>5.Mechanistic Studies</b>	<b>38</b>
5.1Conditioned Media	38
5.2Physical Separation Of Cell Types	39
5.3Agitation	41
<b>6.Optimization Studies</b>	<b>41</b>
6.1Reduction In Fibroblast Number	41
6.2Randomly Distributed Co-Cultures	43
<b>7.Summary</b>	<b>44</b>
<b><i>Characterization: Microfabricated Substrates &amp; Co-Cultures</i></b>	<b>45</b>
<b>1.Overview</b>	<b>45</b>
<b>2.Characterization Of Cell-Free Substrates</b>	<b>46</b>
<b>3.Characterization Of Micropatterned Cultures</b>	<b>48</b>
<b>4.Discussion</b>	<b>54</b>

<b>5.Summary</b>	<b>56</b>
<b><i>Functional Analysis Of Micropatterned Co-Cultures</i></b>	<b>59</b>
<b>1.Overview</b>	<b>59</b>
<b>2.Characterization Of Initial Cell Distribution</b>	<b>61</b>
<b>3.Biochemical Analysis Of Liver-Specific Function</b>	<b>62</b>
<b>4. Hepatocyte Function In Situ: Immunostaining Of Intracellular Albumin</b>	<b>65</b>
<b>5.Hepatocyte Function In Situ: Bile Duct Excretion</b>	<b>67</b>
<b>6.Discussion</b>	<b>69</b>
6.1 Cellular Microenvironment Modulated Liver-Specific Functions	69
6.2 Cellular Microenvironment Induced Spatial Heterogeneity In Hepatocyte Phenotype	71
6.3 Related Observations On Control Of Cell-Cell Interactions	73
<b>7.Summary And Implications</b>	<b>74</b>
<b><i>Probing Mechanisms Of Hepatocyte/Fibroblast Interactions</i></b>	<b>77</b>
<b>1.Overview</b>	<b>77</b>
<b>2. Effect Of Homotypic Hepatocyte Interactions On Spatial Pattern Of Immunostaining</b>	<b>79</b>
<b>3.Use Of Conditioned Media</b>	<b>82</b>
<b>4.Physical Separation Of Cell Populations</b>	<b>83</b>
<b>5.Agitation Of Co-Cultures</b>	<b>85</b>
<b>6.Discussion</b>	<b>86</b>
6.1 Cell-Associated Signal Is Implicated In Induction Of Function	87
6.2 Potential Contributors To Finite Penetration Length	90
6.3 Limitations Of Experimental Method	92
<b>7.Summary And Future Work</b>	<b>93</b>
<b><i>Optimization Of Hepatic Function In Co-Cultures</i></b>	<b>95</b>
<b>1.Overview</b>	<b>95</b>
<b>2. Reduction Of Fibroblast:Hepatocyte Ratio While Preserving Heterotypic Interface In Micropatterned Co-Cultures</b>	<b>96</b>
<b>3. Reduction Of Fibroblast:Hepatocyte Ratio Without Control Of Heterotypic Interface In Conventional, Randomly-Distributed Co-Cultures</b>	<b>100</b>

<b>4. Comparison Of Micropatterned And Randomly-Distributed Co-Cultures</b>	<b>102</b>
<b>5.Discussion</b>	<b>105</b>
5.1 Optimization Of Fibroblast:Hepatocyte Ratio	105
5.2 Kinetics Of Up-Regulation Of Hepatic Functions	107
5.3 Comparison Between In Vivo And In Vitro Values	109
5.4 Design Criteria For Co-Culture-Based Bioreactor	111
5.5 Comparison Of Hypothetical Microfabricated Bioreactor To Existing Technologies	119
<b>6.Summary</b>	<b>120</b>
<b>Conclusions And Outlook</b>	<b>123</b>
<b>1.Summary</b>	<b>123</b>
<b>2.Future Directions</b>	<b>125</b>
<b>References</b>	<b>129</b>
<b>Glossary</b>	<b>141</b>
<b>Index</b>	<b>143</b>



## List of Figures and Tables

<b>Introduction</b>	<b>1</b>
<b>Figure 1.1. Liver Lobule. Schematic view.</b>	<b>3</b>
<b>Figure 1.2. Relationships of branches of portal vein (PV), hepatic artery (HA), and bile duct (BD).</b>	<b>3</b>
<b>Figure 1.3. Schematic of Adult Sinusoid.</b>	<b>4</b>
<b>Figure 1.4. Hepatocyte plasma membrane domains and extracellular spaces.</b>	<b>5</b>
<b>Figure 1.5. Development of the human liver in the A. 4th week and B. 5th week of gestation</b>	<b>10</b>
<b>Table 1.1. Cell Types Utilized in Co-Cultures for Stabilization of Rat Hepatocyte Phenotype</b>	<b>11</b>
<b>Table 1.2 Functions Induced in Hepatocytes by Co-Culture</b>	<b>15</b>
<b>Figure 1.6. Schematic of Conventional Approaches for Control of Cell-Cell Interaction</b>	<b>20</b>
<b>Methodology for Fabrication, Characterization, and Analysis of Micropatterned Co-Cultures</b>	<b>29</b>
<b>Figure 2.1. Schematic of Process to Generate Micropatterned Co-Cultures</b>	<b>30</b>
<b>Figure 2.2. Schematic of Method for Separation of Cell Populations</b>	<b>39</b>

<b>Figure 2.3. Schematic of Strategy for Minimization of Fibroblast Number.</b>	<b>42</b>
<b>Characterization of Microfabricated Substrates and Co-Cultures</b>	<b>45</b>
<b>Figure 3.1 Characterization of Photoresist.</b>	<b>46</b>
<b>Figure 3.2. Differential Hydrophilicity of Aminosilane Modified Pattern.</b>	<b>47</b>
<b>Figure 3.3. Surface Characterization of Collagen.</b>	<b>48</b>
<b>Figure 3.4. Phase Contrast Micrographs of Micropatterned Hepatocytes.</b>	<b>49</b>
<b>Figure 3.5. Micrographs of Micropatterned Hepatocytes and Co-Cultures with 3T3 Fibroblasts.</b>	<b>50</b>
<b>Figure 3.6. Immunofluorescent Staining of Micropatterned Co-Cultures.</b>	<b>51</b>
<b>Figure 3.7. Schematic of Method for Determining, <math>\chi</math>, Heterotypic Interaction Parameter.</b>	<b>52</b>
<b>Figure 3.8. Average Heterotypic Interaction in Co-Cultures</b>	<b>53</b>
<b>Figure 3.9. Distribution of Heterotypic Interactions, <math>\chi</math>, in Co-Cultures</b>	<b>54</b>
<b>Functional Analysis Of Micropatterned Co-Cultures</b>	<b>59</b>
<b>Figure 4.1. Phase Contrast Micrographs of Micropatterned Co-Cultures With Varying Heterotypic Interface But Similar Cell Numbers.</b>	<b>61</b>
<b>Figure 4.2. Biochemical Analysis of Micropatterned Cultures and Co-Cultures.</b>	<b>64</b>
<b>Figure 4.3. Kinetics of Immunostaining of Intracellular Albumin in 490 <math>\mu\text{m}</math> Island Co-Cultures.</b>	<b>66</b>
<b>Figure 4.4 Comparison of Intracellular Albumin Immunostaining in Various Micropatterns at Day 6.</b>	<b>67</b>
<b>Figure 4.5. Functional Bile Canilicular Staining.</b>	<b>68</b>
<b>Probing The Mechanisms Of Hepatocyte/Fibroblast Interactions</b>	<b>77</b>
<b>Figure 5.1. Immunostaining of Intracellular Albumin in Micropatterned Hepatocytes (Only).</b>	<b>80</b>

<b>Figure 5.2. Immunostaining of Intracellular Albumin in Micropatterned Co-Cultures.</b>	<b>81</b>
<b>Figure 5.3. Urea Synthesis in Hepatocytes Treated with Conditioned Media</b>	<b>82</b>
<b>Figure 5.4. Separation of Cell Populations.</b>	<b>84</b>
<b>Figure 5.5. Immunostain of Intracellular Albumin in Separated Cell Populations.</b>	<b>85</b>
<b>Figure 5.6. Immunostain of Intracellular Albumin in Static and Shaken Cultures.</b>	<b>86</b>
<b>Optimization Of Hepatic Function In Co-Cultures</b>	<b>95</b>
<b>Figure 6.1. Phase Contrast Micrograph of Micropatterned Hepatocytes With Reduced Center-to-Center Spacing.</b>	<b>97</b>
<b>Figure 6.2. Phase Contrast Micrograph of Micropatterned Co-Culture with Reduced Spacing.</b>	<b>98</b>
<b>Figure 6.3. Urea Synthesis for Micropatterned Co-Cultures with Reduced Fibroblast:Hepatocyte Ratio and Similar Heterotypic Interface.</b>	<b>99</b>
<b>Figure 6.4. Albumin Secretion for Micropatterned Co-Cultures with Reduced Fibroblast:Hepatocyte Ratio and Similar Heterotypic Interface.</b>	<b>100</b>
<b>Figure 6.5. Urea Synthesis of Randomly-Distributed Co-Cultures with Reduced Fibroblast:Hepatocyte Ratio.</b>	<b>101</b>
<b>Figure 6.5. Albumin Secretion of Randomly-Distributed Co-Cultures with Reduced Fibroblast:Hepatocyte Ratio.</b>	<b>102</b>
<b>Figure 6.7. Comparison of Micropatterned Co-Cultures to Randomly-Distributed Co-Cultures.</b>	<b>103</b>
<b>Figure 6.7B. Pattern Of Induction Of Urea Synthesis Varies In Fibroblast:Hepatocyte Ratio Of 0.5:1.</b>	<b>104</b>
<b>Figure 6.7C. Dose Response of Urea Synthesis as a Function of Fibroblast Number in Micropatterned versus Randomly-Distributed Cultures.</b>	<b>104</b>
<b>Figure 6.7D. Kinetics of Up-Regulation of Urea Synthesis</b>	<b>105</b>
<b>Figure 6.8. Comparison of Albumin Secretion in Hepatic Tissues In Vitro.</b>	<b>110</b>

<b>Figure 6.9. Schematic of Hypothetical Bioreactor. Multi-unit bioreactor with common inlet and outlet.</b>	<b>112</b>
<b>Table 6.1. Effect of Reduced Fibroblast Number on Bioreactor Design</b>	<b>112</b>
<b>Table 6.2. Constants Used in Solution of Transport Equations</b>	<b>114</b>
<b>Figure 6.10. Effect of Flow Rate on Oxygen Concentration along Channel Length.</b>	<b>115</b>
<b>Figure 6.11. Effect of Oxygen Tension on Flow Rate versus Cell Surface Area.</b>	<b>116</b>
<b>Figure 6.12. Effect of Channel Height on Shear Stress and Pressure Drop.</b>	<b>118</b>
<b>Table 6.3. Comparison of a hypothetical microfabricated liver reactor to a spheroid-based, hollow-fiber reactor for replacement of rat liver function.</b>	<b>120</b>

# Chapter 1

## Introduction

### 1. TISSUE ENGINEERING

Every year, the national health care cost for Americans suffering tissue loss or end-stage organ failure exceeds \$400 billion (Langer and Vacanti, 1993). These patients are treated medically by organ transplant, surgical reconstruction, or with mechanical devices such as kidney dialyzers. These therapies, although useful and important, leave much to be desired. Organ transplants are limited by donor shortages, surgical reconstruction by long-term sequelae, and mechanical devices by the inability to mimic all aspects of functional tissues. Recent progress has been made in the area of 'Tissue Engineering' where investigators have attempted to engineer biological, cell-based, tissues *in vitro* to restore, maintain, or improve tissue function. Many of these strategies have focused on manipulation of the cell environment. Development of functional tissue substitutes has been facilitated by the ability to control many relevant environmental influences; however, one key factor, the influence of local cell-cell interactions, has been difficult to manipulate precisely. This study will describe a novel, microfabrication-based, model system that allows the examination of the role of cell-cell interactions in tissue engineering of a particular organ system, the liver.

## **2. WHAT DOES THE LIVER DO?**

This complex organ performs a myriad of vital functions. Located in the right-upper quadrant of the abdomen, the liver is the largest solid organ of the body and is so highly metabolic that it consumes 30% of the oxygen of each breath we take. The many functions of the liver can be divided into four main categories: metabolism, synthesis, detoxification, and formation of bile. These diverse functions are performed by repeating lobular units depicted schematically in Figure 1.1. The precise architecture of the liver facilitates efficient transport of solutes between the blood stream and the hepatocytes (the main functional cell of the liver). Blood enters the organ through two pathways- the highly oxygenated hepatic artery and the portal vein, a comparatively oxygen-poor blood pool that drains the gastrointestinal tract. On the lobular scale, blood enters at the periphery of the lobular structure, and drains centrally along the specialized capillary of the liver- the sinusoid. Along the way, blood interacts directly with cords of hepatocytes, all the while separated by a minimal diffusion distance. The efficiency of this organ is achieved by replication of these many functional units- an example of biological scale-up by 'brute force'. In addition to the vascular network, each lobule contains the fine, intercalated tree of the biliary system. The bile canaliculus consists of domains formed between two hepatocyte neighbors, within which cells excrete bile. Conceptually, each canaliculus is a 'belt' around an individual hepatocyte. When interconnected, the resulting biliary network allows the flow of bile in the opposite direction of the blood flow. Ultimately, the bile network drains into the bile duct which lies adjacent to the portal vein and hepatic artery inlet (Figure 1.2).

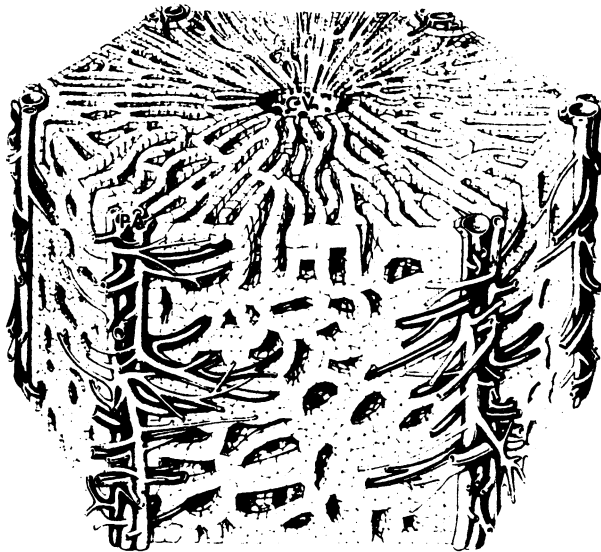


*Figure 1.1.* Liver Lobule. Schematic view. Blood flows from the peripheral portal areas (PA) consisting of branches of the portal vein, hepatic artery, and bile duct to the central vein (CV). (Jones et al, 1977: 702. Reproduced here by kind permission of McGraw-Hill)



*Figure 1.2.* Relationships of branches of portal vein (PV), hepatic artery (HA), and bile duct (BD). (Jones et al, 1977: 703. Reproduced here by kind permission of McGraw-Hill)

The precise architecture of the liver lobule allows for highly efficient transport, and precise variations in physical factors such as oxygen concentration, shear stress, and hydrostatic pressure (progressive reduction from inlet to outlet). In addition, the architecture of the lobule facilitates a variation of precisely defined cell-cell interactions. A sub-set of sinusoids is schematically depicted in Figure 1.3. The sinusoids are lined by a specialized fenestrated (discontinuities in the cytoplasm) endothelium such that transport is maximized between hepatocytes and the blood space while hepatocytes remain proximal to endothelial cells. Hepatocytes are separated from the endothelium only by the Space of Disse- named for its microscopic ‘empty’ appearance, though immunohistochemical stains of the liver show that extracellular matrix proteins are deposited in this space. Locally, this creates a ‘sandwich’ of extracellular matrix for each hepatocyte- an observation that has been exploited in the culture of hepatocytes once they have been removed from the liver.

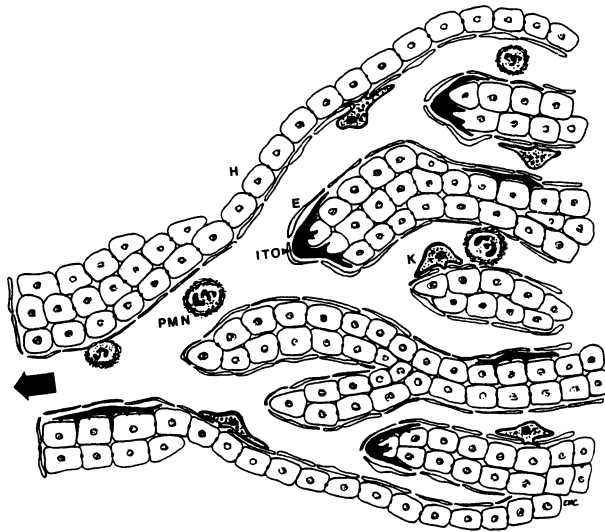


*Figure 1.3.* Schematic of Adult Sinusoid. Hepatocytes are arranged in cords. Sinusoids are lined with endothelial cells (E). Also shown are Ito (fat-storing, stellate), Kupffer cells, and neutrophils (PMN). (Clemens et al, 1994. Reproduced with permission).

In addition, fat-storing, or Ito cells are in direct contact with hepatocytes and intercalated between hepatocyte cords (Figure 1.4). Under normal conditions, these cells regulate the storage of vitamin A; however, when activated by alcohol (or other) injury, these cells become activated and are thought to be responsible for the scarring of



the liver that occurs in cirrhosis. Another cell type, the biliary ductal epithelium, lies within the lobule and has contact with hepatocytes towards the end of the hepatic sinusoid (Figure 1.2). Kupffer cells (the phagocytic cells of the liver) are free to roam through the blood and tissue compartment engulfing biological debris and sometimes becoming activated in concert with the immune system, thus interacting transiently with hepatocytes. Overall, the adult liver provides a scaffold for many complex cell-cell interactions which allow for effective, coordinated organ function. We will see that some of these interactions seem to be important to the function of isolated hepatocytes- interactions that we may now manipulate using microfabrication tools.

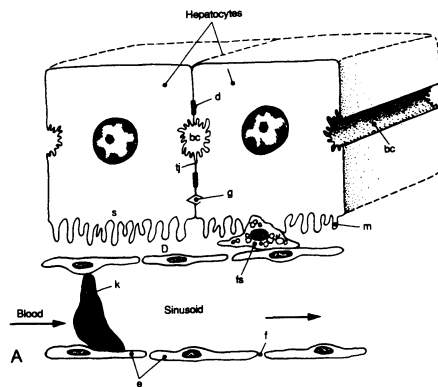


*Figure 1.4.* Hepatocyte plasma membrane domains and extracellular spaces. Two hepatocytes are represented to illustrate a sinusoidal domain (s), an intercellular domain with tight junctions (tj), desmosomes (d), gap junctions (g), and bile canicular domain (bc). Microvilli (m) project into the extracellular-extravascular Space of Disse (D). Also seen are Ito (fat-storing, fs) cells, endothelial cells (e) with fenestrations (f), and Kupffer cells (k) which participate in the removal of large particles. (Kaplowitz, 1992. Reproduced here by kind permission of Williams & Wilkins).

### 3. WHAT HAPPENS WHEN THE LIVER FAILS?

Given the diversity of vital functions that the liver performs, it is not surprising that failure of the liver is fatal. Disturbances in metabolic function lead to fluctuations in blood levels of ammonia and other substances that are toxic in high concentrations. Similarly, synthetic dysfunction causes reduction in albumin synthesis (important component of osmotic drive to keep blood in vessels) and blood

clotting proteins. Patients frequently suffer from ascites (accumulation of liters of fluid in the abdomen) and bleeding disorders. Detoxification dysfunction can alter the response to standard medical therapies by decreased clearance of a drug product-leading to exposure to toxic concentrations of pharmaceutical compounds. Similarly, defects in excretion of bile cause jaundice (yellowing of the skin and eyes) and itching of the skin (due to accumulation of the red blood cell by-product, bilirubin), and gastrointestinal digestive problems. Finally, the most catastrophic product of liver failure is loss of mental status or 'hepatic coma'. The progressive deterioration of mental status, initiates with confusion and progresses to complete unresponsiveness. Despite years of research in this area, and many proposed causes, there has been no single factor associated with this clinical outcome. This particular problem has led many researchers to conclude that nothing short of functional organ replacement will suffice for treatment of liver failure.

Of the 30,000 patients who die from liver failure annually in the U.S., less than 3500 will undergo liver transplantation- currently the only available method for the treatment of severe liver failure (Keefe, 1995). For patients who are not selected for transplantation there is no adequate treatment available and it is estimated that 375 prospective recipients die each year while waiting for a transplant. Replacement of liver function has been attempted by many investigators, but few systems except whole organ transplantation have had even limited success.

Several nonbiological extracorporeal ('outside-the-body') approaches have been used historically, including: (1) dialysis, (2) hemoperfusion, and (3) ion exchange resins. Notwithstanding a few studies which have shown limited positive effects, nonbiological methods, for the most part, are inadequate because of their non-selectivity (i.e. they indiscriminately remove compounds from the blood) and limited function replacement (Nyberg et al 1993; Sussman and Kelly, 1995). Major liver functions (i.e. metabolism, synthesis, and excretion) are ignored in these nonbiological systems. It is also likely that certain toxins remain in the circulation while other desirable compounds are removed.

Conventional wisdom, supported by years of experimentation, therefore suggests that simple approaches such as filtration of blood, exposure to immobilized detoxification enzymes, supplementation of albumin, administration of digestive enzymes, will not be sufficient. Thus, research has turned to development of a 'bioartificial' or 'hybrid' liver device- one that utilizes live liver cells to perform a

myriad of necessary functions, presumably including those necessary to retain normal mental status. Below we detail some previous approaches to 'bioartificial liver' devices, their advantages, their shortcomings, and the role for microfabrication in improving the next generation of devices.

#### 4. HEPATIC TISSUE ENGINEERING

Hepatic tissue engineering describes efforts that attempt to harness the function of live cells (hepatocytes) for therapeutic applications. Research on these cell-based therapies has focused primarily on the creation of an extracorporeal bioartificial liver (BAL) device. Conceptually, this device would be akin to dialysis for kidney failure- i.e. patient blood would be perfused through a device that replaced an array of liver functions. However, unlike the kidney which is essentially a blood filter, the liver must synthesize, metabolize, and detoxify blood components. Thus, it seems clear that utilizing liver cells (hepatocytes) as the "heart" of an artificial liver device would provide the closest tissue replacement to the organ itself.

Applications of extracorporeal devices include treatment for both acute and chronic liver disease. Acute liver failure typically occurs in otherwise healthy patients due to viral infection (viral hepatitis), ingestion of hepatic toxins (certain mushrooms, Tylenol), or traumatic injury. It has long been recognized that this sub-population of liver failure patients will exhibit extraordinary regenerative potential- that is, if stabilized, the liver will literally 'grow back' and patients can be expected to achieve a full recovery *without* transplantation. Thus, for these ~5,000 patients per year the goal would be temporary support on an extracorporeal bioartificial liver device for a period of many weeks. In contrast, chronic liver failure is often accompanied by irreversible scarring- thus, liver regeneration is not an anticipated outcome. The application of these devices in chronic liver disease is focused primarily on bridging medically unstable patients to a successful transplant procedure and stabilization of liver transplant patients post-transplantation. Furthermore, 25% of liver transplant recipients undergo post-surgical complications and require a second surgical procedure- these patients are also candidates for an extracorporeal bioartificial device.

Currently, commercial extracorporeal bioartificial liver systems are based on hollow-fiber (dialysis) technology. Three hollow-fiber based, extracorporeal bioartificial liver systems are under

investigation. The use of hepatocytes varies from so-called 'primary' cells that are isolated from an animal by enzymatic digestion of the liver, to use of well-behaved, liver-derived, tumor cell lines. The hepatoma-based device, utilizes a transformed, contact-inhibited cell line 'C3A' (Sussman et al, 1992). Thus, liver-like cells can be easily grown in hollow-fiber devices to the desired density; however, the use of transformed human cells has some disadvantages as well. First, the cells vary in their ability to perform key liver functions. As noted above, some clinical outcomes have not been linked definitively to a particular marker of liver function- thus, it is difficult to predict whether these devices will replace all necessary liver functions. In addition, the potential of cell migration through the semi-permeable trappings of the hollow fiber to the 'blood compartment' of the device- a clinically undesirable outcome is a major disadvantage of this approach (Rozga et al, 1995).

In contrast to non-transformed cells, under most conditions primary cells undergo minimal division in vitro; therefore, investigators must isolate the necessary cell mass from animals. Due to the large size of the pig liver, porcine hepatocytes have been utilized in this setting. In addition, to cell sourcing, the stabilization of the isolated cells becomes a key factor in these devices. Thus, maximal hepatocyte function is desirable to minimize the necessary cell mass and maximize the lifetime of the device. One group has exploited the concept that hepatocytes are stabilized when they form multicellular spheroids (Wu et al, 1995) by injecting hepatocyte spheroids immobilized in a collagen gel into hollow-fiber devices. Spheroid-based devices, while providing stable cultures, have been limited by insufficient cell numbers to replace the metabolic capacity of at least 10% of the human liver. Finally, hepatocytes are known to be attachment-dependent- that is, they will rapidly die without a substrate on which to attach and spread. Thus, another group has used microcarriers (solid spheres) to create a large surface area for hepatocyte attachment (Rozga et al, 1994). Microcarrier-immobilized hepatocytes are then injected into a hollow-fiber cartridge; however, the use of these devices has been limited, to only a few hours. In addition, this configuration also suffers from insufficient cell numbers to support 10% of the human adult liver. While these devices have set the stage for key issues such as feasibility, clinical implementation, and regulatory approval, major challenges exist in the development future hepatocyte-based bioartificial liver devices. The most significant rate-limiting step will be the development of a scaleable bioreactor that incorporates hepatocytes that have been stabilized to

express high levels of a full complement of liver functions for many weeks.

## 5. HOW CAN HEPATOCYTES BE STABILIZED *IN VITRO*?

The development of an extracorporeal device requires the ability to retain liver functions in hepatocytes that have been enzymatically isolated from a donor (usually porcine) organ. In addition, this stable culture system should promote high levels of liver-specific function and the capacity to be scaled-up to replace approximately 10% of liver function. Hepatocytes, however, are notoriously difficult to maintain *in vitro*. When cultured in monolayer (in petri dishes) cultures they rapidly lose adult liver phenotype (characteristic behavior) within one week of isolation. The hepatocytes detach from the underlying substrate and die. To address this problem, investigators have developed a number of methods to sustain liver-specific functions of primary hepatocytes *in vitro*.

Typical approaches utilize manipulation of the extracellular matrix (insoluble biomolecules), media composition, or cellular environment. Extracellular Matrix (ECM) modulation has included both variations in composition and topology. Matrigel and biomatrix are examples of biologically-derived, basal lamina-like compounds which maintain long-term function (Bissel et al, 1987). Multicellular spheroids produced on nonadherent substrates are also shown to produce high liver-specific activity (Koide et al, 1990) Variations in matrix topology have include floating collagen gels and sandwich culture. Sandwich culture (Dunn et al, 1991) was designed to mimic the microenvironment of the adult hepatocyte seen in Figure 1.3 where cells are sandwiched by extracellular matrix between hepatic cords. Cells in this configuration express many liver-specific functions for weeks; however, attempts to scale-up this culture method have met with limited success thus far.

Media modifications such as hormonally-defined media (Dich et al, 1988) and supplementation of low concentrations of dimethyl sulfoxide (Isom et al, 1985) are known to stabilize hepatocytes in culture; however, these approaches are inapplicable to extracorporeal circuits where patients would encounter systemic exposure to these media components. Finally, the cellular environment of hepatocytes has been modified by the addition of other cell types. These 'co-culture' systems have provided reproducibly high levels of stable,

liver-specific function but their use in bioartificial devices is still in its infancy (Gerlach et al, 1995; Taguchi et al, 1995). A brief review of the benefits and limitations of existing hepatocyte co-culture configurations along with the physiologic basis for complex cell-cell interactions in the liver is seen below.

## 6. HOW ARE CELL-CELL INTERACTIONS IMPORTANT *IN VIVO*?

The importance of cell-cell interactions in the liver can be observed both in fetal development and the adult organ. Developmentally, the liver arises as a bud from part of the foregut. The 'hepatic diverticulum' extends into another structure, the septum transversum, where it rapidly enlarges and divides into two parts: (1) the primordium of the liver and part of the biliary apparatus and (2) the gall bladder and the connecting (cystic) duct. It is thought that the interaction of the bud with this other structure induces the cells to proliferate, to branch, and to differentiate (Gilbert, 1991)- indeed, experimentally separated tissues do not differentiate normally. The proliferating bud then gives rise to interlacing cords of liver cells and the lining of the biliary apparatus. As the liver cords penetrate the septum transversum, they break up two venous networks, creating the lining of the sinusoids (Figure 1.5) (Sadler, 1990, Houssaint et al, 1980).

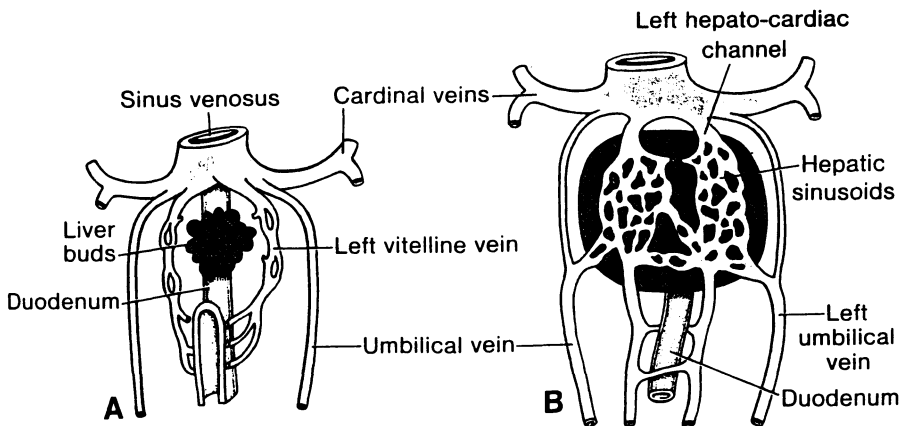


Figure 1.5. Development of the human liver in the A. 4th week and B. 5th week of gestation. (Sadler, 1990. Reproduced here by kind permission of Williams & Wilkins).

Similarly, the adult form of the liver houses many different cell types which interact precisely with one another. As seen in Figures 1.1-2.4, the liver consists of differentiated hepatocytes, endothelial cells, fat-storing cells, biliary ductal cells, and Kupffer cells. As you will see, many of these cell types aid in the stabilization of adult hepatocytes in vitro. Taken together, information about cell-cell interactions in liver development and terminal differentiation imply an essential role for cell-cell signaling. This attribute of the liver has been exploited to obtain stabilize isolated hepatocytes in vitro for fundamental studies as well as towards design of bioartificial liver devices.

## 7. CO-CULTURE

Hepatocyte viability and differentiation have been shown to be extended for several weeks when co-cultured with a variety of other cell types. Due to the many aspects of in vivo function which these co-cultures have been shown to mimic, they have been widely utilized in studies of various physiologic and pathophysiologic processes including host response to sepsis, xenobiotic toxicity, lipid metabolism, and induction of the acute phase response (Clement et al, 1984). In addition, this method of preserving hepatocyte differentiation in vitro may have important applications in bioartificial liver devices.

*Table 1.1. Cell Types Utilized in Co-Cultures for Stabilization of Rat Hepatocyte Phenotype*

LIVER-DERIVED	NON-LIVER DERIVED
Rat Liver Epithelial (Presumed Biliary Origin)	Embryonic Murine (3T3)
Liver-Derived Fat-Storing Sinusoidal Liver Endothelial Kupffer	Rat Dermal Fibroblast Chinese Hamster Monkey Kidney Epithelia Canine Kidney Epithelia
'Non-parenchymal' Fraction of Isolated Population	Bovine Aortic Endothelia Human Fibroblast Human Lung Epithelia

This stabilization of liver-specific functions has been reported for co-cultures with both liver-derived cell types as well as non liver-derived endothelia and fibroblasts (Table 1.1). Liver-derived cell

types include rat liver epithelial cells of presumed biliary origin, Ito (fat-storing) cells, sinusoidal liver endothelial cells, Kupffer cells and the entire 'non-parenchymal' fraction of isolated liver cells. Although this effect on morphologic and functional differentiation was originally thought to be species-specific, many other cell types from other organ systems and species have since been shown to influence isolated rat hepatocytes. This effect has been demonstrated, to varying degrees, using embryonic murine 3T3 and C3H 10T $\frac{1}{2}$  cells, rat dermal fibroblasts, chinese hamster cells, monkey kidney epithelia, canine kidney epithelia, bovine aortic endothelia, and human fibroblasts and lung epithelia.

Typically, cultures have preserved the differentiated synthetic functions for prolonged periods (1 to 10 weeks). The effects on hepatocyte function are inducible for 3-4 days after which hepatocyte 'rescue' is unattainable (Fraslin et al, 1985). In addition, the time-course over which albumin synthetic capability increases, appears to remain fairly constant, 6-10 days.

Culture configurations for many of these systems employed variations in the ratio of cell types and media composition. Typically, investigators have explored ratios of cell numbers of approximately 1:1, (alternative cell type: hepatocyte); however, this has varied between studies from 10:1 (Shimaoka et al, 1987) to 1:10 (Matsuo et al, 1992). In addition, many media formulations have included additions of insulin and glucocorticoids such as hydrocortisone or dexamethosone to inhibit fibroblastic overgrowth. Lastly, both serum-free and fetal bovine serum formulations have been utilized successfully. In addition to viable cells in the above culture configurations, experiments have been performed with feeder layers (irradiated (Langenbach et al, 1979), dessicated and heated (Shimaoka et al, 1987), glutaraldehyde-fixed (Morin et al, 1988) or mitomycin C-treated (Kuri-Harcuch and Mendoza-Figuera, 1989). One study compared the relative effect of viable cells versus feeder layers and reported comparable effects on the examined markers (Shimaoka et al, 1987). Similarly, glutaraldehyde-fixed endothelial cells elicited a comparable response to viable cells (Morin et al, 1986).

In general, a variety of co-culture models have met with significant success in maintenance of many hepatospecific functions. A summary of the existing data on the morphologic, mitotic, and biochemical effects of co-culture on hepatocytes is presented below.



## 7.1 Effects of Co-Culture on Hepatocyte Morphology and Function

Hepatocytes in co-cultures exhibit stereotypical polygonal morphology with distinct nuclei. In addition, co-cultures have been shown to express many liver-specific proteins such as albumin (Table 1.2). Murine 3T3's have been shown to induce the highest levels of albumin synthesis by hepatocytes ( $4.2 \mu\text{g}/10^6$  cells/h) followed by rat liver endothelial cells (3.1), rat dermal fibroblasts (3.1), rat liver epithelial cells (2.9), and bovine aortic endothelial cells (1). Another liver-specific marker, cytochrome P-450 enzyme activity, has also been observed to increase in amount and stability. For the most part, P-450 isoenzymes 1A1 and 3A1 seem to be the best stabilized after 1 week (Utesch et al, 1991; Donato et al, 1994) whereas some isoenzyme activities, such as 2C11, deteriorated completely. In comparison to conventional hepatocyte cultures such as Matrigel, total P-450 content was found to be elevated two-fold in un-induced co-cultures (Donato et al, 1990). In addition, P-450 enzymes were induced above baseline levels, with each isoenzyme showing a different induction pattern; some were inducible for up to 2 months (Naughton et al, 1994).

Functional contacts were also observed in hepatocyte co-cultures. Tight junctions were detected by the presence of ZO-1 in co-cultures (Loreal et al, 1993). Gap junctions (connexin 32) were localized both by indirect immunofluorescence and/or by microinjection of Lucifer Yellow. In general, gap junctions were formed only in homotypic cell interactions (Mesnil et al, 1987). One notable exception is the formation of heterotypic functional gap junctions between hepatocytes and fat-storing cells (connexin 43) (Rojkind, 1995). In addition, the degree of induction of albumin synthesis correlated with increased levels of connexin 43 in various fat-storing cell clones. This observation is particularly significant because fat-storing cells maintain direct contact with hepatocytes *in vivo*. Therefore, although heterotypic gap junctions have not yet been demonstrated *in vivo*, this model suggests that hepatocyte function may be influenced by the degree of heterotypic gap junction formation which in turn is modulated by cell-cell interaction in culture.

Spatial and temporal distribution of homotypic gap junctions were also examined. Mesnil et al. (1987) noted that the number of dye-coupled hepatocytes per injection gradually increased with co-culture time from 1 cell early in co-culture to 9 cells by 25 days. In addition, hepatocytes that were distant from the second cell type

maintained their specific functions (functional gap junctions, intracellular albumin production) if they were, in turn, communicating with hepatocytes which were in direct contact with the second cell type, providing indirect evidence that the differentiation signal is not confined to the interface of heterotypic contact. These results suggest that both temporal and spatial variations in gap junction expression exist in co-cultures. Furthermore, these phenomena may be better examined by utilizing a culture system that produces spatially homogeneous cell-cell interactions.

Due to the relationships described between dedifferentiation in tumors and decrease in gap junctions, studies were also done to assess the necessity of homotypic gap junctional communication for the stabilization of differentiated functions. Traiser et al. (1995) found that gap junction intercellular communication could be effectively blocked with minimal effects on another liver-specific marker, the stabilization of xenobiotic metabolic enzyme activities; however, the results of this study may not be conclusive due to the potential effects of the compounds utilized for interfering with gap junctional communication on induction of P-450 enzymes. The notion that hepatocyte gap junctions may be decoupled from differentiated function is also supported by the lack of observable gap junctions in well-established hepatic culture systems after 24 h.

An additional notable feature of certain co-cultured hepatocytes as compared to pure hepatocyte cultures, is the ability to synthesize DNA *in vitro*. This effect has been noted in hepatocyte co-cultures of both liver-derived and non-liver-derived cell types. An important distinction must be made between DNA synthesis and cell growth *per se*, especially in light of the known ability of hepatocytes to multinucleate both *in vivo* and *in vitro*. Given this caveat, two investigators have reported significant levels of DNA synthesis/division in co-cultures. When rat liver cells were co-cultured with the entire non-parenchymal liver fraction on felt templates, parenchymal cells of 15-30  $\mu\text{m}$  diameter increased in number by 10-fold over 48 days as measured by enzymatic separation of cultures and counts of cell populations by size. In addition, thymidine incorporation was measured over 48 days and found to reach a maximum at 24 days of culture (Naughton et al, 1994). In contrast, Shimaoka et al. (1987), found an increase of labeling index from 13% of hepatocytes in pure cultures to 35% of hepatocytes in co-cultures with non-parenchymal cells. This stimulatory effect of non-parenchymal cells on DNA synthesis by adult hepatocytes varied in a dose-dependent manner where cultures with low hepatocyte densities

demonstrated a two-fold increase in labeling index over high hepatocyte densities. Furthermore, DNA synthesis reached a maximum at 3 days of culture; however, this phenomenon was species specific and therefore limited to rat non-parenchymal cells as compared to other cell lines such as murine Swiss 3T3 cells.

DNA synthesis was also examined by co-culture with non-liver derived 3T3 clones, producing varied results. Some investigators have reported 20-30% labeling indices (Kuri-Harcuch and Mendoza-Figueroa, 1989) while others have reported minimal thymidine uptake (Donato et al, 1990). In other non-liver derived cell types such as human embryonic lung, canine kidney and monkey kidney epithelia, minimal thymidine uptake was reported. Thus, in general, it appears that very little hepatocyte growth occurs in co-culture configurations. This suggests that growth-arrest of the 'alternative cell type' in hepatocyte co-cultures will afford adequate control over preservation of approximately constant cell numbers of both sub-populations.

*Table 1.2 Functions Induced in Hepatocytes by Co-Culture*

---

albumin secretion
cytochrome P-450 activity (isoenzymes 1A1, 3A1)
tight junctions (detection of ZO-1)
gap junctions (detection of connexin 32, microinjection)
other: pyruvate kinase, transferrin, glutathione S-transferase, DNA synthesis

---

Lastly, the level of regulation involved in the reported increases in liver-specific protein production has also been investigated. The cause of the observed increases in protein synthesis and mRNA was studied using *in vitro* transcriptional assays from isolated nuclei as well as 'rescue' experiments wherein mRNA was allowed to decline and then observed to reappear. Albumin, pyruvate kinase, transferrin, and various subunits of glutathione S-transferase were found to be regulated primarily at the transcriptional level with at least some component of post-transcriptional mRNA stabilization (Fraslin et al, 1985, Vanderberghe et al, 1992). The degree to which heterotypic cell-cell interaction contributes to the role of each of these levels of regulation is undetermined and may be elucidated by use of a model system that allows precise control over these interactions as proposed in this study.

## 7.2 Mechanisms of Induction of Liver-Specific Function in Hepatocytes

The precise mechanisms which regulate increases in liver-specific gene transcription and mRNA stabilization have not yet been elucidated. The potential mediators of cell-cell communication include 'freely secreted' signals (i.e. cytokines) or 'cell-associated' signals (i.e. insoluble extracellular matrix or membrane-bound proteins (Table 1.3.)

Table 1.3. Potential Inducers of Hepatocyte Phenotype In Vitro

Freely Secreted	Cell-Associated	
	Extracellular Matrix	Transmembrane Proteins
Co-Cultures - generally no induction observed <sup>†</sup>	Co-Cultures collagenase-sensitive signal	Co-Cultures Connexin (32/43)  Liver Regulating Protein (LRP)
Hepatocytes Alone ?	Hepatocytes Alone Heparan Sulfate Proteoglycan Matrigel/ Biomatrix Collagen I Gels (Sandwich)	Hepatocytes Alone   $\beta$ 1 integrin

<sup>†</sup> partial induction in one study (Schrode et al, 1990)

Many studies attempting to discern the contribution of soluble factors in co-culture systems have produced contradictory results. Morin et al. (1988), reported that a transmembrane culture system utilizing hepatocytes seeded on a 0.45  $\mu$ m pore size filter and endothelial cells in an underlying well, induced similar levels of albumin secretion as control co-cultures with sinusoidal cells in contact with hepatocytes on similar filters. In contrast, Donato et al. (1994), reported no significant improvement in P450 activity when hepatocytes were cultured on the bottom of a similar transwell system with a 0.4  $\mu$ m pore size and MS epithelial cells on top of the insert over pure hepatocyte cultures. In addition, use of conditioned media from pure cultures of the second cell type on pure hepatocyte cultures has been shown, almost universally, to be ineffective (Kuri-Harcuch and Mendoza-Figueroa, 1989; Donato et al, 1990; Shimaoka et al, 1987). At least one dissenting study showed a partial effect of rat liver epithelial cell conditioned media on hepatocyte cultures (half-maximal increases in levels of glutamine synthetase activity relative to control co-cultures). Interestingly, conditioned media from co-

cultures showed no effect implying any potential soluble factor is not present in excess in co-cultures due to its uptake/degradation by hepatocytes (Schrode et al, 1990).

Comparatively, studies on extracellular matrix-mediated effects on liver-specific gene expression have been even less conclusive. Although many groups have reported matrix deposition patterns specific to co-cultures, no causative effects of this matrix have been shown. In particular, reticulin fibers were observed in co-cultures but absent in both types of pure culture (Guguen-Guillouzo et al, 1983, Goulet et al, 1988, Baffet et al, 1991). Other extracellular matrix components have been observed in co-cultures with indirect immunofluorescent techniques including collagen I, IV, fibronectin, laminin, entactin (Clement et al, 1988; Goulet et al, 1988; Loreal et al, 1993).

Mesenchymal cells are typically characterized by their ability to produce collagen I and fibronectin matrix molecules whereas hepatocytes have been shown to primarily produce collagen IV and laminin. As a result, the cellular source of ECM deposition in co-cultures is unclear. In addition, endothelial cells were found to produce perlecan in vivo (heparan sulfate-proteoglycan, a known mediator of some liver-specific functions), which may implicate proteoglycans in some component of the co-culture effect. However, this ECM effect on liver cells is unlikely to be descriptive of the mechanism by which Ito cells induce differentiated hepatic function since they were consistently negative for perlecan. Finally, two groups have attempted to modulate the effect of potentially ECM-mediated events by (1) crudely assessing the distance over which the signal can travel from the heterotypic interface (Shrode et al, 1990), and by (2) treating feeder layers with enzymes specific for ECM destruction (Shimaoka et al, 1987). Shrode et al (1990) found up-regulation of glutamine synthetase production up to a few millimeters from the heterotypic interface; they suggest that large, insoluble, ECM molecules are likely mediators since they would have limited diffusivity at critical concentrations. In contrast, the effects of direct cell contact communicated via gap junctions are discounted by the authors as they hypothesize that such a signal would travel over a limited distance. Finally, Shimaoka et al (1987), reported that the DNA synthesis which they monitored in co-cultures, was acid, trypsin and collagenase-sensitive, implicating some protein containing collagen. In addition, pre-cultured feeder layers induced DNA synthesis earlier than fresh feeder layers, indicating the presence of some material was rate-limiting. The authors suggest that the

insoluble molecules (ECM or membrane receptors) in the feeder layers were responsible for the observed effects, although soluble factors which had become entrapped in the feeder layers may also have played a role.

Until recently, the role of direct contact of cells, the other potential mechanism involved with induction of liver-specific function, has remained unclear. Mesnil et al. (1987) showed that only hepatocytes in close proximity to epithelial cells in sparse cultures remained viable and differentiated as compared to those which appeared to lack heterotypic contact. The authors suggest the importance of cell contact based on this indirect evidence; however, it seems clear that local deposition of ECM or local concentrations of critical soluble factors cannot reliably be ruled out as causes for the preservation of viability and differentiation. More rigorous evidence supporting the role of membrane contact as a potential mechanism was reported in 1991. Corlu et al (1991) identified a cell surface protein, LRP or liver regulating protein which seemed to be involved in the establishment and maintenance of hepatocyte differentiation in co-culture with liver epithelial cells. They demonstrated the ability to modulate albumin secretion, cytoskeletal organization, and ECM deposition by addition of a monoclonal antibody against LRP. Furthermore, the authors discount extracellular matrix as potential ligand for LRP due to the inability of anti-LRP antibody to modulate cell adhesion to immobilized ECM. In addition, this inhibitory effect was only produced upon addition of the antibody early in culture. The authors suggest that this time-dependence supports the role of cell-cell contact in the co-culture effect due to the indirect evidence that establishment of cell-cell contacts occurs during the same time frame in culture. Finally, it seems that LRP is almost certainly not the whole story; although some cell types which induce liver-specific functions in hepatocytes stained positive for LRP (sinusoidal cells and Ito cells), other cell types did not (vascular endothelia, biliary ductal cells). Therefore, although the presence of LRP may modulate hepatocyte function in epithelial co-culture, the absence of LRP in co-culture with other cell types does not seem to prevent induction of liver-specific functions.

Other modes of direct contact such as gap junctional communication may also play a role in cell signaling. In one study, levels of connexin 43 (cx43) protein expressed by fat-storing cell subclones, correlated with albumin mRNA levels in co-cultured hepatocytes. Functional heterotypic gap junctions were observed as a result of cx43 protein synthesis by microinjection of Lucifer Yellow.

This mode of cell signaling may be particularly important in hepatocyte interaction with Ito cells as compared to other cell types due to the potential relevance of this signaling mechanism in vivo (Clemens et al, 1994 ).

In summary, despite the substantial data existing on potential mediators of cell communication in co-cultures (receptors, gap junctions, cytokines, ECM), the mechanisms by which co-culture of hepatocytes with other cell types induce increased liver-specific function and viability are undefined. Elucidation of the role of cell-cell interaction in mediating this response will provide valuable insight into the design of a bioartificial liver (BAL) system. Specifically, maximal metabolic capacity will require optimal hepatocellular function with a minimum number of fibroblasts. In addition, the potential elucidation of the components of cell signaling responsible for hepatic differentiation offers the hope of eliminating the need for fibroblasts entirely. In either case, we are posed with an engineering problem which necessitates a quantitative understanding of mesenchymal-parenchymal interactions.

## **8. PREVIOUS ATTEMPTS TO CONTROL CELL-CELL INTERACTIONS**

Co-culture systems discussed above have utilized a variety of techniques to examine the role of cell-cell interactions in a semi-quantitative manner. Here, we critically review existing approaches in hepatocyte co-culture and demonstrate the need for better methodologies (See Figure 1.6).

Control of cell-cell interactions fall into two general categories: (1) prevention of contact or (2) modulation of the degree of contact. Prevention of contact has been achieved by co-cultures with porous filter inserts, insertion of crude spacers, or conditioned media experimentation. As detailed above, these culture configurations have produced inconsistent results due to the variations in media sampling, storage, filter material, and cell seeding densities. In addition, absolute lack of contact is difficult to ensure; for example, transfer of detached cells in conditioned media or protrusion of cell processes through the porous filter is difficult to completely rule out.

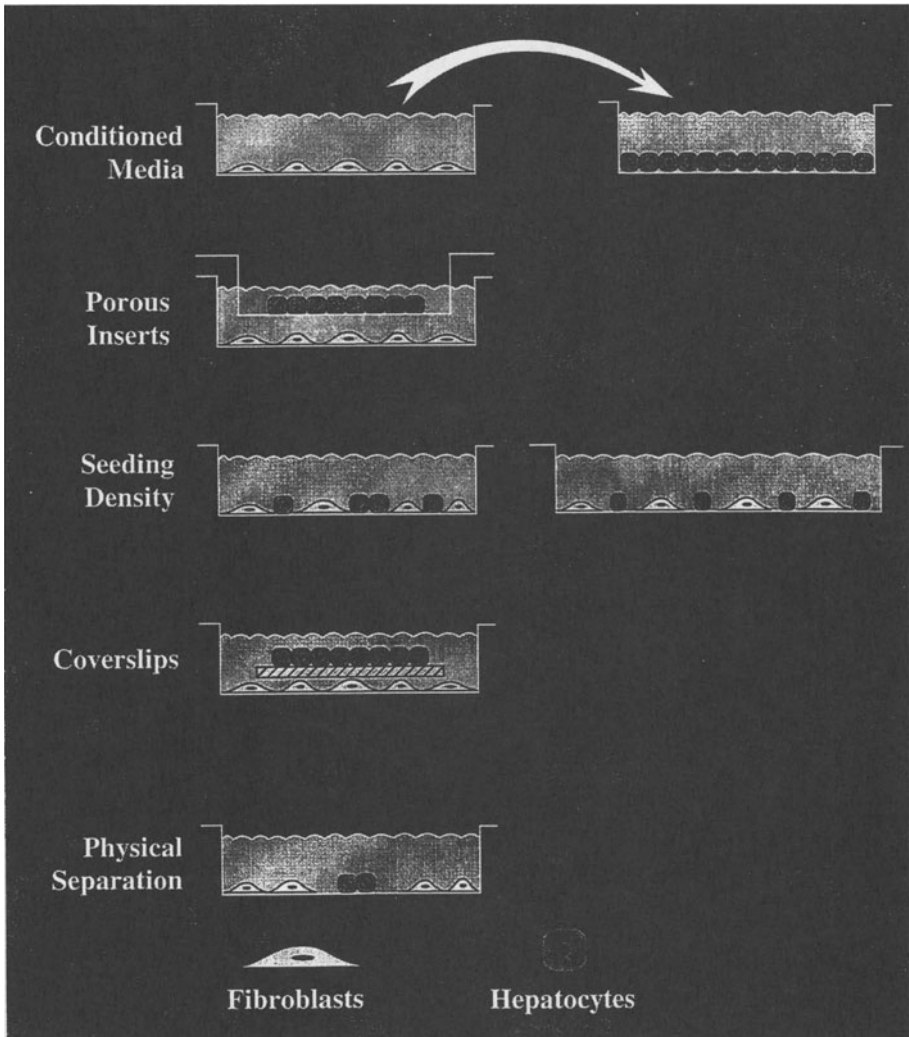


Figure 1.6. Schematic of Conventional Approaches for Control of Cell-Cell Interaction

Another approach at prevention of contact was reported by Shrode et al (1990). Creation of a cell-free annulus has been crudely attempted through the addition of a polymer spacer to a culture dish



by use of rubber cement adhesive. This spacer was then removed resulting in a defined, relatively large (~mm) cell-free annulus between the cell populations. This method is limited by the undefined underlying substrate (residual adhesive) and relegation to relatively large dimensions of annuli (spacers must be large enough to manipulate manually).

In addition to control of cell-cell interactions by prevention of contact, modulation of the degree of cell contact has also been attempted. Both conventional techniques (variations in seeding density) as well as more specialized systems (addition of confluent coverslips to confluent cultures) have been utilized. Variations in seeding density were used by Guguen-Guillouzo et al. (1986) to study effects of cell contact on hepatocyte differentiation. They examined effects of lower seeding densities by seeding the same cell numbers in a two different size flasks. This method is limited by heterogeneous cell contacts that occur due to random aggregation during cell seeding. In addition, a confounding factor is the ability of the second cell type to divide- lower seeding densities may then result in increased cell number and the accompanying soluble factors synthesized by these cells.

Another group examined the role of cell contact by addition of confluent cultures of hepatocytes on a coverslip to the center of confluent cultures of either fibroblasts or fibroblast/hepatocyte co-cultures. This experimental method is limited due to cell death underlying the coverslip and the significant topological variations in the culture (height of a coverslip is typically 100-300 microns) (Shimaoka et al, 1987).

We shall pursue techniques of controlling cell-cell interactions which will significantly advance the current state-of-the-art reviewed here. These methods should allow control over the spatial distribution of two cell types in planar cultures while maintaining constant cell number as well as allowing cell-free areas between cell populations. Below we discuss review existing methods micropatterning cellular structures and their applicability to our goals.

## 9. MICROPATTERNING OF CELLS

The spatial control of cells in culture has been achieved, in some form, since 1912 when cultured cells on spider webs were shown to influence cell movement (Harrison, 1912). Recently, especially in the last decade, the field of micropatterning has advanced significantly

due to marked improvements in the techniques for generating defined surfaces. Many of the methods employ variations of photolithographic processes developed for the manufacture of integrated circuits, resulting in the ability to achieve spatial resolution on the order of 0.5 microns. A wide array of biological phenomenon have been investigated using these model systems including cell guidance, effects of cell shape on function, and cell-signaling. Most approaches can be categorized into one of the following areas: manipulation of surface topology alone, modification of glass/silicon with inorganic compounds, modification of glass/silicon with biomolecules, or immobilization of biomolecules on polymeric substrates.

Variation in surface topology alone (i.e. chemically identical regions) has been reviewed extensively elsewhere (Singhvi et al, 1994) and is typically achieved by anisotropic chemical or plasma etching of silicon or glass. Many investigators have reported a phenomenon now commonly known as 'contact guidance' whereby cells become oriented in response to the underlying topography. In addition, some have shown that parallel grooves of certain dimensions can increase cell adhesion by confining them. Currently, mechanistic studies are underway to assess the relative importance of various cytoskeletal elements in directed locomotion. Oakley and Brunette (1995) recently reported that microtubules do not seem to be required to establish or maintain directed locomotion provided that an alternate oriented cytoskeletal component is available. Our interest has been in the localization of cells on planar surfaces; therefore, we will focus primarily on chemical modification of 'flat' surfaces as compared to topological variations on chemically uniform ones.

Chemical modification of glass and silicon substrates with inorganic compounds has primarily been approached in two ways: selective coupling of hydrophilic and hydrophobic silanes, and vapor deposition of metals. Localized vapor deposition is typically achieved by the deposition of palladium through a microfabricated mask onto a non-adhesive (i.e. poly-hydroxyethyl methacrylate) background (O'Neill et al, 1990; Letourneau et al, 1975; Harris et al, 1973; Ireland et al, 1987; Carter et al, 1965). A variety of cell types (mouse fibroblasts, chick myocytes, chick neuronal cells) were shown to selectively attach and spread on the metallic areas and were examined for degree of attachment, distribution of focal contacts, cell shape, locomotion, cytoskeletal structure and growth. Despite the ability to mediate selective cell attachment, the chemical composition of the modified surface has been restricted to gold or palladium; therefore,

more flexible techniques of chemical modification with silanes have also been developed.

Typically, silanes reacting with hydroxyl groups on glass, quartz, or silicone to form silane-modified surfaces. The terminal silane groups dictate the resultant surface properties: therefore, methyl or perfluorinated terminations result in hydrophobic surfaces whereas amine terminations result in hydrophilic surfaces. Many groups have used photolithography to pattern non-permissive hydrophobic silane groups that prevent cell attachment adjacent to primary amine chemistries that are permissive towards cell attachment (Healy et al, 1994; Stenger et al, 1992; Kleinfeld et al, 1988; Clark et al, 1992; Georger et al, 1992; Britland et al, 1992; Matsuda et al, 1990). This process was originated by Kleinfeld et al (1988) with the intent of controlling outgrowth of disassociated neurons. Ranieri et al (1993) recently showed that this avoidance of the hydrophobic region by certain cell types was dependent on the initial adsorption conformation of albumin from the media. These studies have illuminated some of the underlying factors contributing to cell attachment, spreading, and guidance; however, they do not offer much insight into binding of cells to natural ligands such as ECM molecules. As a result, a number of groups have moved towards systems which allow immobilization of biomolecules of greater interest such as proteins and synthetic peptides.

Localization of biomolecules is achieved either by protein adsorption, selective photo-inactivation, or immobilization via silanes or alkanethiols. Protein deposition techniques have included use of capillary action on a metal grid, micro-pipetting (Gundersen et al, 1987), suction through a capillary-pore filter (Baier et al, 1992) and even re-fitting of an ink-jet printer to print fibronectin solutions (Klebe et al, 1988). These methods have the benefit of utilizing the protein in its native form; however, the resolution on 'wet' techniques ranges from 25-300 microns. In comparison, methods which utilize light as the vehicle for surface modification (photolithography or photo-(in)activation) have resolutions in the vicinity of 1-5 microns. Photo-inactivation of laminin and photoablation of poly-L-lysine have both been utilized successfully in studies of the effect of substrate adhesivity on neuronal guidance in vitro (Corey et al, 1991; Hammarback et al, 1985, 1988). Similarly, albumin-agarose gels were cross-linked with ultraviolet light resulting in preferential adsorption of laminin and irradiation caused immobilization of collagen in collagen-doped hydrogels (Hammarback et al, 1986; Yamazaki et al, 1994).

Although these techniques offer significant improvement over non-biological substrates and 'wet' protein deposition methodologies, the variations in adhesive properties of the immobilized biomolecules is not well understood. As a result, techniques whereby substrates are coated uniformly and inactivated in selected regions, do not provide a versatile model system to examine a variety of biomolecules of interest. Alternatively, immobilization of biomolecules in selected areas has been achieved using silane and alkanethiol linkers. Britland et al. (1992) reported immobilization of bovine serum albumin and horse radish peroxidase with retained catalytic activity. They first coupled hydrophobic silanes to micropatterned glass substrates, removed residual photoresist, and coupled aminosilanes to the newly exposed sites. Subsequently, glutaraldehyde was used to link protein groups to bound amine groups. Non-specifically bound protein was removed from the hydrophobic sites by denaturation in urea solution. Although effective, this technique proved difficult to generalize due to the variability in protein denaturation (collagen, for example, does not desorb from hydrophobic sites in the presence of urea). Lom et al (1993) improved on this technique by first binding aminosilane to glass and selectively linking proteins to exposed aminosilane groups. One drawback of this technique is the necessity of exposing proteins to acetone, or a similar solvent, in order to remove the residual patterning materials. In spite of this theoretical limitation, this method was utilized successfully for the micropatterning of bioactive laminin, fibronectin, collagen IV, and bovine serum albumin. Another, equivalently versatile approach was reported by Singhvi et al (1994) whereby adhesive biomolecules are selectively immobilized using gold-sputtered surfaces 'stamped' with alkanethiols. This allows binding of adhesive biomolecules to the stamped areas as well as non-adhesive poly-ethylene glycol groups to the surrounding regions. This technique, unlike those utilizing photolithography for individual substrate modification, utilizes microfabrication to create a template for the generation of a reusable polymeric stamp. However, this system also has some potential drawbacks due to the heterogeneity implicit in a 'stamping' process and the necessity of gold-sputtering every substrate.

Thus, the ability to micropattern cells via non-specific as well as receptor-specific interactions on underlying solid substrata (glass and silicon) has advanced significantly. Recently, this has been improved upon by micropatterning of biomolecules on polymeric substrates, thereby creating model systems for research in implantation biology (Ranieri et al, 1994; Bellamkonda et al, 1993;

Valentini et al, 1993). These techniques are similar to those detailed above; however, the polymers (fluorinated ethylene propylene, polyvinylidene) are first chemically activated through a mask with a radio frequency glow discharge process that covalently replaces surface fluorine atoms with reactive hydroxyl groups. Subsequently, coupling agents are utilized to link receptor-specific oligopeptide sequences derived from laminin by either the N- or C-terminus. Receptor-specific binding of neurons was demonstrated through competitive binding assays with soluble oligonucleotides. This approach offers great promise in the area of patterning biomolecules on biomaterials; however, the versatility of the technique remains to be demonstrated. For example, experiments to assess the ability to couple larger molecules without incurring non-specific adsorption to the underlying polymer will need to be performed on a case-by-case basis. Finally, microfabrication technology is rapidly advancing from patterning technology to development of precisely controlled 3-dimensional microenvironments (Desai et al, 1998).

Despite the extensive literature reviewed above, investigators have not yet demonstrated the ability to control the spatial location of two or more cell types simultaneously. We have modified techniques of Lom et al. (1993) to allow precise control over cell-cell interactions in two-phase cultures.

## 10. SCOPE OF THIS STUDY

Based on mesenchymal induction of hepatic differentiation in utero coupled with knowledge about cell-cell interactions in the adult liver and results of in vitro co-culture experiments, we propose that a quantitative study of cell-cell interactions would have tremendous impact in hepatic tissue engineering, in particular, and liver physiology, in general. In addition, although co-culture of hepatocytes with other cell types has proven to be a promising way to obtain a wide array of differentiated hepatic functions in vitro, there is a paucity of data on the mechanisms behind the well-characterized 'co-culture' effect. Furthermore, cell-cell interactions have not been quantitatively controlled in such a way that useful 'design parameters' could be inferred for the design of a BAL. Thus, the use of microfabrication for the quantitative control of cell-cell interactions in co-culture would provide a system with significance in vivo, relevance to an important clinical need, and the potential to be easily

generalized to many other fields of developmental biology and tissue engineering.

In Chapter 2, we describe an adaptable method for generating two-dimensional, anisotropic, model surfaces capable of organizing a single cell type or two different cell types in discrete spatial locations. We utilized photolithography to pattern biomolecules on glass substrates which mediated cell adhesion of the first cell type, hepatocytes. The second cell type, 3T3-J2 fibroblasts, underwent non-specific, serum-mediated attachment to the remaining unmodified areas. The versatility of photolithography was exploited to generate an array of homotypic and heterotypic interactions while maintaining identical cell numbers of both cell populations. We further describe methods utilized for characterization of these substrates and resulting co-cultures, and the techniques utilized in subsequent biological investigations.

In Chapter 3, we characterize patterned substrates before and after the localization of proteins and cells. We demonstrate the versatility and utility of this technique in reproducibly achieving control over cell-cell interactions.

In Chapter 4, the reproducible control over cellular microenvironments was utilized to study the effects of homotypic and heterotypic interactions on the liver-specific functions *in vitro*. Microfabrication was utilized as a vehicle for control over cell-cell interactions without significant variations in cell numbers. The effect of modulation of the heterotypic interface on bulk tissue function was examined. The level of heterotypic interactions was found to dramatically alter liver-specific markers of metabolic, synthetic, and excretory functions in the composite tissues.

In Chapter 5, the mechanisms by which these local influences from the cellular microenvironment modify hepatocyte function were probed. In addition to demonstrating that liver-specific tissue function can be modulated by controlling heterotypic cell-cell interactions, it was determined that hepatocyte function varied with distance from the heterotypic interface. Liver-specific function was observed to be increased in the vicinity of the heterotypic interface, indicating a local fibroblast-derived signal. We attempted to classify this signal broadly as cell-associated as compared to freely secreted for fundamental and practical purposes.

Finally, in Chapter 6, we defined a framework for manipulation of the cellular microenvironment based on these data in order to optimize tissue function for use in a BAL device. By utilization of microfabrication and polymer masking techniques, we

determined optimal fibroblast:hepatocyte ratios for use in such a hypothetical bioreactor. Furthermore, we observed significant improvements in hepatic function as compared to other methods of promoting stable hepatic function in vitro. Last, approximations of oxygen transport and viscous energy losses in a hypothetical reactor were utilized to generate design criteria for a co-culture based bioreactor. This approach will have important implications not only in the assembly of BAL devices, but the potential to be generalized to many other organ systems as well.

## Chapter 2

# Methodology for Fabrication, Characterization, and Analysis of Micropatterned Co-Cultures

### 1. OVERVIEW

In this chapter, we describe an adaptable method for generating two-dimensional, anisotropic, model surfaces capable of organizing a single cell type or two different cell types in discrete spatial locations. We have chosen a primary rat hepatocyte/3T3 fibroblast cell system due to its potential significance in clinical applications and based on widely reported interactions observed in this co-culture model (Shimaoka et al, 1987; Goulet et al, 1988; Donato et al, 1990; Langenbach et al, 1979; Kuri-Harcuch et al, 1989). We have used photolithography to pattern biomolecules on glass substrates which mediate cell adhesion of the first cell type, hepatocytes. The second cell type, 3T3 fibroblasts, undergoes non-specific, serum-mediated attachment to the remaining unmodified areas. Here, we describe the specifics of our methodology and discuss its facility and versatility as compared to other existing micropatterning techniques. The remaining portion of the chapter details the methodologies utilized in characterization of substrates and subsequent experimentation. These studies include examination of function based on variations of cell-cell interaction, probing for mechanisms of cell-cell interaction, and optimization of micropatterned co-cultures for bioreactor applications.



## 2. FABRICATION OF MICROPATTERNED CO-CULTURES

As seen in Figure 2.1, microfabrication techniques were first used to modify glass substrates with biomolecules. These modified substrates were then utilized to pattern a single cell type or micropattern co-cultures in various configurations. Each critical processing step is described in detail below.

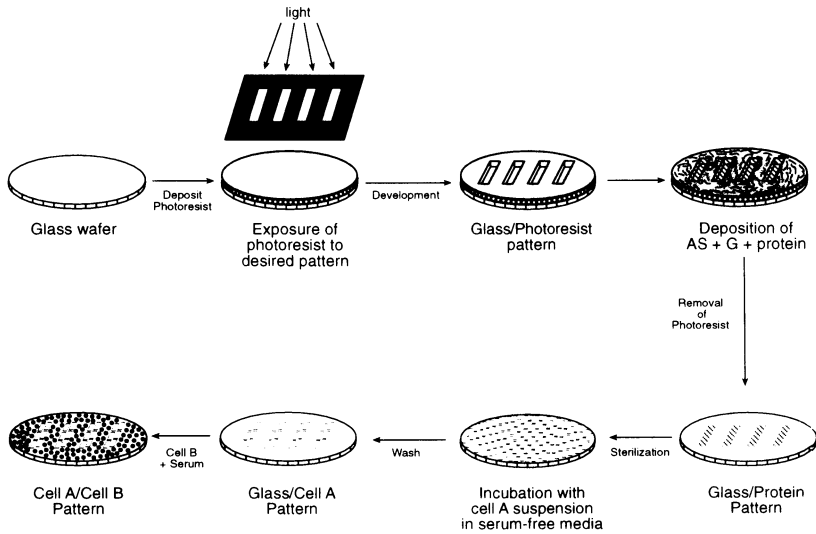


Figure 2.1. Schematic of Process to Generate Micropatterned Co-Cultures

### 2.1 Microfabrication of Substrates

The experimental substrates were produced utilizing standard microfabrication techniques at Microsystems Technology Lab, MIT, Cambridge, MA. Chrome masks of the desired dimensions were generated on a pattern generator (Gyrex) which transferred the pattern to a chromium coated quartz plate using a contact printer and a developer. Round, 2" diameter X 0.02" thickness borosilicate wafers (Erie Scientific) were cleaned in a piranha solution (3:1 H<sub>2</sub>SO<sub>4</sub>: 30% H<sub>2</sub>O<sub>2</sub>) for 10 min, rinsed, and blown dry with a N<sub>2</sub> gun. Wafers were then dehydrated by baking for 60 min at 200° C. Discs were subsequently coated with positive photoresist (OCG 820-27 centistokes) on a Headway spin-coater with vacuum chuck as follows: dispense photoresist at 500 RPM for 2 s, spread photoresist at 750 RPM for 6 s, spin at 4000 RPM for 30 s, resulting in a 1 μm coating (Step A, Figure 2.1). Wafers were then pre-baked for 5 min at 90°C to remove

residual solvent and anneal any stress in the film. Wafers were exposed in a Bottom Side Mask Aligner (Karl Suss) to ultraviolet light through the desired chromium mask to create a latent image in the resist layer. Exposure occurred under vacuum-enhanced contact for 3 s. Exposed photoresist was then developed to produce the final three-dimensional relief image for 70 s in developer (OCG 934 1:1), rinsed three times under running deionized water and cascade rinsed for 2 min (Step B, Figure 2.1). Subsequently, discs were hard-baked for 30 min at 120° C to remove residual developing solvents and promote adhesion of the film. Finally, substrates were exposed to oxygen plasma at 250 W for 4 min to remove unwanted resist in areas to be subsequently modified. Wafers were stored at room temperature for up to 2 months. Substrates were subsequently re-exposed to oxygen plasma 24 h prior to further processing to ensure availability of borosilicate for surface modification on a Plasma Day Etcher at a base vacuum of 50 mTorr and O<sub>2</sub> pressure of 100 mTorr at a power of 100W for 2-4 min.

## **2.2 Surface Modification of Substrates**

Substrates were modified using experimental methods similar to those developed by Lom et al. and Britland et al (Step C, Figure 2.1) (Stenger et al, 1992; Lom et al, 1993). Briefly, substrates were rinsed 2X in distilled, deionized (DD) water and allowed to air dry. Silane immobilization onto exposed glass was performed by immersing samples for 30 s in freshly prepared, 2% v/v solution of 3-[(2-aminoethyl)amino] propyltrimethoxysilane (AS, Hüls America) in water followed by 2 rinses in 200 mL DD water. Wafers were then dried with nitrogen gas and baked at 120 ° C for 10 min. Next, discs were immersed in 20 mL of 2.5% v/v solution of glutaraldehyde in PBS (pH 7.4) for 1 h at 25° C. Substrates were then rinsed twice in fresh PBS, and immersed in a 4 mL solution of a 1:1 solution of 1 mg/mL collagen I (preparation described in detail elsewhere) (Dunn et al, 1991): DD water for 15 min at 25 °C. Discs were subsequently immersed in acetone and placed in a bath sonicator (Bransonic) for 15 min to remove residual photoresist ultrasonically (Step D, Figure 2.1). Wafers were then rinsed twice in DD water, and soaked overnight in 70% ethanol for sterilization (Step E, Figure 2.1).

## **2.3 Cell Culture**

### **2.3.1 Hepatocyte Isolation and Culture**

Hepatocytes were isolated from 2- to 3-month-old adult female Lewis rats (Charles River) weighing 180-200g, by a modified procedure of Seglen

(1976). Detailed procedures for isolation and purification of hepatocytes were previously described by Dunn et al (1989). Briefly, the liver is perfused with a collagenase solution and dispersed hepatocytes are purified by gradient centrifugation. Routinely, 200-300 million cells were isolated with viability between 85% and 95%, as judged by Trypan blue exclusion. Non-parenchymal cells, as judged by their size ( $< 10 \mu\text{m}$  in diameter) and morphology (nonpolygonal or stellate), were less than one percent. Culture medium was Dulbecco's modified Eagle's Medium (DMEM, Gibco) supplemented with 10% fetal bovine serum (FBS, JR Scientific), 0.5 U/mL insulin, 7 ng/mL glucagon, 20 ng/mL epidermal growth factor, 7.5  $\mu\text{g}/\text{mL}$  hydrocortisone, 200 U/mL penicillin, 200  $\mu\text{g}/\text{mL}$  streptomycin and 50  $\mu\text{g}/\text{mL}$  gentamycin ('hepatocyte media with serum'). Serum-free culture medium was identical except for the inclusion of 40  $\mu\text{g}/\text{mL}$  of L-Proline (Sigma) and exclusion of FBS (Lee et al, 1993) ('serum-free hepatocyte media').

### **2.3.2 NIH 3T3-J2 Culture**

NIH 3T3-J2 cells were the gift of Howard Green, Harvard Medical School. Cells grown to pre-confluence were trypsinized in 0.01% trypsin (ICN Biomedicals)/0.01% EDTA(Boehringer Mannheim) solution in PBS for 5 minutes and then resuspended in 25 mL media. Approximately 10% of the cells were inoculated into a fresh tissue culture flask. Cells were passaged at pre-confluency no more than 12 times. Cells were cultured in 75  $\text{cm}^3$  flasks (Corning) at 10%  $\text{CO}_2$ , balance moist air. Culture medium consisted of DMEM (Gibco) with high glucose, supplemented with 10% bovine calf serum (BCS, JRH Biosciences) and 200 U/mL penicillin and 200  $\mu\text{g}/\text{mL}$  streptomycin. In some cases growth-arrested cells were obtained for DNA analysis by incubation with 10  $\mu\text{g}/\text{mL}$  mitomycin C (Boehringer Mannheim) in media for 2 h (reconstituted just prior to use) followed by three washes with media. Mitomycin C-treated fibroblasts were shown to have constant levels of DNA for 10 days of culture, verifying lack of fibroblast growth under these conditions.

## **2.4 Cell Culture on Modified Surfaces**

Wafers were rinsed in sterile water, and incubated in 0.05 % w/w bovine serum albumin in water at 37°C for 1 h to pre-coat substrates with a non-adhesive protein. Substrates were then washed twice with serum-free media. Next, hepatocytes were seeded at high density ( $4 \times 10^6/\text{mL}$ ) in serum-free media for 1.5 h at 37°C, 10%  $\text{CO}_2$ , balance air (Step E, Figure 2.1). Surfaces were then rinsed twice by pipetting and then aspirating 4 mL of serum-free

media, re-seeded with hepatocytes for 1.5 h, rinsed with 4 mL of serum-free media, and incubated overnight (Step F, Figure 2.1). The following day, 3T3 cells were trypsinized as described above, counted with a hemocytometer and plated at  $1 \times 10^6$  /mL in 2 mL of serum-containing, high glucose DMEM, and allowed to attach overnight (Step G, Figure 2.1). 'Randomly-distributed' co-cultures consisted of hepatocyte seeding in the desired number (usually 250,000) on a uniformly collagen-derivatized surface followed by 3T3 seeding after 24h.

### **3. SURFACE CHARACTERIZATION OF SUBSTRATES**

Microfabricated substrates were characterized at various stages of processing: after photoresist development, after collagen immobilization, and after cell seeding. Below we describe the methodologies that were utilized to evaluate the substrates at these various points. The results of these experiments are detailed and discussed in Chapter 3.

#### **3.1 Autofluorescence**

Photoresist patterned wafers were observed using a Nikon Diaphot microscope equipped with a Hg lamp and power supply (Nikon). The autofluorescence of photoresist (excitation: 550 nm, emission: 575 nm) was used to visualize micropatterned substrates prior to surface modification. Absence of autofluorescence after sonication was taken to verify removal.

#### **3.2 Profilometry**

Profilometry was performed on photoresist patterned wafers to characterize surface topology at the Center for Material Science Engineering (CMSE), MIT, Cambridge, MA on a Dektak 3 Profilometer ( Veeco Instruments) with a 12.5  $\mu\text{m}$  radius probe at a scan rate of 100  $\mu\text{m/s}$ .

#### **3.3 Atomic Force Microscopy (AFM)**

AFM was performed on collagen-derivatized substrates in order to characterize the spatial distribution of immobilized groups at the CMSE, MIT on a Nanoscope 3 (Digital Instruments) equipped with a standard 117  $\mu\text{m}$  silicon cantilever operating in tapping mode with a scan size of 100  $\mu\text{m}$ .

### **3.4 Indirect Immunofluorescence of Collagen I**

Immunoreactivity and localization of collagen was confirmed by indirect immunofluorescent visualization of collagen-derivatized substrates. After collagen immobilization and photoresist removal, wafers were incubated at 37°C with undiluted Rabbit Anti-Rat Collagen I Antisera (Biosciences), by inverting substrates onto parafilm which contained a droplet of (50  $\mu$ L) of antisera for 1 h. Substrates were then washed thoroughly in PBS and placed on a rotating shaker at 25 °C for 30 min. This washing procedure was repeated twice. Next, discs were inverted onto parafilm with 50  $\mu$ L (1:20) of Dichlorotriazinylamino Fluorescein (DTAF)-conjugated Donkey Anti-Rabbit IgG (Jackson) in blocking solution. Blocking solution consisted of 3% w/w bovine serum albumin, 1% donkey serum, 0.04 % sodium azide, pH 7.4. Finally, substrates were washed in PBS overnight, and observed by fluorescence microscopy (excitation: 470 nm, emission: 510 nm).

### **3.5 Immunofluorescent Staining**

Subsequent to cell seeding, micropatterned co-cultures were visualized by fluorescent staining of two cytoskeletal elements- actin and cytokeratin. Cultures were washed 2 $\times$  with 2mL PBS, fixed and permeabilized with 10 mL of acetone at -20° C for 2 min, and washed 2 $\times$  in 10 mL PBS. Cultures on wafers were incubated at 37°C with undiluted Rabbit Anti-Rat Pan Cytokeratin Antisera (Accurate Chemical), by inverting substrates onto parafilm containing a 50  $\mu$ L droplet of antisera for 1 h. Substrates were then washed, incubated with secondary antibody, and washed as described above (See Indirect Immunofluorescence of Collagen). Secondary antibody also included rhodamine-phalloidin (1:100, Molecular Probes) for fluorescent labeling of F-actin. Specimens were observed and recorded using fluorescence microscopy.

### **3.6 Image Analysis**

Finally, micropatterned co-cultures were visualized under phase contrast optics to estimate the degree of cell-cell interaction that was achieved. To quantitatively describe the extent of heterotypic interactions we measured the fraction of projected cell perimeter in contact with adjacent cells of a different cell type ( $\chi$ ). For example,  $\chi=1$  for a single cell island whereas  $\chi=0$  for a cell amidst hepatocyte neighbors. Images were acquired as described above and analyzed with MetaMorph Image Analysis System. Cells were sampled from each field and manually outlined to obtain individual cell perimeters, P. Subsequently, the regions of heterotypic cell-

cell contact were similarly delineated,  $F$ . Each cell was assigned its characteristic  $\chi = F/P$  and these values of  $\chi$  were averaged over 20-50 cells for each condition. For population distributions, individual values of  $\chi$  were assigned to an appropriate 'bin', and histograms plots were generated. A representative image used for analysis is depicted in Chapter 3.

## **4. FUNCTIONAL ANALYSIS OF MICROPATTERNED CO-CULTURES**

In Chapter 4 we examine the functional impact of varying cell-cell interactions through micropatterning. Here, we present the experimental design used for this study and various assays for probing hepatocellular function.

### **4.1 Experimental Design**

Spatial configurations of micropatterned co-cultures were manipulated by varying mask dimensions. Transparent circular areas (or 'holes') on chrome masks correspond to derivatized, and ultimately hepatocyte-adhesive, areas of glass substrates. In order to achieve identical hepatocyte numbers across varying micropatterned configurations, the total surface area of all 'holes' was kept constant across all masks despite changes in hole diameter and center-to-center spacing. All arrays were hexagonally packed with the exception of the largest dimension hole which consisted of a single unit of 17800  $\mu\text{m}$  diameter. Thus, pattern dimensions varied as follows (hole diameter, center-to-center spacing): 36, 90; 100, 250; 490, 1229; 6800, 16900; and a single unit of 17800  $\mu\text{m}$  diameter, where the resulting total hepatocyte-adhesive area on 2" diameter glass substrates would be identical in all cases.

### **4.2 Analytical Assays**

Co-cultures were probed for urea synthesis, a marker of metabolic hepatocyte function, and albumin secretion, a marker of synthetic function. Media samples were collected daily and stored at 4°C for subsequent analysis for urea and albumin content. Urea synthesis was assayed using a commercially available kit (Sigma Chemical Co., kit No. 535-A). Reaction with diacetyl monoxime under acid and heat yields a color change detected at 540 nm. Albumin content was measured by an enzyme-linked immunosorbent assay (ELISA) using a horse-radish peroxidaase conjugated

antibody to albumin as described previously (Dunn et al, 1991). Rat albumin and anti-rat albumin antibodies were purchased from Cappel Laboratories (Cochranville, PA).

DNA analysis was also performed to estimate the size of cell populations. Since measurement of DNA content included both fibroblast and hepatocyte DNA, in some cases fibroblasts were growth-arrested (holding DNA content) to isolate changes in hepatocyte DNA. DNA analysis was adapted from a method of MacDonald and Pitt (1991). Cells were sacrificed at the indicated time of culture by washing with PBS, removal and immersion of wafer into PBS to eliminate dead cells underneath the substrate, and subsequent incubation with 0.05% (w/v) type 4 collagenase (Sigma) in Krebs's Ringer Buffer at 37° C for 30 min to release the cell layer from the underlying substrate. Next, cells were removed with a rubber policeman and the cell/collagenase mixture was removed. The substrate was washed with PBS which was then combined with the above solution. The resulting solution was combined with an equivalent volume of hepatocyte media for neutralization of collagenase, followed by centrifugation at 1000 RPM for 5 minutes. The supernatant was aspirated, and cells were resuspended in 2 mL PBS. Subsequently, the samples were frozen at -80°C for up to 1 month. Upon analysis, the frozen samples were rapidly thawed in a 37° C water bath to promote membrane rupture. Freeze-thaw protocols have been established as an effective way to rupture the cell membrane in order to gain access to cellular contents (Rago et al, 1990). To ensure complete cell lysis, samples were then sonicated using a probe sonicator (Branson) for 10 s at 4°C. Samples were vortexed and 20 µl samples were placed into a 96-well plate (NUNC, Denmark). Similarly, 20 µl of DNA standard (double stranded Calf Thymus DNA, Sigma) in PBS from 100 to 0 µg/mL were vortexed and placed on each plate. This volume was combined with 100µl salt/dye buffer (2 M NaCl, 10mM Tris, 1mM EDTA, 1.6 µM Hoechst 33258 (Molecular Probes, Eugene, OR)). Samples and standards were allowed to incubate with salt/dye buffer at room temperature in the dark for 30 min before reading on a Spectrofluorometer (Millipore, Bedford, MA) Excitation 360 nm, ½ bandwidth 40 nm, Emission, 460 nm, ½ bandwidth 40 nm.

Analysis of total DNA content in cultures with growth-arrested fibroblasts was conducted as follows. Fibroblasts were growth arrested by incubation with 10 µg/mL mitomycin C (Boehringer Mannheim) in media for 2h (reconstituted just prior to use) followed by three washes with media. Cells were trypsinized and 1.5 X 10<sup>6</sup> fibroblasts were counted with a hemocytometer and added to micropatterned hepatocyte cultures. Replicate cultures were either sacrificed 6 h after fibroblast seeding or after 9 days of co-culture and assayed for total DNA as described above.

### **4.3 Immunohistochemistry**

In order to visualize the spatial distribution of liver-specific functions in micropatterned hepatocytes, immunohistochemical techniques were utilized to stain intracellular albumin. Cultures were washed twice with PBS, fixed with 4 % paraformaldehyde in PBS for 30 minutes, and permeabilized for 10 min with 0.1% Triton in PBS. Endogenous avidin-binding activity of hepatic tissue was blocked by 20 minute incubations with 0.1% avidin and 0.01% biotin in 50 mM Tris-HCl respectively (Biotin Blocking System X590, DAKO, Carpinteria, CA). Endogenous peroxidase activity was blocked by 30 minute incubation with a hydroxgen peroxide and sodium azide solution (Peroxidase Blocking Reagent, DAKO). Rabbit anti-rat albumin antibodies (Cappell) were utilized with horse-radish peroxidase visualization by use of a biotinylated secondary antibody to rabbit IgG, streptavidin-labelled horse radish peroxidase, and hydrogen peroxide in the presence of 3-amino-9-ethylcarbazole as a substrate (Rabbit Primary Universal Peroxidase Kit #K684, DAKO).

### **4.4 Functional Bile Duct Staining**

Polarized hepatocytes with functional bile caniluculi can be visualized by use of a fluorescent dye that accumulates after excretion across the apical membrane. Thus, function of the biliary system was probed in micropatterned co-cultures using carboxyfluorescein diacetate (CFDA, Molecular Probes). Cultures were washed three times with media and incubated for 5 h with 2  $\mu\text{m}$  CFDA in an adapted method of LeCluyse et al (1994). Subsequently, cultures were washed again three times and examined microscopically. Digital images were obtained on a Nikon Diaphot microscope equipped with Hg lamp and excited at 470 nm excitation and 510 nm emission.

### **4.5 Image Acquisition and Analysis**

Digital image acquisition was conducted using a Nikon Diaphot microscope (Nikon) equipped with a Hg lamp and power supply (Nikon), light shuttering system (Uniblitz D122), CCD camera (Optitronics CCD V1470), and MetaMorph Image Analysis System (Universal Imaging). Image analysis on immunostained images was performed utilizing the thresholding function in MetaMorph and visual correlation with brightfield images.



## 4.6 Statistics and Data Analysis

Experiments were repeated two to three times with duplicate or triplicate culture plates for each condition. Two duplicate wells were measured for biochemical analysis. One representative experiment is presented where the same trends were seen in multiple trials but absolute rates of production varied with each animal isolation. Each data point represents the mean of three dishes. Error bars represent standard error of the mean. Statistical significance was determined using one-way ANOVA (analysis of variance) on Statistica (StatSoft) with Tukey HSD (Honest Significant Difference) Post-Hoc analysis with  $p < 0.05$ .

## 5. MECHANISTIC STUDIES

In Chapter 5, we present and discuss the results obtained from a number of studies aimed at investigating the mechanisms by which these two cell types interact. Experiments were performed to probe the modes of heterotypic cell-cell interaction: secreted factors (through use of conditioned media), cell contact (separated co-cultures), and diffusive versus convective transport of secreted factors (agitated cultures). Here we describe the methodology utilized in these experiments.

### 5.1 Conditioned Media

Conditioned media is the term used to describe media that has been incubated with a live cell culture, thereby 'conditioned' by secreted biochemical factors. Conditioned media experiments were performed in unpatterned configurations. Glass substrates were modified by aminosilane, glutaraldehyde, and collagen I as described in Chapter 3, resulting in collagen I immobilization over the entire wafer. Hepatocytes were seeded in 'hepatocyte media with serum' as described previously, at a density of 250,000 per P-60. Four different culture configurations were investigated. First, in order to control for baseline degradation of biochemical compounds in media at 37°C, hepatocytes were fed daily with 2 mL of media which had been previously incubated for 24 h in tissue culture plastic. Second, in order to examine the effects of fibroblast secreted products, hepatocytes were fed daily with 2 mL of media which had previously incubated for 24 h with (750,000 initially seeded) NIH 3T3-J2 cells on an unmodified glass wafer. Third, in order to probe the effects of fibroblast secreted products which require hepatocyte interaction for their up-regulation, hepatocytes were fed daily with 2 mL of media which had been previously incubated for 24 h with

a co-culture of (750,000 initially seeded) NIH 3T3-J2 cells and 250,000 hepatocytes on an, unpatterned, collagen-modified wafer. Last, in order to generate a 'positive control' for comparison, hepatocytes were co-cultured with NIH 3T3-J2 fibroblasts by the addition of 750,000 fibroblasts on day 2 of culture and fed with fresh media daily. Media was collected daily and stored at 4°C.

## 5.2 Physical separation of cell types

Co-cultures were performed in a configuration that would allow diffusion of soluble factors yet eliminate signaling via cell contact. These separated co-cultures consisted of two distinct cell populations separated by a region of 'bare' substrate. Cell populations then grew together and could be probed for liver-specific functions at various designated time points. Hepatocytes and fibroblasts were separated within a co-culture by the following general protocol: placement of a polymer annulus on glass substrate, surface modification of glass within the annulus by adsorption of collagen I, attachment of hepatocytes to central, collagen-immobilized region, 'capping' of hepatocyte population during fibroblast seeding to prevent access of fibroblasts to top surface of hepatocytes, and removal of cap and annulus. Differential spacing was achieved by variation in annulus width resulting in identical inner diameter (and therefore size of hepatocyte island) and larger outer diameter (resulting in larger separation between cell populations). Figure 2.2 depicts a schematic overview of method.

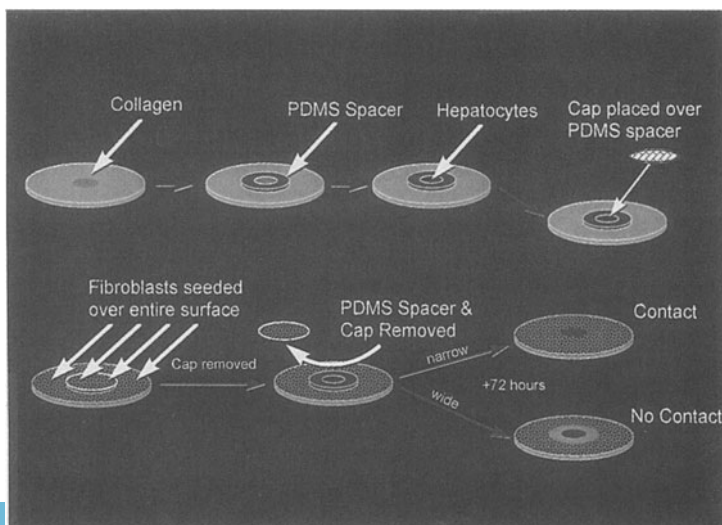


Figure 2.2. Schematic of Method for Separation of Cell Populations

Annuli were fabricated with polydimethylsiloxane (PDMS) (Sylgard 184, Dow Corning, Lansing, MI). Stock sheets of 500  $\mu\text{m}$  thickness were prepared by casting polymer solution (mixed as described by the manufacturer) in polystyrene tissue culture plastic for 2 h at 65°C. Annuli were fabricated with inner diameter of 0.6 cm and various outer diameters using disposable skin punch biopsy cutting tools. To limit potential cytotoxicity, PDMS annuli were then coupled to collagen I with aminoethylaminopropyltrimethoxysilane and glutaraldehyde as previously described. 'Caps' were fabricated from sheets of polyethylene terephthalate (PET) by use of a standard paperpunch to generate 0.6 cm disks from 7 mil thickness mylar film (Kodak). Discs were soaked in 70% ethanol in water for 2 h followed by rinsing in media.

Annuli were affixed to clean, 2" diameter, borosilicate wafers, and subsequently 'heat-fixed' to prevent detachment via three consecutive exposures to a heat gun at a distance of 10 cm for 5 s. Collagen adsorption to the inner circular region of exposed glass was achieved by addition of 200  $\mu\text{l}$  of collagen I: water in 1:1 ratio, pH 5.0, and incubation at 37°C for 45 min. Wafers were then sterilized overnight in 70% ethanol in water, rinsed in water, exposed to 0.05% bovine serum albumin and rinsed with serum-free hepatocyte media (as previously described). Hepatocytes were seeded in serum-free media as previously described and allowed to spread overnight.

The following day, PET caps were applied to PDMS annuli under sterile conditions, growth-arrested (described in Section 2.3) fibroblasts were seeded and allowed to attach for 1 h, rinsed twice with 'fibroblast media', followed by removal of annuli and cap. The separated co-culture was rinsed once more with fibroblast media and fibroblasts were allowed to spread for 6 h prior to replacement of fibroblast media with 'hepatocyte media with serum'. Control co-culture was performed by standard micropatterned co-culture methods described previously on 0.68 cm hepatocyte island patterns (see Section 2). Briefly, glass was modified by immobilization of collagen I, hepatocytes were seeded followed by fibroblasts. No cap or polymer annulus was applied in this condition.

Finally, absence of overlying fibroblasts on hepatocyte island was confirmed using fluorescent labels CMFDA (chloromethylfluorescein diacetate, C-2925, Molecular Probes) and CMFTR (chloromethylbenzoylaminotetramethyl rhodamine, C-2927). Cells were loaded by incubation in 25  $\mu\text{M}$  dye in media for 45 min, rinsed, and incubated for 30 min prior to a final rinse. Fibroblasts were then trypsinized as previously described and utilized in the above protocol. Separated co-cultures were rinsed and imaged 7 h after initial fibroblast seeding.

### **5.3 Agitation**

In order to examine the influence of fluid convection on transport of potential biochemical mediators to patterned hepatocytes, co-cultures were conducted in static and 'shaken' conditions. One representative pattern was utilized for this study. Micropatterned co-cultures were generated utilizing 490  $\mu\text{m}$  hepatocyte islands with 1230  $\mu\text{m}$  center-to-center spacing as described previously. 750,000 NIH 3T3-J2 fibroblasts were added 24 h after initial hepatocyte seeding. Replicate cultures were then cultured under two different conditions: (1) under static culture conditions as previously described and (2) under 'shaken' conditions by culturing on a rocking platform at approximately 1 Hz within a separate incubator. Media (2 mL) was replaced daily. Cultures were fixed and stained for intracellular albumin at indicated times.

## **6. OPTIMIZATION STUDIES**

Incorporation of micropatterned co-cultures in a bioreactor configuration presents a paradox. Fibroblasts are required to induce liver-specific functions in hepatocytes, yet they occupy surface area that would otherwise be available for attachment of additional hepatocytes. Thus, we conducted experiments that probed the impact of reduction of fibroblast number. The versatility of microfabrication allowed these experiments to be conducted while preserving the heterotypic interface, therefore the effect of fibroblast number on hepatocyte function was examined in isolation. These data were compared to cultures with similar cellular constituents in unpatterned (randomly-distributed) configurations to assess the impact of controlling the heterotypic interface.

### **6.1 Reduction in fibroblast number**

Reduction of fibroblast number with preservation of heterotypic interface was achieved by reduction of surface area dedicated to fibroblasts in each set of wafers. This was accomplished by reducing the total patterned area by using a polymer mask to cover certain regions, while also reducing the island spacing. In this manner, the total number of patterned hepatocyte islands per wafer as the heterotypic interface was preserved between various cultures of decreasing numbers of fibroblasts (Figure 2.3). Micropatterned spatial configurations were spacing modifications of one, representative hepatocyte island diameter, 490  $\mu\text{m}$ - notable for the lack of cellular reorganization and high level of hepatic function. Chrome, 5" masks were obtained with

hexagonally packed ‘holes’ of 490  $\mu\text{m}$  diameter and four different center-to-center spacings of 1230  $\mu\text{m}$ , 930, 650, and 560  $\mu\text{m}$  (Advanced Reproductions, N. Andover, MA). Masks were used to obtain photolithographic patterns over the entire surface of a 2” diameter borosilicate wafers. Wafers were processed as described previously with immobilization of aminoethylaminopropyltrimethoxysilane, glutaraldehyde, and collagen I, sterilization, and rinse in sterile water.

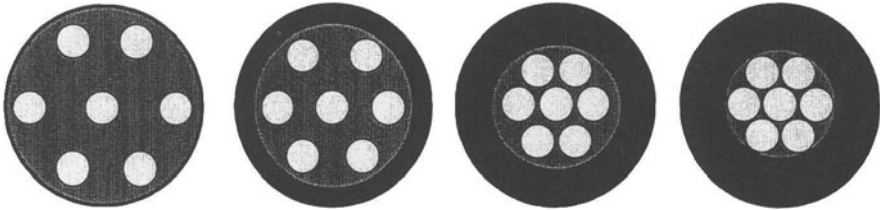


*Figure 2.3.* Schematic of Strategy for Minimization of Fibroblast Number. Lighter, smaller circles indicate islands of hepatocytes surrounded by fibroblasts. Black region indicates bare glass.

In order to reduce the fraction of each patterned wafer which would promote cellular micropatterning, portions of wafers were masked with polydimethylsiloxane (PDMS) elastomer prepared as follows. PDMS was polymerized as described previously (Section 5.2) to create relatively thin elastomeric films (< 1 mm thickness). PDMS was then cut into annuli of the following dimensions (inner diameter, outer diameter): 1.5”,2”; 1.06”,2”; 0.94”,2” corresponding to center-to-center spacing of 560, 650, and 930  $\mu\text{m}$ , respectively. The largest center-to-center spacing (1230  $\mu\text{m}$ ) did not require a PDMS annulus because the entire wafer was intended to be available for cell adhesion. These annuli were modified with previously described silane chemistry and 0.05% bovine serum albumin (BSA) in water for two reasons: (1) to prevent potential toxicity of unmodified polymer to hepatocytes, and (2) bovine serum albumin was utilized instead of collagen I because it was desirable to deter hepatocyte attachment to the surface of annuli during cell seeding, leaving more hepatocytes for attachment to collagen-modified micropatterned areas. BSA is known to deter hepatocyte attachment in vitro (Bhatia et al, 1994). Annuli were then sterilized in 70% ethanol, dried, mounted on corresponding collagen-micropatterned wafers, and ‘heat-fixed’ with a hot air gun to prevent detachment of elastomeric masks.

Composite PDMS/micropatterned glass wafers were then utilized for cell culture as described previously- sterilized, rinsed, treated with BSA,

rinsed, and seeded repeatedly with hepatocytes in serum-free media. The following day, growth-arrested fibroblasts (described in Section 2.3) were seeded as follows:  $1.5 \times 10^6$  for 1230  $\mu\text{m}$  spacing,  $1.3 \times 10^6$  for 930  $\mu\text{m}$ , and  $0.88 \times 10^6$  for 650  $\mu\text{m}$ , and  $0.59 \times 10^6$  for 560  $\mu\text{m}$  spacing. The fibroblasts attached with equal efficiency to both PDMS and exposed glass; therefore, these seeding densities corresponded to fibroblast number in the central patterned region of  $1.5 \times 10^6$ ,  $0.75 \times 10^6$ ,  $0.25 \times 10^6$ , and  $0.125 \times 10^6$ . Finally, the next day PDMS annuli (with adherent fibroblasts) were removed resulting in micropatterned co-cultures with the same number of hepatocytes and heterotypic interface and fibroblast:hepatocyte ratios of 6:1, 3:1, 1:1, and 0.5:1.

## 6.2 Randomly Distributed Co-Cultures

In order to achieve a reduction in fibroblast number without controlling the heterotypic interface, randomly-distributed cultures were performed with varying fibroblast:hepatocyte ratios but no attempt at micropatterning or polymer masking was made. Reduction in fibroblast number was achieved by seeding progressively fewer fibroblasts on each set of wafers. A thorough description of wafer preparation and cell seeding follows.

Glass wafers were first modified with collagen I by washing in Chem-Solv Detergent (Mallinckrodt, Paris, KY) prepared as directed by the manufacturer, followed by 2 rinses in water, and exposed to aminoethylaminopropyltrimethoxysilane, glutaraldehyde, and collagen I as described previously. In order to treat the immobilized collagen in the same fashion as collagen on the micropatterned wafers, discs were subsequently sonicated in acetone for a fixed time (2-5 min), rinsed in water, sterilized in 70% ethanol, rinsed in sterile water, treated with 0.05% sterile BSA in water, and finally rinsed in water followed by serum-free media. Since numbers of attached hepatocytes in micropatterned conditions is dictated by modified surface area, micropatterns were seeded in serum-free conditions to maximize specificity of attachment. In this case, however, randomly distributed cultures are on uniformly modified glass; therefore, number of attached hepatocytes is dictated by number of viable, seeded cells. As a result, hepatocytes were seeded in serum-containing media to maximize efficiency of attachment. The next day, growth-arrested fibroblasts (Section 2.3) were trypsinized, counted with a hemocytometer, and plated in 3 mL of fibroblast media. After 24 h, media was replaced with 2 mL of 'hepatocyte media with serum' and subsequently changed daily.

## 7. SUMMARY

This chapter is intended to serve as a reference for the experimental methods utilized in subsequently described studies. We have presented techniques for fabrication, characterization, and analysis of micropatterned cultures composed of two distinct cell types. In many cases, these techniques may be generalized to different substrates, immobilized biomolecules, methods of immobilization, pattern configuration, and/or choice of cell types.

## Chapter 3

# Characterization of Microfabricated Substrates and Co-Cultures

### 1. OVERVIEW

The methods described in the previous chapter were utilized to create micropatterned cultures of two distinct cell types and characterize these cultures for subsequent experimentation. We have used photolithography to pattern biomolecules on glass substrates which mediate cell adhesion of hepatocytes (liver cells). Subsequently, fibroblasts (another cell type typically found in supporting structures of the body) were attached to the remaining unmodified areas to allow creation of micropatterned co-cultures. This methodology provides a versatile tool to control and vary cell-cell interactions for studies on cell function. Since the methodology presented here represents significant modification of many existing techniques, we initially performed surface characterization studies on substrates in the absence of cells to validate our ability to obtain spatially-defined surface chemistries. Subsequently, the ability to micropattern single cell cultures, co-cultures of two different cell types, and the ability to vary cell-cell interactions was investigated. Microfabricated substrates were characterized at various stages of processing: after photoresist development, after collagen immobilization, and after cell seeding. In this chapter, the results of these characterization studies are presented, analyzed, and discussed in detail.



## 2. CHARACTERIZATION OF CELL-FREE SUBSTRATES

Substrates were first characterized in the early stages of processing- prior to collagen or cell exposure (See Figure 3.1). Topological and spatial uniformity of photoresist patterns were assessed using profilometry and autofluorescent properties of photoresist. The photoresist coating was found to be approximately 1.35  $\mu\text{m}$  in thickness using the specified spin-coating parameters (see Figure 3.1B). Furthermore, the thickness of photoresist varied  $<5\%$  within each scan. Autofluorescence of photoresist was utilized to examine integrity and distribution of photoresist prior to and during processing. Figure 3.1A and 3.1B demonstrates autofluorescent regions corresponding to  $\sim 1 \mu\text{m}$  variations in thickness. Absence of any contaminant fluorescence in the dark lanes indicates complete, uniform removal of exposed photoresist during development.

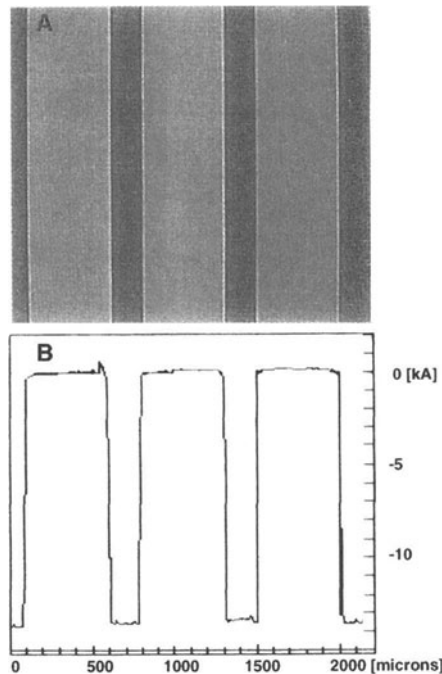


*Figure 3.1* Characterization of Photoresist. A. Fluorescent micrograph of autofluorescent photoresist. B. Profilometry scan of surface of photoresist pattern.

In order to verify regional aminoethylaminopropyl trimethoxysilane (AS) modification of borosilicate, substrates were exposed to AS followed by

removal of photoresist. Aminosilane modification has been previously reported to modify the three-phase contact angle of water with the surface (Lom et al, 1993); therefore, the perimeter of a single water droplet should display microscopic undulations on patterns of varying hydrophilicity. These undulations are exhibited in Figure 3.2 where 20  $\mu\text{m}$  AS modified lanes exhibit differential wetting properties relative to the adjacent 50  $\mu\text{m}$  unmodified lanes. Therefore, selective AS modification of exposed glass was verified in the pattern of the original 20  $\mu\text{m}$ /50  $\mu\text{m}$  striped photoresist pattern, indicating the ability for photoresist to serve as a 'chemical mask' to AS modification of underlying glass.

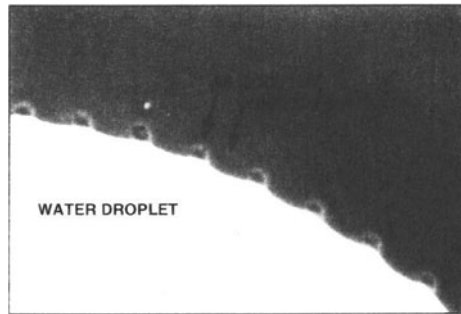


Figure 3.2. Differential Hydrophilicity of Aminosilane Modified Pattern. Water droplet on 20  $\mu\text{m}$  aminosilane-modified/50  $\mu\text{m}$  bare glass lanes

Collagen immobilization via glutaraldehyde derivatization of patterned AS surfaces was also characterized. The fluorescence micrographs in Figure 3.4A show the results of indirect immunofluorescent staining of areas of presumed collagen immobilization. Fluorescent regions, corresponding to regions of collagen localization, were patterned uniformly with spatial resolution on the micron level. Furthermore, fluorescent patterns corresponded to initial photoresist patterns without evidence of undercutting. More importantly, despite processing in acetone and 70% ethanol, collagen retained sufficient immunoreactivity for antibody binding.

Collagen-derivatized surfaces were also analyzed with AFM (Figure 3.4B) to determine differences in topology between unmodified and modified borosilicate. Modified regions with a width of 20  $\mu\text{m}$  were found to have an average height of 4 nm above the unmodified, 50  $\mu\text{m}$  lanes. These data can be utilized to approximate the number of collagen monolayers atop AS.

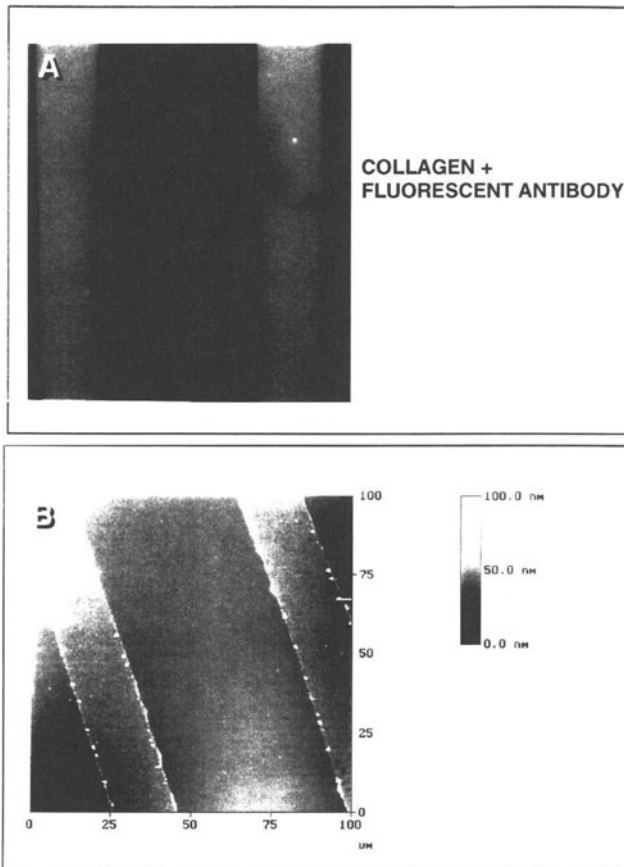


Figure 3.3. Surface Characterization of Micropatterned Collagen. A. Fluorescent micrograph of indirect immunofluorescent stain of collagen I. B. Atomic force micrograph of 50  $\mu\text{m}$  lanes of borosilicate alternating with 20  $\mu\text{m}$  lanes of collagen-modified glass.

### 3. CHARACTERIZATION OF MICROPATTERNED CULTURES

Given the ability to reproducibly utilize photoresist patterns to generate immobilized collagen patterns, the applicability of these techniques to cellular micropatterning was examined. Seeding of the first cell type, hepatocytes, resulted in localization to collagen-derivatized regions and normal polygonal morphology. The cellular configurations were dictated by the positioning of collagen on glass which was in turn controlled by the

choice of chromium mask in the microfabrication procedure (Figure 3.4, 3.5A,B). Furthermore, hepatocytes conformed to the edges of the collagen pattern on the modified glass. Typical hepatocyte diameter in suspension is 20  $\mu\text{m}$  whereas upon attachment and unconstrained spreading, cell diameters increases to 30-40 microns. Therefore, after attachment to 20  $\mu\text{m}$  lines, cells were observed to elongate in the axial direction upon spreading (Figure 3.5B). Similar cytoskeletal changes were observed in cells on corners of larger patterns or on the perimeter of circular patterns.

The versatility of this technique is seen in representative phase-contrast micrographs in Figures 3.4 and 3.5. Initial hepatocyte patterns of 200 $\mu\text{m}$  and 20  $\mu\text{m}$  (3.5 A,B) were modified by the addition of fibroblasts in serum-containing media. Fibroblasts were observed to localize to unmodified (glass) regions of patterned substrates resulting in micropatterned co-cultures of 200 $\mu\text{m}$ /500 $\mu\text{m}$  and 20 $\mu\text{m}$ /50 $\mu\text{m}$  (3.5C,D). The grating pattern utilized was chosen for its illustrative potential; however, in principle, co-cultures can be achieved in any desired configuration. Thus, our approach is clearly adaptable to both micropatterning of single cell cultures and co-cultures of two different cell types.

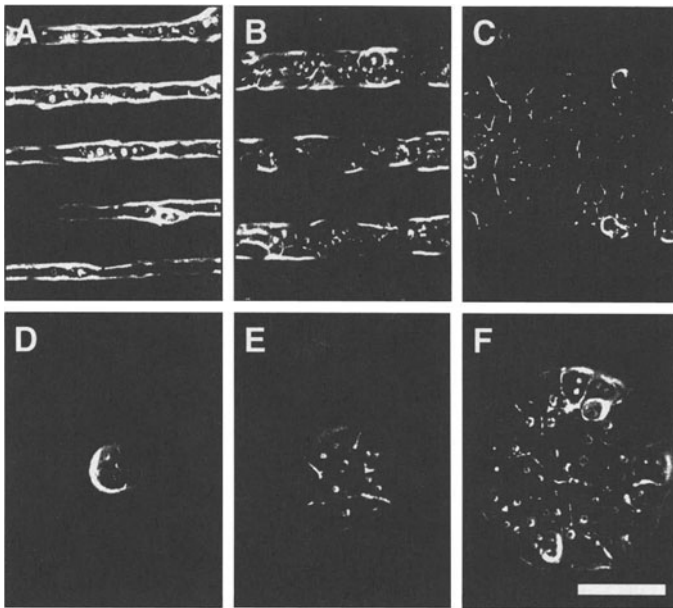
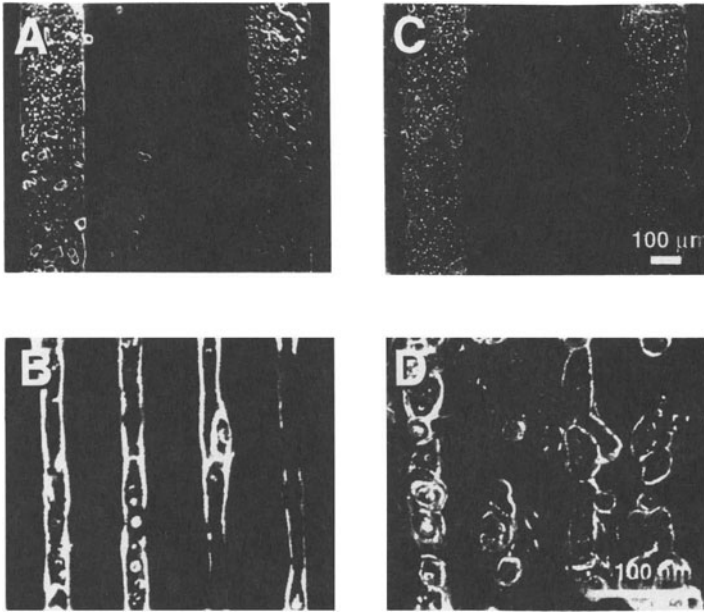


Figure 3.4. Phase Contrast Micrographs of Micropatterned Hepatocytes. Hepatocytes attached to linear strips of width: A. 20  $\mu\text{m}$ , B. 50  $\mu\text{m}$ , and C. 200  $\mu\text{m}$ , and circular patterns of diameter D. 50  $\mu\text{m}$ , E. 100  $\mu\text{m}$ , and F. 250  $\mu\text{m}$ . Scale bar indicates 100  $\mu\text{m}$ .



*Figure 3.5.* Micrographs of Micropatterned Hepatocytes and Co-Cultures with 3T3 Fibroblasts. Hepatocytes attached to A. 200  $\mu\text{m}$  and B. 20  $\mu\text{m}$  lanes. Co-cultures of hepatocytes and fibroblasts on C. 200/500  $\mu\text{m}$  and D. 20/50  $\mu\text{m}$  patterns.

Spreading of the primary cell type typically resulted in negligible residual sites of collagen-derivatization. Therefore, attachment of the secondary cell type would theoretically be limited either to unmodified glass or the surface of the primary cell type. In a separate set of studies, we determined that 3T3 fibroblasts do not undergo significant attachment to hepatocyte surfaces by performing plating experiments of fibroblasts on monolayers of hepatocytes which showed no attachment even after a 4 h incubation (data not shown). In addition, fibroblast attachment and spreading on glass was characterized by seeding cells in serum-containing media on glass coverslips where they were observed to attach and spread with high efficiency within 4 h (data not shown).

Indirect immunofluorescence was utilized to selectively stain cell populations and aid in visual discrimination between different cell types. Figure 3.6 compares presence of cytokeratin (A,B), an intermediate filament expressed in hepatocytes but absent in mesenchymal cells, to F-actin (C,D),

a cytoskeletal protein present in all mammalian cells. The figure also contains a comparison of a patterned co-culture of 200  $\mu\text{m}$ / 500 $\mu\text{m}$  (A,C) compared to a 'randomly distributed' (see Chapter 2) co-culture (B,D) with identical attached cell numbers of both cell populations. Of note, is the level of homotypic (between cells of the same type) hepatocyte interaction in Figure 3.6A, a 200  $\mu\text{m}$  stripe, versus Figure 3.6B, a random distribution of cells. Hepatocytes in Figure 3.6A had primarily homotypic contacts whereas those in 3.6B had predominantly heterotypic (between cells of different types) contacts. Furthermore, the distribution of heterotypic interaction over a patterned cell population is observed to be greatly reduced over random co-cultures where hepatocytes are shown to be present in single cell islands, doublets, and triplets (Figure 3.6B).

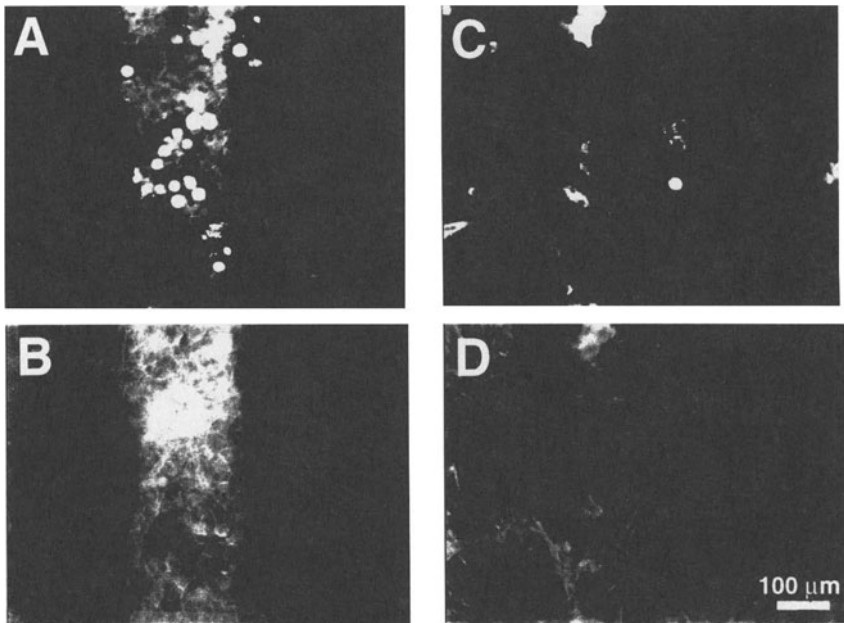


*Figure 3.6.* Immunofluorescent Staining of Micropatterned Co-Cultures. Micrograph of indirect immunofluorescence of cytokeratin in A. Micropatterned and B. Randomly-distributed co-cultures. F-actin localization in C. Micropatterned and D. Randomly-distributed co-cultures.

To quantitatively describe the extent of heterotypic contact, we used image analysis and perimeter tracing to define the fractional cell perimeter engaged in heterotypic cell contact as  $\chi$  (see Chapter 2). Figure 3.7 schematically depicts sample perimeter tracings (black lines) with highlighted interfaces of heterotypic contacts corresponding to hepatocytes in a

digitally-acquired phase micrograph. This particular pattern (200 $\mu\text{m}$ /500 $\mu\text{m}$ ) has very little heterotypic contact as is visually observed; therefore, the average  $\chi$  over the population is small due to the majority of cells with  $\chi=0$ .

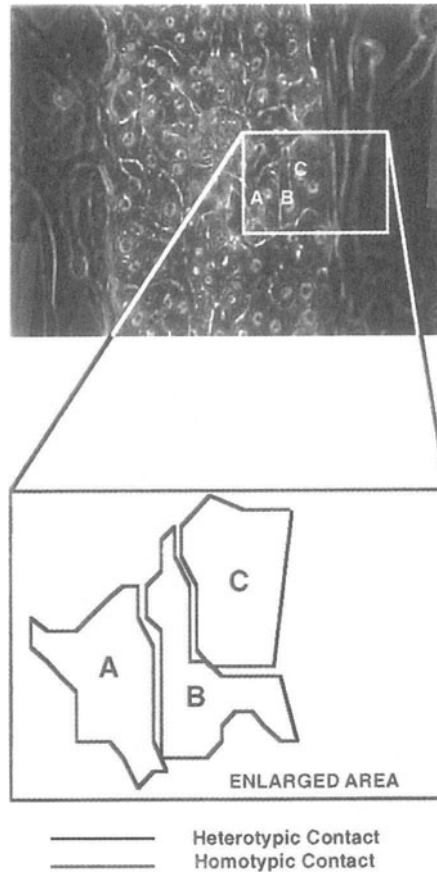


*Figure 3.7.* Schematic of Method for Determining,  $\chi$ , Heterotypic Interaction Parameter. Cells were outlined as shown using image analysis software

In Figure 3.8, we demonstrated the ability to vary the mean value of  $\chi$  over a cell population from 0.7 in the randomly distributed culture to 0.08 using micropatterning. Moreover, different patterns (20/50) produce distinct mean values of  $\chi$  ( $\chi = 0.55$ ).

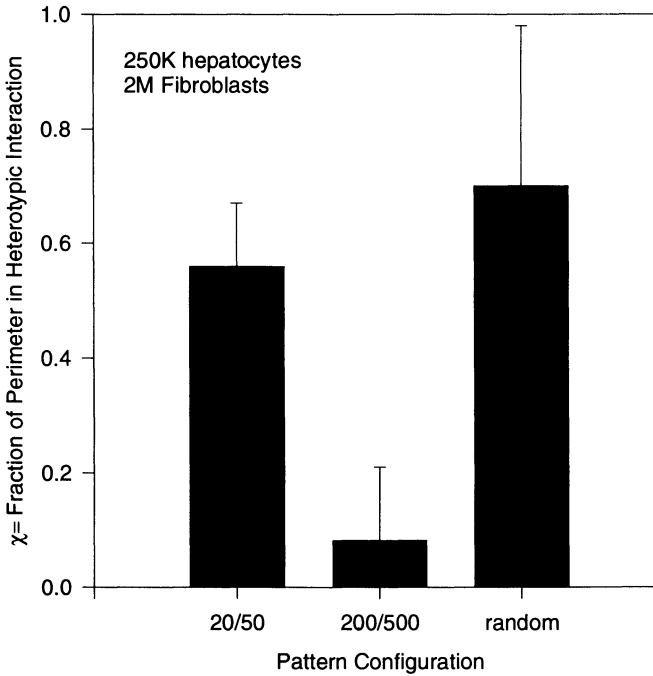


Figure 3.8. Average Heterotypic Interaction in Co-Cultures

Variations of  $\chi$  from the mean were also examined for randomly distributed cultures as compared to defined patterns (20/50). As observed microscopically in Figure 3.6B, hepatocytes in randomly distributed cultures experience heterogeneous microenvironments- single hepatocytes, doublets, and multicellular aggregates can be observed within a given culture. Quantitative analysis of population distributions corroborate the variability in  $\chi$  in randomly distributed cultures as compared to micropatterns (20/50 and 50/50) which exhibited a relatively small variance around the mean value of  $\chi$  (Figure 3.9). Thus, variations in cellular microenvironment, both in amount and variability, were achieved without varying the numbers of cells in each sub-population.



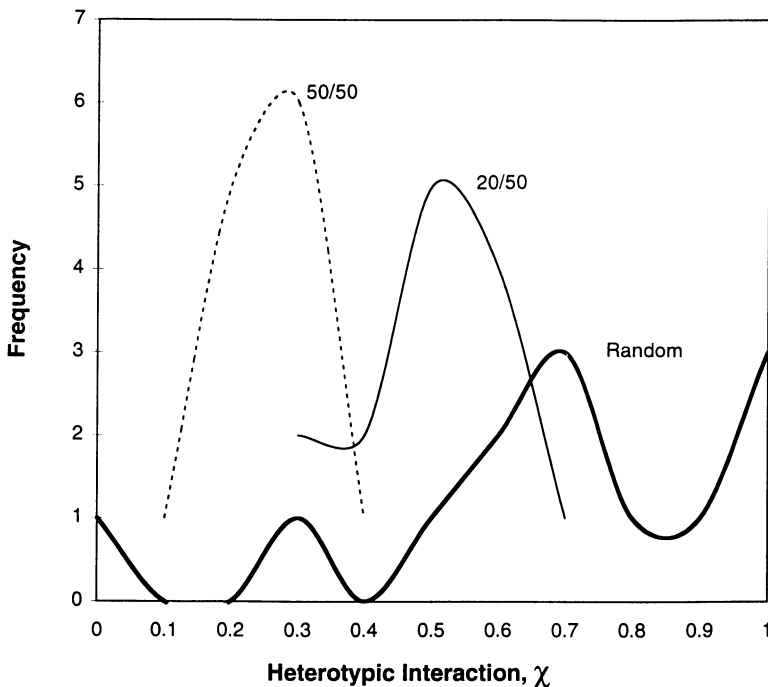


Figure 3.9. Distribution of Heterotypic Interactions,  $\chi$ , in Co-Cultures

#### 4. DISCUSSION

Traditional co-culture systems have been limited by the inability to vary cell local seeding density independently of the cell number as well as inherent variations in the distribution of cell contacts over a population of cells. We have developed a versatile technique for the micropatterning of two different cell types based on existing strategies for surface modification with aminosilanes linked to biomolecules and the manipulation of serum content of cell culture media. This co-culture technique allows the manipulation of the initial cellular microenvironment without variation of adhered cell number. Specifically, we were able to control both the degree and type of initial cell-cell contact. Differences in homotypic and heterotypic interaction were demonstrated allowing variations in exposure to cell-surface receptors, locally secreted extracellular matrix, and local concentrations of soluble factors.

The patterning methodology utilized in this study represents significant modification of many existing techniques. Specifically, our

approach differs from other patterning techniques in the method and timing of surface modification AS. AS was applied after photoresist patterning but before photoresist lift off. This differs from Lom et al (1993) who apply AS before photoresist application. The microfabrication facility utilized for the manufacture of these substrates, like many others, restricts presence of class III-V compounds for quality control of semiconductor fabrication; therefore, AS modification of borosilicate cannot be performed prior to photoresist application. In contrast, other groups (Stenger et al, 1992; Kleinfeld et al, 1988) typically modify exposed glass with alkylsilanes in solvents which do not attack photoresist, such as chlorobenzene. Subsequently, photoresist is lifted-off in acetone and AS is deposited in ethanol on newly exposed glass. In these systems, incubation with biomolecules, such as horseradish peroxidase, results in adsorption to both regions which becomes specific after denaturation of non-specifically bound protein in 8M urea. Many proteins, such as collagen, undergo irreversible adsorption (Deyme et al, 1986) and will therefore not desorb from unmodified regions. We preserved the integrity of the photoresist throughout the surface modification process and removed the photoresist after the deposition of collagen. This was achieved by deposition of AS in water, which does not normally attack photoresist. AS is known to oligomerize in aqueous solution (Arkles et al, 1991), but is stable at least for a period of hours. In this way, we utilized photoresist to mask the borosilicate from non-specific protein adsorption and did not need to rely on protein denaturation and desorption nor on AS deposition prior to photoresist patterning.

Atomic force microscopy was utilized to approximate the depth of the immobilized collagen layer. Modified regions were ~4 nm above the unmodified regions. AS molecules have been estimated to have a height of 1.2 nm end-to-end (Lom et al, 1993). In the helical configuration, collagen I fibrils have dimensions of 300 nm in length and 1.2 nm in diameter (Darnell et al, 1990). These data suggest that we have only 1-2 layers of collagen fibrils, configured lengthwise, despite the high concentration of collagen solution utilized in the immobilization procedure, corresponding to an upper limit of  $0.1 \mu\text{g}/\text{cm}^2$  per monolayer of 'side-on' packed fibrils (Deyme et al, 1986). Therefore, achievable collagen surface concentrations are within an order of magnitude those observed in adsorbed collagen systems ( $0.37 \mu\text{g}/\text{cm}^2$ ) (Deyme et al, 1986). Another consideration is the bioactivity of biomolecules after exposure to acetone and ethanol. We have demonstrated preservation of bioactivity of collagen I via cell attachment and spreading as well as by antibody binding for indirect immunofluorescence. Others have shown functional integrity of laminin, fibronectin, collagen IV, and bovine serum albumin (Lom et al, 1993).

Proteins sensitive to acetone may require adaptation of the photoresist lift-off procedure.

In the described technique, selective cell attachment to immobilized collagen was enhanced by adsorption of bovine serum albumin to the surface to deter non-specific adhesion. This has been shown to be effective for hepatocytes, neuroblastoma cells (Lom et al, 1993; Miyamoto et al, 1993; Bhatia et al, 1994), and many antibody-antigen interactions. In contrast, albumin adsorption to (mono)aminosilane on fluorinated ethylene propylene films has been shown to have the opposite effect of mediating attachment of aortic endothelial cells (Ranieri et al, 1993); therefore, this aspect of the procedure may require optimization for generalization to other cell types.

Using primary rat hepatocytes and 3T3 fibroblasts, we demonstrated the ability to vary initial heterotypic ( $\chi$ ) interactions over a wide range while preserving the ratio of cell populations in culture. Thus, co-culture interactions may be manipulated in an entirely new dimension. In addition, micro-patterned co-cultures were observed to have less variation in the level heterotypic contacts ( $\chi$ ) than random co-cultures. Therefore, measurement of macroscopic biochemical quantities in micro-patterned co-cultures will be better representations of specific cell-cell interactions than those seen in random co-cultures.

In general, this methodology for micropatterning co-cultures can also be applied to other techniques of patterning biomolecules, such as self-assembled monolayers. In addition, three-phase co-cultures can be theoretically established by patterning of two different, cell-specific biomolecules. The versatility of the technique is, however, limited by a number of experimental constraints. First, this methodology only allows manipulation of initial culture conditions. Motile and mitotic cells will eventually intermix although the time scale of interest may not exclude meaningful experimentation. A variety of strategies to prevent this intermixing could be explored including cytoskeletal agents (cytochalasins, phalloidin), topological modification of the surface (i.e. seeding cells in grooves), and mitotic agents (mitomycin C). These approaches may be tailored to each culture system to minimize the degree of deviation from the initial pattern. Indeed, we will utilize mitomycin C in subsequent chapters specifically to reduce the contribution of fibroblast growth to changes in total DNA.

## 5. SUMMARY

In summary, we have developed a simple, versatile technique for controlling homotypic versus heterotypic interactions of at least two cell

types in culture, by modification of existing micropatterning technologies and utilization of serum-protein adsorption to facilitate cell attachment. We have shown that one can vary  $\chi$  (heterotypic interface) without changing the number of cells in each sub-population and therefore the ratio of cell types in a given culture. In the next Chapter, we use this methodology to evaluate the role of heterotypic interactions in modulation of liver-specific functions.

## Chapter 4

# Functional Analysis Of Micropatterned Co-Cultures

### 1. OVERVIEW

Communication between distinct cell types or 'heterotypic cell-cell interaction' is central to the function of many organ systems. A common theme for heterotypic cell-cell interactions is the interaction of parenchymal cells (the functional cell of an organ) with stromal neighbors (typically components of supporting organ structures). Often this interaction results in modulation of cell growth, migration, and/or differentiation of either cell type. These interactions are of fundamental importance in embryonic development, and adult liver, skin, vasculature, muscle, and hematopoietic physiology. In some cases, studies on parenchymal interaction with supporting stroma have led to important *in vitro* systems for expansion and differentiation of human cells for therapeutic applications (bone marrow-Trentin, 1989; and skin- Boykin and Molnar, 1992). These complex interactions are also implicated in normal physiology of repair and regeneration as well as in the dysregulated growth of cancer (Goldberg and Rosen, 1995). Further understanding of how cell-cell interactions modulate tissue function will allow us to gain fundamental insight into mammalian physiology as well as suggest approaches which will allow the manipulation of tissue function *in vitro* for therapeutic applications.

The diversity of cellular signaling mechanisms has made quantitative study of the effects of cell-cell interaction on tissue function difficult. These include a complex interplay between soluble factors, insoluble extracellular matrix, and transmembrane cellular proteins as well as second-order signals such as co-receptors, matrix-immobilized growth

factors, and cooperative cellular signals inherent to multicellular systems. In Figure 1.6, we reviewed some conventional model systems that have been utilized to study key aspects of cell-cell interactions. Despite the apparent utility of such model systems, these approaches are limited in their scope due to the fundamental inability to independently vary 'local' cell-cell interactions and examine their effects on cellular function.

We developed and characterized a method that would allow reproducible control over local cellular microenvironments (Chapters 2 and 3). Using these techniques, the effects of homotypic and heterotypic cell interaction on cellular phenotype *in vitro* can be examined. In this chapter, we designed a series of micropatterned co-cultures that allowed us to independently control heterotypic interactions in order to gain some insight into how local tissue microenvironments modulate bulk tissue function. Specifically, we tested the hypothesis that the same cellular constituents, when rearranged spatially, would produce variations in the functionality of the resultant tissue.

The experimental design for this study (described in detail in Chapter 2) allowed the generation of micropatterned co-cultures with variations in heterotypic interface, yet identical surface area (i.e. cell numbers) dedicated to both hepatocyte and fibroblast adhesion (Figure 4.1). Five different configurations, consisting of hepatocyte islands of various sizes and center-to-center spacing, ranged from maximal heterotypic interface (smallest islands) to minimal heterotypic interface (single island). The resultant micropatterned co-cultures were characterized for expression of liver-specific function by use of markers of bulk tissue function (albumin and urea synthesis in media), localized markers of tissue function (intracellular albumin immunostaining, bile duct excretion), and total cell number (approximated by DNA content).

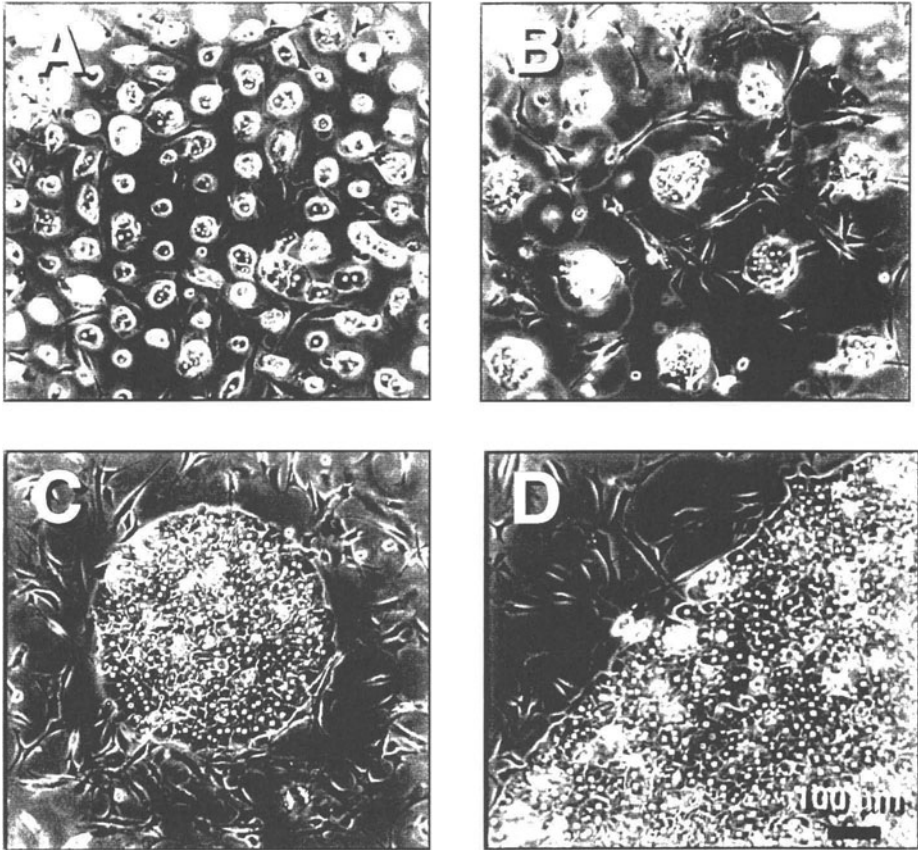


*Figure 4.1.* Phase Contrast Micrographs of Micropatterned Co-Cultures With Varying Heterotypic Interface But Similar Cell Numbers. A. 36 B. 100 C. 490 and D. 6800  $\mu\text{m}$  hepatocyte islands, background fibroblasts.

## 2. CHARACTERIZATION OF INITIAL CELL DISTRIBUTION

All 5 micropatterns were designed to have similar levels of hepatocyte-adhesive surface area ( $2.5 \text{ cm}^2$ ), which should ultimately correspond to identical number of attached hepatocytes. Variations in spatial configurations were utilized to generate differences in total perimeter of hepatocyte islands from 5.6 cm to 2800 cm, which, upon addition of fibroblasts, should correspond to variations in the total heterotypic interface.

Micropatterns ranged from many single hepatocyte islands of 36  $\mu\text{m}$  diameter to a single island of 17.8 mm diameter (Figure 4.1). Micropatterned hepatocytes were found to adhere predominantly to collagen-modified areas in all 5 conditions with close agreement between theoretical and observed values for total initial hepatocyte island perimeter (data not shown).

To verify similar numbers of attached hepatocytes across various spatial configurations, we measured DNA content of micropatterned hepatocyte cultures 24 h after hepatocyte seeding (i.e. prior to fibroblast seeding). All cultures had statistically similar levels of DNA ( $8 \pm 1.8 \mu\text{g}$ ) with the exception of increased DNA content ( $18 \pm 3.3 \mu\text{g}$ ) on the smallest island (36  $\mu\text{m}$  diameter) micropatterns. The smallest islands were designed to produce single cell islands. The dimensions of these islands (36  $\mu\text{m}$  diameter) was chosen to correspond with the experimentally determined projected surface area of a single, spread hepatocyte on immobilized collagen I of  $1000 \mu\text{m}^2$  (data not shown); however, isolated rat hepatocytes have a diameter of approximately 20  $\mu\text{m}$ , allowing the potential for individual islands to retain more than one hepatocyte upon seeding with a concentrated cell suspension. In addition, hepatocytes have been shown to have an increased mitotic index at low seeding densities (Nakamura et al, 1983) which may have contributed to increased hepatocyte DNA in this condition. To distinguish between increased cell number as compared to increased ploidy, image analysis of one thousand 36  $\mu\text{m}$  micropatterned islands was completed at 6 h after initiation of cell seeding. This analysis demonstrated more than one cell per island in 57 % of cases with an average of  $1.9 \pm 1.2$  cells per island. Therefore, we concluded that increased DNA was due to increased hepatocyte number on the smallest pattern.

Addition of 3T3-J2 fibroblasts to micropatterned hepatocytes resulted in micropatterned co-cultures with marked alterations in initial heterotypic interface despite similar numbers of fibroblasts and hepatocytes across conditions. Phase contrast micrographs of 4 of the 5 configurations are shown in Figure 3.1 demonstrating the significant variation in hepatocyte microenvironment which was achieved by altering micropattern dimensions.

### **3. BIOCHEMICAL ANALYSIS OF LIVER-SPECIFIC FUNCTION**

To determine the effect of modulation of the local hepatocyte environment on liver-specific function, albumin secretion and urea synthesis were measured as markers of hepatocellular function (Figure 4.2). These two markers were measured as a function of micropattern dimensions in the



presence and absence of fibroblasts. In cultures of fibroblasts alone, albumin secretion and urea synthesis by fibroblasts was found to be undetectable, therefore changes in these markers in co-cultures were attributed to differences in hepatocyte metabolism.

Albumin secretion for five different spatial configurations was determined for pure hepatocyte cultures. Figure 4.2A demonstrates a rapid decline in liver-specific functions for all five conditions from initial values of  $8.8 \pm 0.9$   $\mu\text{g}/\text{day}$  to undetectable levels. In contrast, Figure 4.2B depicts albumin secretion for the same five micropatterns with the addition of fibroblasts. Albumin synthesis increased over time in culture in all configurations from less than 10  $\mu\text{g}/\text{day}$  to greater than 34  $\mu\text{g}/\text{day}$  indicating up-regulation of this liver-specific function due to co-culture with fibroblasts. These micropatterned co-cultures had decreasing amounts of initial heterotypic contact with maximal levels occurring at the smallest hepatocyte island dimension (36  $\mu\text{m}$ ) and minimal levels occurring at the single large hepatocyte island (17.8 mm). Smaller islands with high levels of heterotypic contact demonstrated greater albumin secretion than larger islands (less heterotypic contact) after day 5 of culture. Two fundamental patterns of up-regulation were observed: (1) dramatic up-regulation to similar levels of albumin secretion in the three smallest island configurations (19 to 26-fold of initial levels) and (2) relatively modest up-regulation (~7-fold) in the two larger island configurations. Therefore, a three-fold increase in albumin production was achieved in certain pattern configurations by modulation of the initial cellular microenvironment.

Analysis of urea synthesis in micropatterned co-cultures revealed similar qualitative results (Figure 4.2C). Urea synthesis was either constant over culture or increased from less than ~100  $\mu\text{g}/\text{day}$  to 160  $\mu\text{g}/\text{day}$  indicating up-regulation of another liver-specific function due to co-cultivation with fibroblasts. In addition, two patterns of up-regulation were observed using this marker of differentiated function: (1) up-regulation of urea synthesis to similar levels in the three smallest island configurations (up to 2-fold increase), and (2) relatively little up-regulation in the two larger island configurations. Therefore, a two-fold increase in urea synthesis production was achieved in certain pattern configurations by modulation of the initial cellular microenvironment. Asterisks indicate  $p < 0.05$  in Tukey post-hoc analysis of variance.

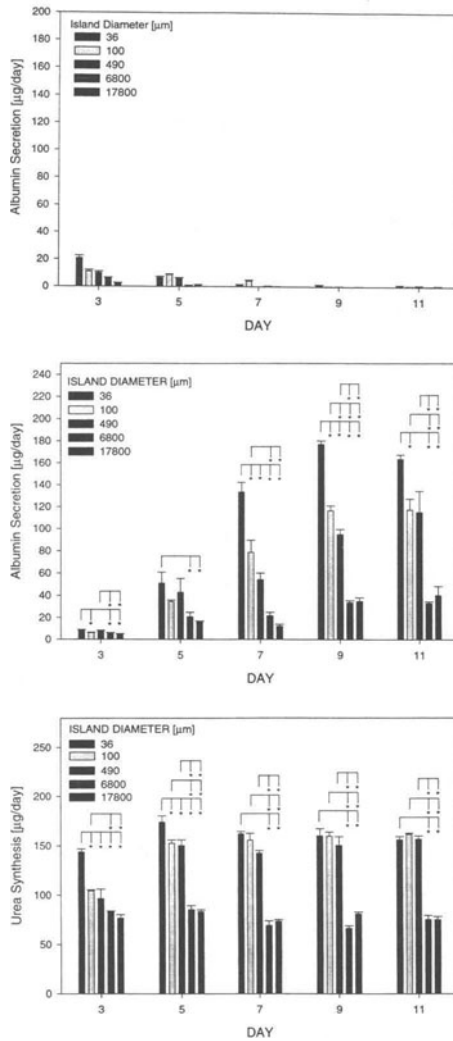
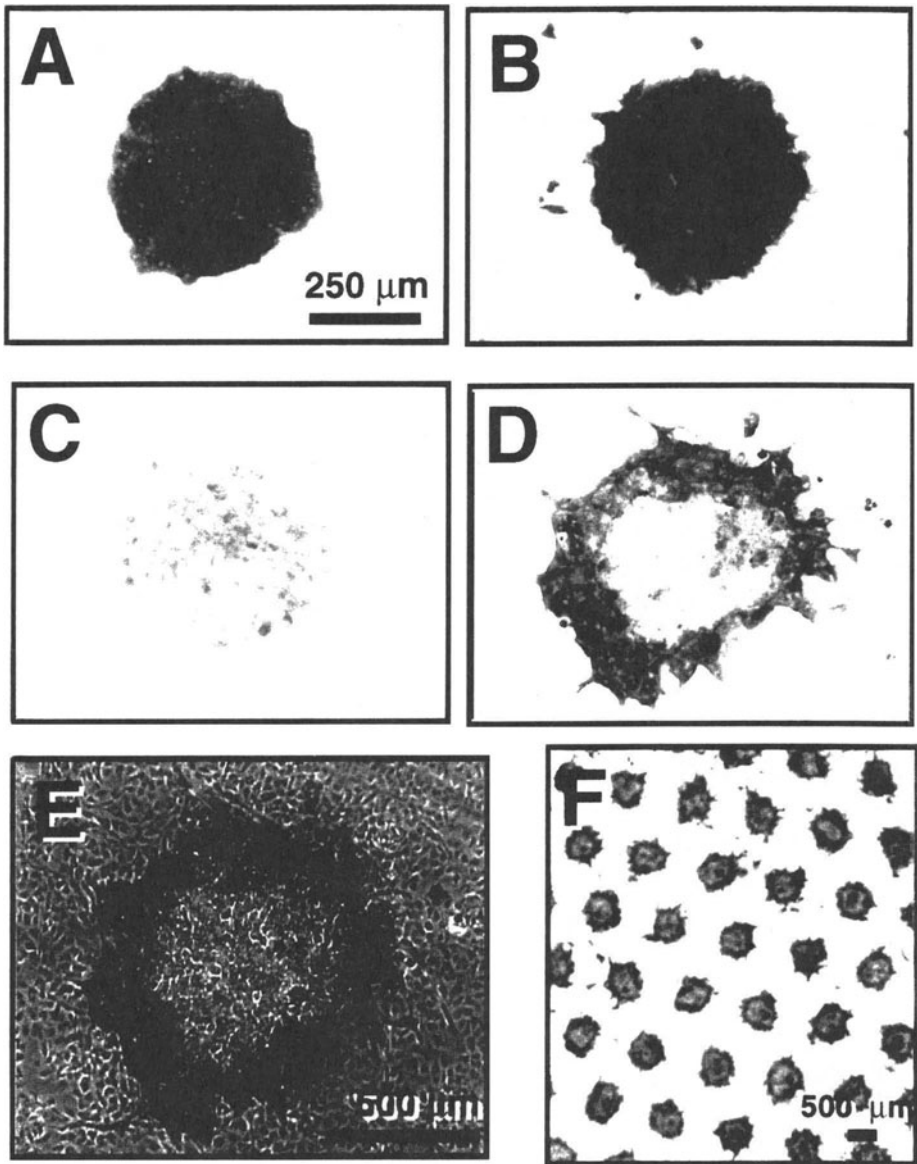


Figure 4.2. Biochemical Analysis of Micropatterned Cultures and Co-Cultures. A. Albumin Secretion in Micropatterned Hepatocyte Cultures B. Albumin Secretion in Micropatterned Co-Cultures C. Urea Synthesis in Micropatterned Co-Cultures

#### **4. HEPATOCYTE FUNCTION IN SITU: IMMUNOSTAINING OF INTRACELLULAR ALBUMIN**

In order to further examine the observed variations in liver-specific function exhibited by various micropatterned co-cultures, we studied the hepatocyte phenotype in situ by immunostaining of intracellular albumin. Specifically, we first focused on the distribution of albumin staining as it related to the heterotypic interface in one representative pattern, 490  $\mu\text{m}$  hepatocyte islands (Figure 4.3B at day 2, 4.3D at day 6). In addition, in order to distinguish between homotypic effects on differentiation and the effects arising from varying the heterotypic interface, we performed immunostaining on micropatterned pure hepatocyte cultures (Figure 4.3A at day 2, 4.3C at day 6). Our results show that hepatocytes alone stained uniformly for intracellular albumin at 48 h after isolation. The level of protein declined subsequently on the order of days. In comparison, micropatterned co-cultures displayed a more complex behavior. They, too, displayed initial uniform staining for intracellular albumin. Over 6 days, however, hepatocytes close to the heterotypic interface stained for high levels of intracellular albumin whereas protein levels in hepatocytes far from the heterotypic interface ( $> 3\text{-}4$  cells) continued to decline as in the pure hepatocyte cultures. To ensure that this 'ring' of intense staining was due to variations in intracellular albumin content of hepatocytes as opposed to the detachment of hepatocytes or fibroblasts from the lightly-stained areas, phase contrast microscopy of these cultures was performed. Figure 4.3E clearly depicts the presence of fibroblasts in the periphery of the hepatocyte island and cellular structures in the center of the hepatocyte island. Finally, Figure 4.3F demonstrates the reproducibility of this peripheral 'ring' of intense staining observed across a 490  $\mu\text{m}$  micropatterned co-culture.



*Figure 4.3. Kinetics of Immunostaining of Intracellular Albumin in 490  $\mu\text{m}$  Island Co-Cultures. A, C. Micropatterned hepatocytes alone (day 2, 6) B, D. Micropatterned co-cultures (day 2, 6) E. Phase contrast micrograph of micropatterned co-culture depicting presence of fibroblasts (day 6) F. Low magnification bright field of micropatterned co-culture (day 6).*

In order to correlate the pattern of immunostaining with variations we observed by biochemical analysis of secreted products in media, we also examined the distribution of high levels of intracellular albumin in comparatively small (100  $\mu\text{m}$ ) and large (6800  $\mu\text{m}$ ) micropatterned co-cultures (Figure 4.4.). These micrographs demonstrate uniform intense staining in smaller islands (initial island size 100  $\mu\text{m}$ , Figure 4.4A), a well-demarcated ring of  $\sim 120$   $\mu\text{m}$  in intermediate size islands (initial size 490  $\mu\text{m}$ , Figure 4.4B), and a well-demarcated ring of  $\sim 380$   $\mu\text{m}$  in larger islands (initial size 6800  $\mu\text{m}$ , Figure 4.4C); indicating a negative correlation between differentiated hepatocyte phenotype and distance from the heterotypic interface.

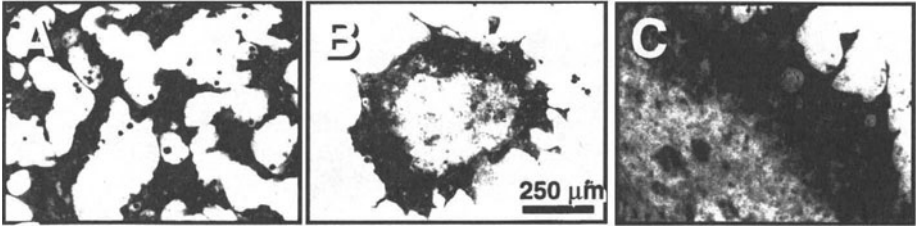
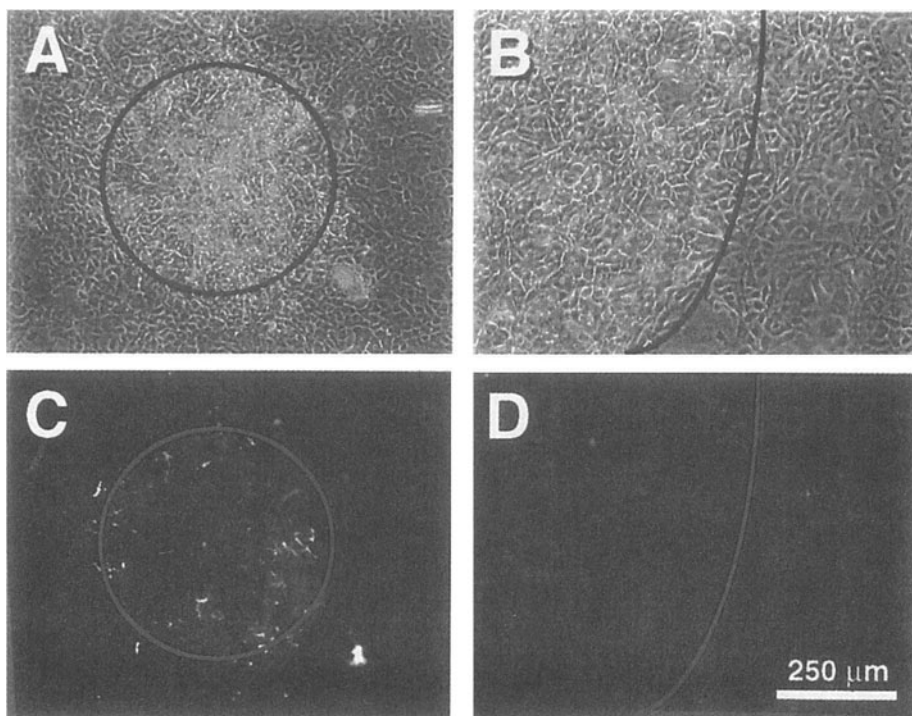


Figure 4.4 Comparison of Intracellular Albumin Immunostaining in Various Micropatterns at Day 6. A. Initial 100  $\mu\text{m}$  hepatocyte island co-culture B. Initial 490  $\mu\text{m}$  island co-culture C. Initial 6800  $\mu\text{m}$  island co-culture.

## 5. HEPATOCYTE FUNCTION IN SITU: BILE DUCT EXCRETION

Another in situ marker of liver-specific function is the formation of functional bile canaliculi between hepatocytes. Carboxyfluorescein diacetate (CFDA) is taken up by hepatocytes, cleaved by intracellular esterases, and in the presence of normal biliary transport, is excreted across the apical membrane of the hepatocyte. The presence of normal biliary transport of the dye as well as functional integrity of the tight-junctional domains bounding the canaliculus, causes illumination of visibly fluorescent bile duct structures between hepatocytes. We probed two patterns, one from a highly functioning co-culture (490  $\mu\text{m}$  circles) and one from a poorly functioning group (17800  $\mu\text{m}$  circle) as determined by albumin and urea production in order to examine this marker of liver-specific function. Figure 4.5 depicts phase contrast micrographs of both cultures (Figure 4.5A,B) where a dark

of demarcation has been included to emphasize the hepatocyte region. We found that 490  $\mu\text{m}$  patterns developed functional bile canaliculi, especially in the island periphery, whereas fluorescent bile duct staining was not observed on 17800  $\mu\text{m}$  islands (Figure 4.5C,D).



*Figure 4.5.* Functional Bile Canicular Staining. (line indicates approximate heterotypic interface). A. Phase contrast micrographs of 490  $\mu\text{m}$  island co-culture. B. Phase contrast micrograph of 17800  $\mu\text{m}$  island co-culture. C. CFDA staining of functional bile ducts in 490  $\mu\text{m}$  island co-culture D. in 17800  $\mu\text{m}$  island co-culture.

## 6. DISCUSSION

In this study, we demonstrated that liver-specific tissue function can be modulated by controlling initial heterotypic cell-cell interactions despite use of identical cellular components. Furthermore, it was determined that these differences in bulk tissue properties as a function of cellular microenvironment were generated by induction of spatial heterogeneity in the hepatocyte phenotype. Hepatocytes in the vicinity of the heterotypic interface had a relative increase in levels of liver-specific function; therefore, spatial configurations with maximal initial interface exhibited superior function.

### 6.1 Cellular Microenvironment Modulated Liver-specific Functions

Evidence that liver-specific function could be controlled by variations in initial cell-cell interactions is seen in the functional differences between predominantly heterotypic cultures (smallest islands of 36  $\mu\text{m}$  diameter) and predominantly homotypic (largest island of 17800  $\mu\text{m}$  diameter) as assessed by markers of metabolism (urea synthesis), synthetic function (albumin secretion and cytoplasmic content), and apical transport (biliary excretion). These cellular microenvironments significantly altered liver-specific functions as follows: increasing hepatocyte island size correlated with a relative decline in urea synthesis, albumin secretion, intracellular albumin staining, and effective biliary excretion. Smaller hepatocyte islands of 36, 100, and 490  $\mu\text{m}$  initial diameter yielded three-fold steady-state increase in albumin secretion and two-fold steady-state increase in urea synthesis over 6800 and 17800  $\mu\text{m}$  islands (Figure 4.2). Similarly, a smaller pattern (490  $\mu\text{m}$  initial diameter) exhibited functional biliary excretion as assessed by accumulation of a fluorescent compound within bile canilicular structures between hepatocytes whereas larger islands (17800  $\mu\text{m}$  initial diameter) showed reduced functional biliary excretion with no evidence of focal fluorescence (Figure 4.5). The presence of fluorescent biliary structures between hepatocytes was correlated by LeCluyse et al (1994) to biliary structures observed on electron microscopic analysis. The absence of fluorescent biliary structures was attributed to either (1) low rate of excretion across apical domain (2) absence or loss of function of tight junctions at borders of apical membrane or (3) decreased uptake of dye by hepatocytes. The lack of fluorescent biliary structures in 17800  $\mu\text{m}$  pattern indicates some such functional deficit. Therefore, hepatocytes in large island co-cultures have impaired biliary transport as well as relative deficiencies in other liver-specific functions due to alterations in the initial cellular microenvironment.

Our conclusion that bulk tissue function (secreted albumin and urea) was modulated by initial cellular microenvironment required evaluation of hepatocyte number to ensure that changes in these liver-specific markers were due to changes in level of hepatocellular function as opposed to cell division. In order to determine the relative contribution of hepatocyte division as compared to up-regulation of functions, fibroblasts were growth-arrested and total DNA in co-cultures was measured- in this way, changes in total DNA could be attributed solely to hepatocytes. Total DNA of co-cultures was measured at 6 h of co-culture and compared to DNA content at 9 days of co-culture. This analysis demonstrated that no significant increase in total DNA occurred in co-cultures over 9 days indicating increases in hepatic functions were due to up-regulation of synthesis rather than a marked increase in hepatocyte population (data not shown). These data correlate well with reports of minimal hepatocyte division under various co-culture configurations (Guguen-Guillouzo, 1986; Kuri-Harcuch and Mendoza-Figuera, 1989; Donato et al, 1990). Furthermore, this result correlated well with visual observation of larger micropatterns (490 micron island diameter and greater) where hepatocyte island size was observed to be relatively constant over the course of culture (Figure 4.3., 4.4.), indicating a lack of significant cell division. Taken together, these data suggest that variations in hepatic functions between culture configurations were due predominantly to relative levels of hepatic up-regulation as opposed to hepatocyte division.

The conclusion that bulk tissue function was modulated by variation of the cell-cell interactions at the heterotypic interface also required confirmation of similar initial hepatocyte numbers to ensure that changes in secreted products were due to up-regulation of liver-specific functions rather than differences in numbers of initial hepatocytes. Comparison of initial total hepatocyte DNA in all five micropatterns showed this to be a valid approximation ( $8 \pm 1.8 \mu\text{g DNA}$ ) with the exception of the smallest ( $36 \mu\text{m}$ ) islands which were found to have two-fold elevated levels of DNA. This may be due to the potential for more than one unspread hepatocyte ( $20\mu\text{m}$  diameter) to adhere to  $36 \mu\text{m}$  islands. One approach to this potential cause of increased hepatocyte number would be the alteration of island diameter to  $\sim 20\mu\text{m}$ ; however, some studies suggest that cell shape alters expression of liver-specific markers thereby confounding our findings (Singhvi et al, 1994b). Alternatively, hepatocytes, known to have a higher mitotic index at sparse seeding densities (Nakamura et al, 1983), may divide over the course of the first 24 h of culture, resulting in increased hepatocyte numbers in smaller patterns. In either case,  $36 \mu\text{m}$  patterns included greater numbers of hepatocytes than other micropattern conditions; therefore,  $36 \mu\text{m}$  islands may not have been the highest producers of liver-specific markers on a per cell basis. Further experimental methods need to be developed to



specifically compare the smallest islands to intermediate island sizes; however, the trend to increased long-term liver specific function resulting from maximal initial heterotypic interface remained a consistent finding.

Previous studies examining the effect of initial cellular microenvironment on tissue function are scant due to the limitations of existing experimental methods. Co-cultures of hepatocytes with other cell types generate heterogeneous cell-cell interactions which are dictated entirely by seeding density and cell aggregation (see Chapter 2). One study conducted to examine the effect of modulation of the local microenvironment was attempted by variations in cell seeding density achieved by variation in size of culture plate (Guguen-Guillouzo, 1986). This study of human hepatocytes co-cultured with rat liver epithelial cells (RLEC) utilized the same numbers of cells in 25 cm<sup>2</sup> and 75 cm<sup>2</sup> dishes. The data suggests two-fold higher albumin secretion in sparser cultures consistent with our data showing smaller micropatterns producing three-fold higher albumin than large micropatterns. However, sparse seeding of rat liver epithelial cells would allow for increased epithelial cell division in larger plates resulting in the ratio of hepatocytes: RLEC to vary between culture conditions. In contrast, our study was conducted with the same surface area dedicated to fibroblasts in all conditions. This allowed examination of the local cellular environment as an isolated variable without differences in cell numbers and resultant variations in concentrations of potential signaling factors (such as humoral factors in media). In addition, our study allowed simultaneous control over both oxygen delivery to hepatocytes as well as amount of media. In contrast, variation of culture plate area necessitates either a change in media volume to preserve the depth of media above the cell population (and the diffusion of oxygen) or a change in media depth to preserve media volume. Therefore, our approach to controlling cellular environment has definitively demonstrated the importance of local cellular microenvironment as an isolated modulator of liver-specific function.

## **6.2 Cellular Microenvironment Induced Spatial Heterogeneity in Hepatocyte Phenotype**

In addition to demonstrating that liver-specific tissue function can be modulated by controlling initial heterotypic cell-cell interactions, this study determined that spatial heterogeneity in the induction of the hepatocyte phenotype was the primary cause of these variations in function. In situ immunostaining of intracellular albumin on micropatterned hepatocyte/fibroblast co-cultures displayed increased staining in the vicinity of the heterotypic interface, indicating up-regulation of this marker of

differentiated function. Specifically, smaller (100  $\mu\text{m}$  islands) stained throughout hepatocyte regions whereas larger islands (490  $\mu\text{m}$  and greater) exhibited intense staining in a well-demarcated ring in the periphery (Figure 4.4). This pattern of staining was highly reproducible both spatially and across various conditions. The differentiated hepatocyte phenotype seemed to dominate within 100-400  $\mu\text{m}$  of the heterotypic interface; therefore, it seems reasonable that patterns with greater interfacial regions displayed superior tissue function.

In order to verify that variations in intracellular albumin represented variations in hepatocyte phenotype due to heterotypic interactions, the effect of homotypic hepatocyte interactions on the spatial distribution of intracellular albumin in one representative pattern (490  $\mu\text{m}$ ) was assessed. Our results revealed uniform staining in pure hepatocyte cultures with decreased staining over a period of one week, consistent with decline in secreted albumin (Figure 4.2) and previous studies showing residual albumin mRNA hepatocyte immediately after isolation with decline of mRNA over 1 week (Dunn et al, 1992); therefore, we concluded that patterns of immunostaining in co-cultures were indeed due to interactions with fibroblasts rather than homotypic interactions.

In an attempt to correlate intracellular albumin staining with albumin secretion data, image analysis was performed on immunostained co-cultures. Specifically, we estimated the fraction of hepatocytes contributing to albumin secreted into the media. Image analysis of intracellular albumin staining revealed  $\sim 100\%$  of hepatocytes stained intensely in 100  $\mu\text{m}$  patterns,  $\sim 65\%$  in 490  $\mu\text{m}$  patterns, and  $\sim 20\%$  in 6800  $\mu\text{m}$  patterns. By assuming negligible contribution of weakly staining hepatocytes to albumin production, we calculated that hepatocytes adjacent to the heterotypic interface in larger patterns may have produced 35-50% more albumin per cell than those in 100  $\mu\text{m}$  micropatterns. More quantitative assessment of intracellular albumin content must be completed to assess the significance of these results; however, this data suggests there may be a further increase in albumin production in hepatocytes adjacent to relatively undifferentiated homotypic neighbors. Interestingly, this could be experimentally examined by micropatterning co-cultures as annuli (i.e. assess function of co-cultures with same heterotypic interface but absence of hepatocytes in center of island).

While our data on modulation of liver-specific functions of co-cultures by variations in cell-cell interactions agree generally with Guguen-Guillouzo et al (1986), the immunostaining data contradict existing reports. Mesnil et al (1987) examined intracellular albumin in rat hepatocytes co-cultured with rat liver epithelial cells after 10 days of co-culture and observed that aggregates of hepatocytes were stained uniformly for albumin.

The authors infer the potential for hepatocytes to communicate with one another since hepatocytes away from the heterotypic interface stained for albumin. The validity of the assumption that the signal for up-regulation of liver-specific functions can be propagated to the entire hepatocyte colony, is limited in these studies by the colony size. In our study, micropatterning co-cultures allowed the creation of larger hepatocyte colonies than those that come about by random aggregation and cell migration; therefore, this study was able to demonstrate a finite penetration length of the differentiation signal to the interior of a large hepatocyte colony. This result contradicts the notion that hepatocytes are able to communicate effectively throughout a hepatocyte colony and in fact, our results indicate significant variations in hepatocyte albumin expression within a co-culture. This type of data may lead to new mechanistic information with regard to homotypic cell communication.

### **6.3 Related Observations on Control of Cell-Cell Interactions**

While the ability to micropattern co-cultures offers the ability to modulate tissue function via the initial cellular microenvironment, the inherent dynamics of cell adhesion and motility may further modify these engineered tissues. The degree of morphogenesis varied remarkably with hepatocyte island size. In these experiments, hepatocyte islands of 490  $\mu\text{m}$  with center-to-center spacing of 1230  $\mu\text{m}$  produced a relatively stable configuration whereas hepatocytes in islands of 100  $\mu\text{m}$  and smaller reorganized into cord-like structures (see Figure 4.4B). Reorganization of tissue may be prevented by cytoskeletal toxins such as cytochalasin D; however, these compounds have been reported to alter vesicular trafficking in hepatocytes and could confound the data. Despite the tendency for some spatial configurations to reorganize, the perturbations which were achieved in 'initial' cellular microenvironment were found to have significant long-term impact on tissue function. Interestingly, this morphogenetic behavior may provide insight into relative cellular adhesivity and tissue reorganization in future studies.

Another variable which can influence the intended cell-cell interactions, is relative cell adhesion of fibroblasts to serum-adsorbed proteins on glass versus the surface of spread hepatocytes. In order to determine the degree of fibroblast attachment to the surface of hepatocytes, dual label vital fluorescent dye studies were performed (data not shown). These data indicated a relative lack of fibroblast adhesion to the surface of hepatocyte islands on smaller hepatocyte islands (36 and 100  $\mu\text{m}$ ); however, at larger island sizes, fibroblasts seemed to attach on both hepatocyte islands as well as adjacent glass. Interestingly, fibroblasts adherent to the surface of

hepatocytes do not seem to produce up-regulation of albumin secretion throughout larger islands- i.e. the character of the fibroblast signal from the surface of the hepatocyte is altered relative to fibroblasts on adjacent glass. Fibroblasts have been reported to alter their response to local stimuli (growth factors) based on the underlying matrix (Xu and Clark, 1996); therefore, the overlying fibroblasts may have altered expression of critical factors for the induction of hepatocyte differentiation. Despite the addition of this variable to the experimental system, it should be noted that changes in tissue function do not seem to be primarily altered by this phenomenon. For example, 490  $\mu\text{m}$  islands are highly functional despite overlying fibroblasts whereas hepatocytes in a 17800  $\mu\text{m}$  island with overlying fibroblasts have relatively impaired liver-specific function.

## 7. SUMMARY AND IMPLICATIONS

This study utilized microfabrication as a vehicle for control over heterotypic cell-cell interactions without significant variations in cell numbers. Unprecedented modulation of heterotypic interface as an independent variable was achieved. This modulation of the heterotypic interface over three orders of magnitude dramatically altered levels of detectable liver-specific function in the resulting composite tissues as measured by markers of metabolic, synthetic, and excretory function. Variations in function were due to modulation of the hepatocyte phenotype: specifically, epithelial differentiation varied inversely with distance from the heterotypic interface causing cultures with a relative increase in cell interaction to exhibit superior function. The ability to control heterotypic cell-cell interactions and probe the resulting tissue for evidence of cell communication will have applications both in basic science and development of functional tissue constructs for medical applications.

From a fundamental perspective, these techniques can be exploited to offer new insight into the mechanisms by which cells communicate. Indeed, our study alone, resulted in the novel finding that unlimited homotypic hepatocyte signaling to differentiate is not achievable. We will explore these findings further in subsequent chapters. Another area which could benefit from these techniques is the area of developmental biology. Transdifferentiations of mesenchyme to epithelium is of fundamental importance in embryonic development and the cellular cues which induce differentiation of many different cell types may be an important application of this work (Hay and Zuk, 1995). Finally, in the area of tissue engineering, the ability to modulate function of multicellular systems could allow

unprecedented level of control over the in vitro reconstruction of skin, bone marrow, muscle, and many other tissues.

## Chapter 5

# Probing The Mechanisms Of Hepatocyte/Fibroblast Interactions

### 1. OVERVIEW

We have demonstrated that variations in tissue function can be achieved by modulation of spatial configuration of co-cultures of hepatocytes and fibroblasts. In Chapter 4 we showed that these differences in function were dependent on the degree of heterotypic interaction that occurred between cell populations. Furthermore, these findings correlated with the observation that hepatocellular islands of a critical size displayed spatial heterogeneity in the pattern of induction of hepatocyte differentiation- i.e. within a given hepatocyte population, hepatocytes close to the heterotypic interface demonstrated increased albumin production as compared to more central hepatocytes. Thus, evidence from markers of both bulk and localized liver-specific function suggested that the heterotypic interface between cell populations was an important determinant of the level of tissue function in the resultant tissue.

Further examination of our novel finding that hepatocytes adjacent to the heterotypic interface up-regulate liver-specific functions such as albumin synthesis could have important implications. Understanding of spatial heterogeneity in vitro could allow insight into many physiologic processes in the liver which also exhibit spatial heterogeneity. For example, in a healthy liver acinus, many functions display zonal heterogeneity (i.e. variations in gene expression in the pericentral, middle, and periportal zones) (Bhatia et al, 1996). In particular, glutamine synthetase has a similar pattern

of expression as that observed for albumin in our study- a well-demarcated zone of intense protein expression in the pericentral cell population (Gebhardt and Mecke, 1983). Another example of spatial heterogeneity *in vivo* is the zone of hepatocyte injury and repair induced by certain ingested toxins (Carbon Tetrachloride damages pericentral hepatocytes preferentially, cirrhosis is thought to initiate as fibrosis in the perivenous region- Zucker and Gollan, 1995). Finally, mechanistic information regarding causes of spatial heterogeneity *in vitro* could shed light on kinetics of hepatocyte signaling and proliferation in liver regeneration where periportal hepatocyte division precedes pericentral events by 1-2 days (Michalopoulos and DeFrances, 1997). From a more practical perspective, mechanistic information on modes of communication between hepatocytes and fibroblasts could influence the design of a bioartificial liver. Data on whether the signal(s) to differentiate is cell-associated or freely secreted will dictate (1) whether cells need to share the same compartment of the bioreactor, (2) whether cell populations can be sequentially perfused, and/or (3) whether fibroblasts could be replaced entirely by some humoral factor(s).

Many investigators have attempted to examine the mechanisms by which mesenchymal cells induce the hepatocyte phenotype (see Chapter 1 for review). Overall, the initiating signal for differentiation is thought to be mesenchymal cell-associated (Mesnil et al, 1987; Corlu et al, 1991; Clemens et al, 1994) and hepatocytes are thought to be capable of transmitting this signal to their homotypic neighbors (Guguen-Guillouzo, 1986; Mesnil et al, 1987). However, as detailed in Chapter 1, experimental examination of these issues have been fraught with confounding factors. In this chapter, we used microfabrication techniques as well as conventional culture methodologies to examine the mechanism of induction of hepatocyte functions at the heterotypic interface. We asked the specific questions: What is the relative importance of 'cell-associated' signals which we defined to include membrane-bound receptors, locally secreted extracellular matrix, and local matrix or cell-bound growth factors, as compared to 'freely secreted' signals which we defined to include humoral factors such as soluble cytokines and growth factors, in the induction of liver-specific functions? As you will see, our data indicated a predominantly 'cell-associated' signal for induction of hepatic functions. This will have important implications in the design of a co-culture based bioartificial liver.

## **2. EFFECT OF HOMOTYPIC HEPATOCYTE INTERACTIONS ON SPATIAL PATTERN OF IMMUNOSTAINING**

We extensively probed the previously described (Chapter 4) observation that co-culture with fibroblasts induced spatial heterogeneity in intracellular albumin staining. Specifically, we examined the potential contribution of homotypic hepatocyte interaction to spatial heterogeneity by studying micropatterns with different levels of homotypic interaction both in the presence and absence of fibroblasts. Figure 5.1 compares patterns of intracellular albumin for five different micropatterned hepatocyte configurations after 48 (A,C,E,G) and 144 h (B,D,F,H) of culture. Notice uniform distribution of intracellular albumin at 48 h in all patterns which diminished over the time. In comparison, Figure 5.2 depicts micropatterned co-cultures (i.e. addition of fibroblasts at 24 h of culture). Initially, uniform distribution of intracellular albumin similar to that observed in micropatterned hepatocyte cultures is demonstrated (A,C,E,G). After 6 days of culture, however, hepatocytes display differential levels of staining. Hepatocytes far from the heterotypic interface exhibit a similar behavior to hepatocytes cultured in the absence of fibroblasts, low levels of staining (Figure 4.3 B,D,F,H). In contrast, hepatocytes proximal to the heterotypic interface exhibit relatively high levels of intracellular albumin. Thus, homotypic hepatocyte interactions do not seem to be the sole contributor to the observed spatial heterogeneity in hepatocyte phenotype.



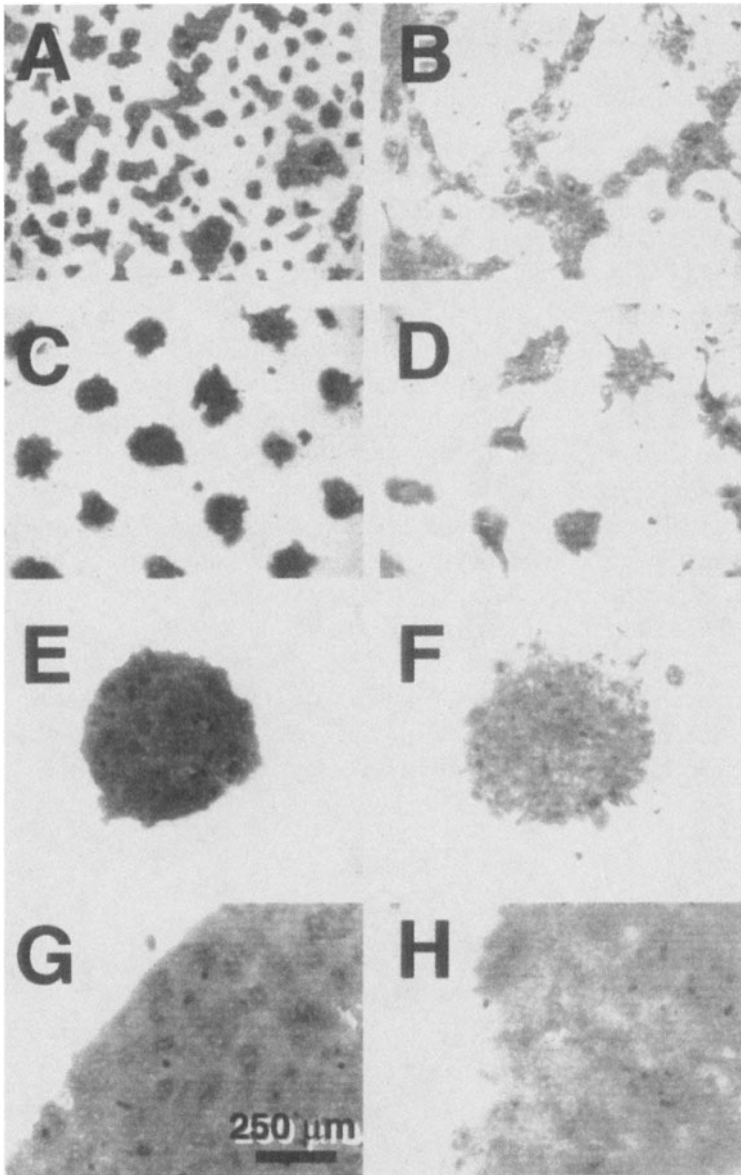


*Figure 5.1.* Immunostaining of Intracellular Albumin in Micropatterned Hepatocytes (Only).  
Stained on: day 2 of culture A. 36  $\mu\text{m}$ , C. 100  $\mu\text{m}$ , E. 490  $\mu\text{m}$ , G. 6800  $\mu\text{m}$ , and day 6 of  
culture B. 36  $\mu\text{m}$ , D. 100  $\mu\text{m}$ , F. 490  $\mu\text{m}$ , and H. 6800  $\mu\text{m}$ .

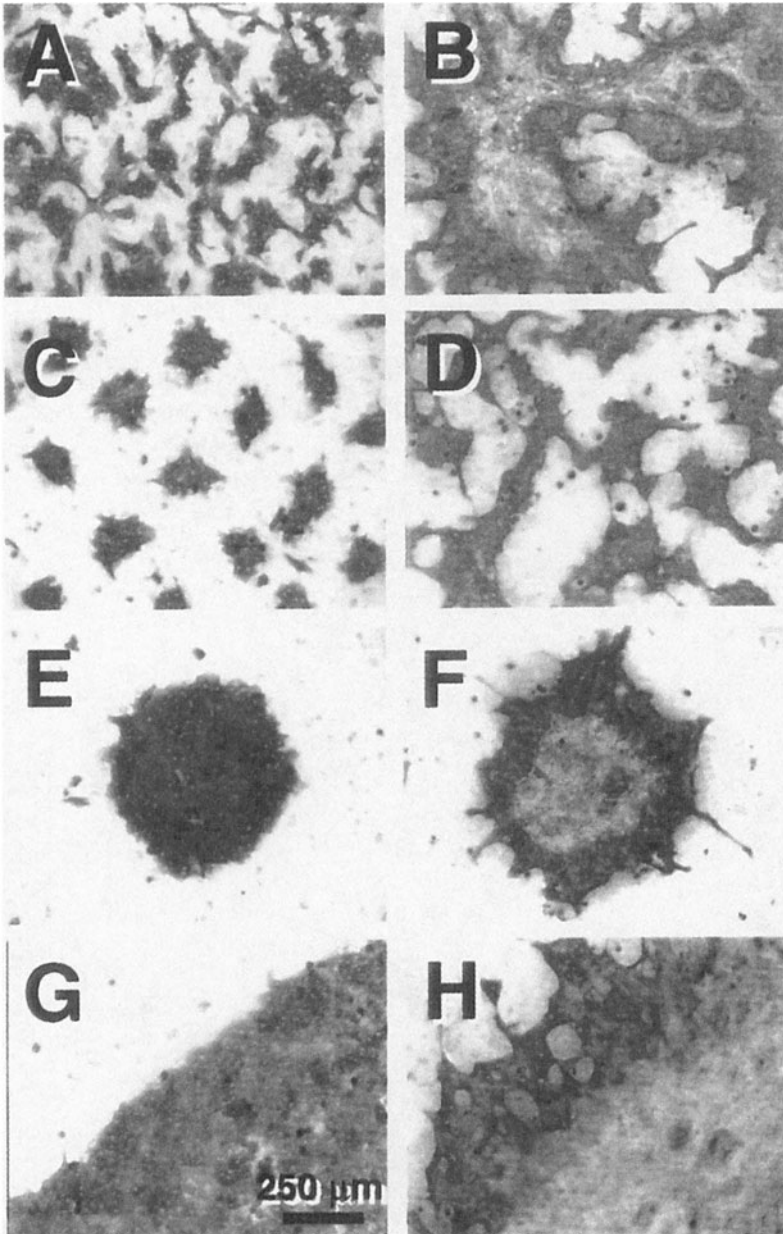


Figure 5.2. Immunostaining of Intracellular Albumin in Micropatterned Co-Cultures. Stained on: day 2 of co-culture A. 36  $\mu\text{m}$ , C.100  $\mu\text{m}$ , E. 490  $\mu\text{m}$ , G. 6800  $\mu\text{m}$ , and day 6 of co-culture B. 36  $\mu\text{m}$ , D. 100  $\mu\text{m}$ , F. 490  $\mu\text{m}$ , and H. 6800  $\mu\text{m}$ .

### 3. USE OF CONDITIONED MEDIA

In order to examine the possible induction of hepatic differentiation by secreted fibroblast products, experiments were conducted with hepatocytes treated with 'conditioned media'. Figure 5.3 displays urea synthesis measured as a marker of liver-specific function in a variety of such culture conditions. Media was 'conditioned' by 24 h incubation with (1) tissue culture plastic as a control (hepatocytes + media), (2) fibroblasts alone (hepatocytes + fibroblast conditioned media), or (3) co-culture of fibroblasts and hepatocytes (hepatocytes of co-culture conditioned media). These data were compared to co-cultured fibroblasts and hepatocytes which served as a positive control for the expected level of liver-specific function (co-culture + media).

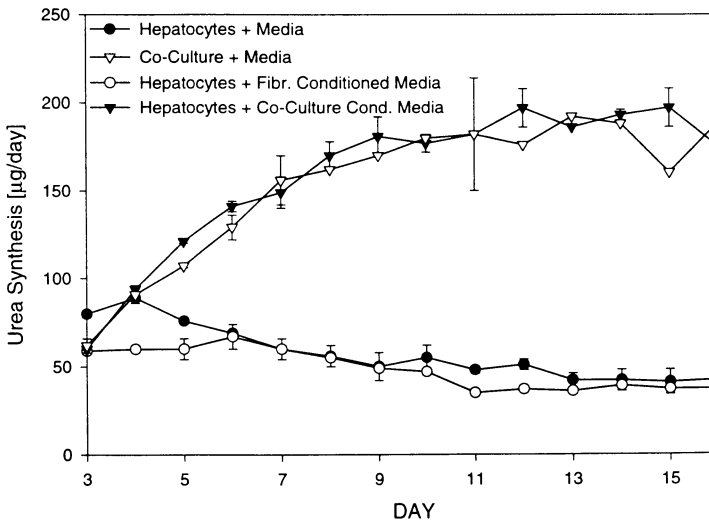


Figure 5.3. Urea Synthesis in Hepatocytes Treated with Conditioned Media

These data indicate an expected decline in liver-specific function in pure hepatocyte over the first week of culture to less than 50 µg/day. A similar decline in liver-specific function was observed in cultures treated with fibroblast conditioned media indicating insufficient concentration of humoral factors for induction of hepatic differentiation. In contrast, co-cultures of hepatocyte and fibroblasts displayed up-regulation of urea

synthesis from ~ 60 µg/day to ~175 µg/day over 10 days of culture followed by stable production of urea. Some cultures were treated with co-culture conditioned media to probe for humoral factors present only when both cell types were allowed to communicate. These did not display any further induction of liver-specific function over that observed in co-culture controls indicating insufficient concentration of humoral factors for induction of hepatic differentiation (note: detection of urea in this media was due to production of urea by the co-culture utilized for conditioning media- any induction of urea synthesis in the target hepatocyte population would therefore have generated a further increase in urea production over control co-cultures).

#### **4. PHYSICAL SEPARATION OF CELL POPULATIONS**

Hepatocyte and fibroblast populations were co-cultured in the same dish yet separated by an annulus of bare glass to probe the role of labile, freely secreted factors in induction of hepatic functions. Figures 5.4B,C show phase contrast micrographs of two different initial annuli dimensions translating to two different achievable separation widths. Growth-arrested fibroblasts migrated towards the central hepatocyte region at a rate of approximately 500 microns per day. After 3 days, the 1500 µm initial separation was observed to have diminished completely and cell contact occurred at the periphery of the hepatocyte island. Subsequently, cells were allowed to interact for 8 days ('contact' condition). In contrast, initial cell separation of 6000 microns narrowed to 500 microns over the same time frame ('non-contact'). This experimental design allowed the examination of the role of cell proximity/cell contact in induction of hepatic functions as well as the elimination of overlying fibroblasts as confirmed by fluorescent dye labeling (Figure 5.4A).

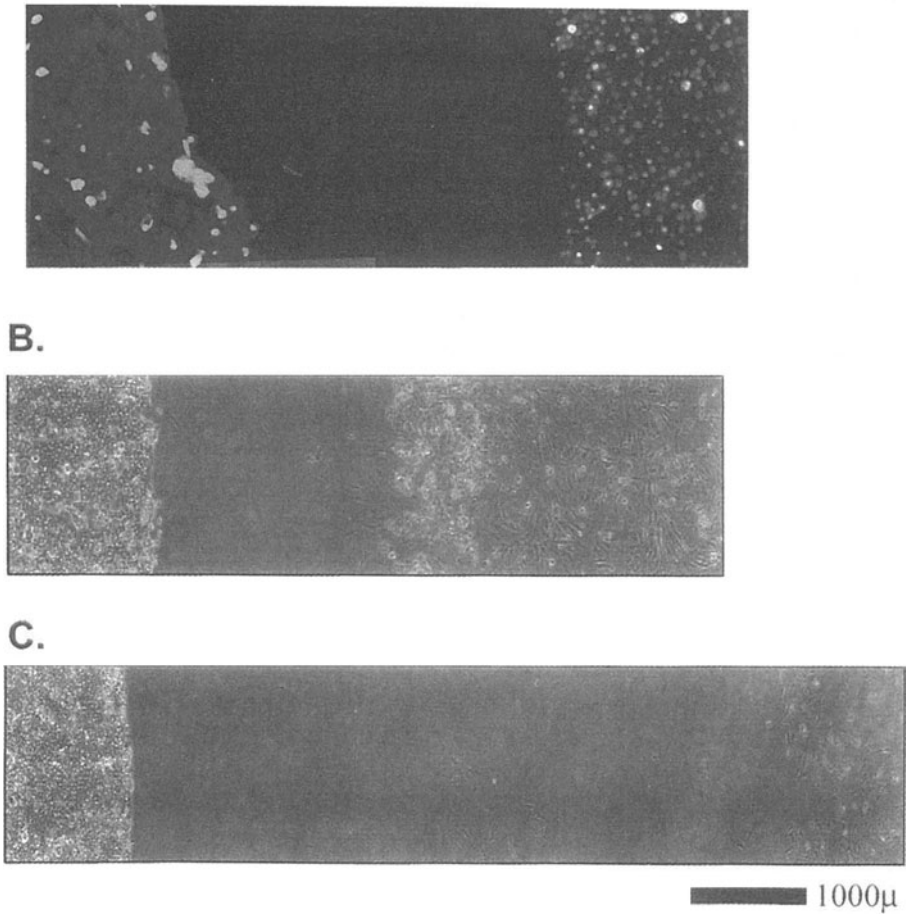


*Figure 5.4. Separation of Cell Populations. A. Fluorescent micrograph of separated, fluorescently-labeled cell populations (left=hepatocytes, right=fibroblasts). B.Phase contrast micrographs-differential spacing in narrow [2500  $\mu\text{m}$ ] and C. wide [6000 $\mu\text{m}$ ] spacing.*

Hepatocytes in the 'contact' condition exhibited an intense staining pattern in the periphery of the hepatocyte island Figure 5.5B similar to the

Hepatocytes in the ‘contact’ condition exhibited an intense staining pattern in the periphery of the hepatocyte island Figure 5.5B similar to the peripheral ring of staining observed in the control co-culture (Figure 5.5A). In contrast, hepatocytes in the ‘non-contact’ condition lacked significant staining for intracellular albumin (Figure 5.5C). These results indicated the importance of cell proximity ( $< 500 \mu\text{m}$ ) for differentiation of hepatocytes. Furthermore, spatial heterogeneity in hepatocyte phenotype persisted despite absence of fibroblast adhesion to surface of hepatocytes, indicating that regional differences in hepatocyte staining is not due to overlying fibroblasts.

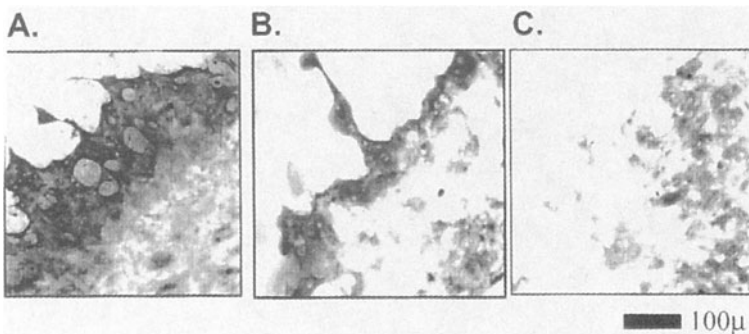


*Figure 5.5.* Immunostain of Intracellular Albumin in Separated Cell Populations. A. Micropatterned Control Co-Culture, stained at day 6 of co-culture. B. ‘Contact’ co-culture; initial separation  $2500 \mu\text{m}$ , contact occurred after 72 h, stained day 8 after contact. C. ‘Non-contact’ co-culture; initial separation  $6000 \mu\text{m}$ , stained day 11, prior to contact.

## 5. AGITATION OF CO-CULTURES

Another method of examining the potential role of secreted products by fibroblasts was the addition of fluid convection to co-cultures. Under these ‘shaken’ conditions, humoral factors which theoretically require a high local concentration for their bioactivity would be diluted in the bulk fluid phase and the resulting pattern of hepatocyte differentiation would differ from static conditions. In addition, agitation of culture media would allow mixing of nutrients (oxygen, glucose) and thereby alleviate potential transport limitations to the center of large hepatocyte islands.

Figure 5.6 demonstrates the effect of agitation of one representative micropatterned co-culture,  $490 \mu\text{m}$  as compared to static conditions. Phase contrast micrographs (5.6A,B) demonstrate that agitation did not cause any overt fibroblast damage due to mechanical shear. In addition, low magnification, bright field images of cultures stained for intracellular albumin demonstrated no significant differences in patterns of spatial

heterogeneity (Figure 5.6C,D). The ‘penetration’ length of the signal for hepatocyte differentiation from the heterotypic interface did not vary significantly when compared to static cultures. These data suggested (1) spatial heterogeneity of hepatocyte phenotype in static cultures was not caused by significant nutrient limitation due to diffusional transport and (2) dilution of secreted factors by mixing did not modulate the observed pattern of spatial heterogeneity.

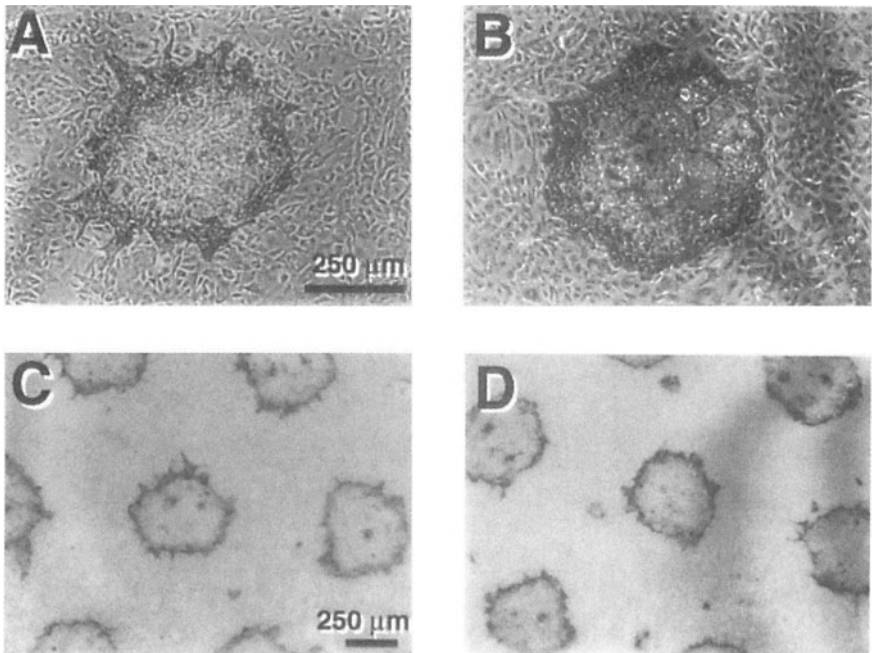


*Figure 5.6.* Immunostain of Intracellular Albumin in Static and Shaken Cultures. A. Phase contrast micrograph of immunostained static culture, day 4, B. shaken, day 4. C. Bright field, low magnification of immunostained static culture, day 4. D. shaken, day 4.

## 6. DISCUSSION

We previously reported the local induction of hepatic function in primary hepatocytes by co-cultivation with murine 3T3-J2 fibroblasts. Our aim in this study was to probe the mechanisms by which these cells interact using both conventional and microfabrication techniques. Due to the potential significance in bioreactor design, our initial efforts were focused on classification of the signal(s) broadly as cell-associated or freely secreted.

Furthermore, we examined potential contributors to the finite 'penetration' length of this signal leading to spatial heterogeneity in the hepatocyte phenotype (See Chapter 4 for details).

## **6.1 A Cell-Associated Signal is Implicated in Induction of Hepatic Function**

Studies attempting to classify the differentiation signal as free versus bound provided evidence that the signal(s) is cell-associated. No single experiment we conducted could adequately address the biochemical nature of the signal; however, taken together, use of conditioned media, separation of cell populations within a co-culture, and agitation of micropatterned co-cultures point towards cell-associated molecules. Neither fibroblast conditioned media nor co-culture conditioned media were able to induce hepatocellular functions in target hepatocytes, indicating the absence of freely soluble signaling molecule (Figure 5.3). These data are supported by the general lack of induction of hepatic function using mesenchyme conditioned media or transwells by other investigators (Shimaoka et al, 1987; Morin et al, 1988; Kuri-Harcuch and Mendoza-Figueroa, 1989; Donato et al, 1990). However, this experimental method is limited due to the inability to probe the role of two possible types of signaling molecules: (1) freely soluble factors which degrade in less than 24 h or (2) freely soluble factors whose bioactivity depends on a high local concentration and is therefore diluted in conditioned media. Further studies with co-cultures with separated cell populations and agitated co-culture suggest that these types of factors are not solely responsible for the effects we observed.

We deduced the implausibility of a freely soluble, highly labile signal from co-cultures performed with separated cell populations. Our data indicated that cell contact (or very close proximity,  $< 5 \mu\text{m}$ ) correlated with induction of liver-specific function in hepatocytes whereas lack of contact ( $> 500 \mu\text{m}$ ) did not induce an observable signal as measured by immunostaining of intracellular albumin (Figure 5.6). With the exception of some unique biochemicals such as nitric oxide, other highly labile signals would be expected to signal hepatocytes across  $500 \mu\text{m}$  in this separated culture configuration. These data correlate well with morphologic evidence that hepatocytes require cell proximity to retain viability in co-cultures (Mesnil et al, 1987). Similarly, we examined morphology of hepatocytes separated from underlying fibroblasts by a 1 mm thick collagen I hydrogel and observed fibroblastic, de-differentiated morphology after a few days of culture, further indicating the lack of a freely soluble, highly labile signal (data not shown).



The potential role of freely soluble factors whose bioactivity depends on a high local concentration was also found to be minimal by the combined results of conditioned media and agitation experiments. Any soluble factor which did not induce a signal in conditioned media due to its dilution in the larger media volume, would also be diluted in agitation experiments due to fluid convection in the media. Therefore, if fluid mixing causes reduction of the concentration of some putative soluble signaling factor below its bioactive concentration, one would not expect local induction of hepatocyte function in agitation experiments. In fact, we found similar patterns of local induction of intracellular albumin in hepatocytes in micropatterned co-cultures as compared to static controls, indicating dilution of soluble factors was not a critical limitation in induction of hepatocellular function (Figure 5.6).

Taken together, the results of conditioned media, separated co-culture, and agitation experiments suggested a 'cell-associated' signal which promotes up-regulation of liver-specific functions. The specific molecular basis for this signal remains unclear; however, below we attempt a comprehensive discussion of existing data on (1) putative signaling molecules in other hepatic co-cultures, (2) other signals that induce hepatocyte differentiation *in vitro*, (3) known products of fibroblasts which could be involved in induction of hepatocellular function, (4) known products of hepatocytes which could signal fibroblasts, and (5) signals involved in general mesenchyme to epithelial transformation. While we have included many potential factors, it should be noted that differentiation in most tissues depends on the synergy of many factors; therefore, it is unlikely that any one of these molecules will provide the entire repertoire of signals necessary for induction of hepatic function.

Putative signaling molecules identified in hepatic co-cultures have been limited to one candidate cell surface protein thus far, liver regulating protein (LRP). The ligand for LRP has not yet been determined; however monoclonal antibodies against LRP modulated albumin secretion, cytoskeletal organization, and extracellular matrix deposition in one co-culture model (Corlu et al 1991). While these data suggest that LRP may be important in the induction of hepatic function in co-cultures, analysis of many different tissues showed that LRP was not present in some tissues known to induce the co-culture response (i.e. vascular endothelium, biliary ductal cells) indicating that the absence of LRP does not prevent induction of hepatic functions.

Hepatocyte differentiation *in vitro* has also been studied without co-culture techniques. A subset of these have focused on the alteration of cell-matrix interactions via manipulation of matrix composition (Matrigel-Bissel et al, 1987), matrix organization (sandwich culture- Dunn et al, 1991),

matrix production (cis-hydroxyproline induced- defect in collagen synthesis, Lee et al, 1992, 1993), integrin interaction with matrix (function-blocking anti-integrin antibodies- Moghe et al, 1997), or addition of matrix products to media (Fujita, 1987; Caron, 1990). These studies have highlighted the importance of hepatocyte-matrix interactions and have specifically implicated Heparan Sulfate Proteoglycan,  $\beta_1$  integrin, and collagen I as important modulators of hepatocyte phenotype. Fibroblasts in vivo and in vitro are well-known to synthesize these and other matrix products and could well be modulating hepatocyte phenotype in co-culture by local deposition of extracellular matrix.

Cell-associated or matrix-bound cytokines could also play a role in our co-culture model. In fact, as with other modes of cell communication, cytokine signaling can modify both hepatocyte and fibroblast function. Fibroblasts are known to secrete a number of cytokines for which hepatocytes have been shown to be responsive. These include interleukin-1, interleukin-6, hepatocyte growth factor (scatter factor), fibroblast growth factor-7 (keratinocyte growth factor), leukemic inhibitory factor, and transforming growth factor- $\beta$  (Michalopoulos et al, 1982; Bauman et al, 1984; Ramadori et al, 1985; Stoker and Perryman, 1985; Stoker et al, 1987; Baumann et al, 1989; Banner and Patterson, 1994; Chedid et al, 1994; Fini et al, 1994; Hirano, 1994; Sporn and Roberts; Strain et al, 1994; 1990). Indeed, many of these cytokines have been reported to have membrane-bound forms including IL-1 $\alpha$  (Dinarello et al, 1991) and matrix-binding characteristics including heparin-binding of KGF (Rubin et al, 1989), ECM-localized binding protein of LIF (Rathgen et al, 1990; Mereau et al, 1993), and collagen-binding of TGF- $\beta$  (Paralkar et al, 1991; Vukicevic et al, 1992). Similarly, hepatocytes have been found to produce a variety of cytokines known to modulate fibroblast behavior including: interleukin-1, acidic fibroblast growth factor, and scatter factor-inducing factor (Bergsteinsdottir et al, 1991; Tsukui et al, 1994; Kan et al, 1989; Baird and Bohlen, 1990; Rosen et al, 1994). Therefore, although our evidence indicated the likelihood of a 'cell-associated' signal to be necessary for induction of hepatic function by fibroblasts, the role of cell or matrix-bound cytokines may also be important.

Finally, we consider the general mechanisms by which mesenchyme transdifferentiate to epithelium during embryonic development (Hay and Zuk, 1995). Such tissue transdifferentiations are essential to normal development and are precisely controlled at many different stages. Gene products implicated in these transformations include cell surface molecules such as E-cadherin a cell-cell adhesion, calcium-dependent protein (Vanderberg and Hay; 1994, Watabe et al, 1994),  $\alpha_6$  integrin (Ekblom, 1989; Ekblom et al, 1994), and the cell surface proteoglycan

syndecan (Kato et al, 1995). In addition, extracellular matrix molecules such as laminin and nidogen may also be important (Ekblom et al, 1994). Soluble growth factors such as hepatocyte growth factor and its interaction with its membrane-bound, tyrosine kinase receptor c-Met have been implicated in transdifferentiation phenomena (Sonnenberg et al, 1993) as well as a host of other gene products involved in expression of epithelial characteristics such as factors found in the spinal cord which promote nephrogenesis (wnt-1, Pax 2; Nusse and Varmus, 1992; Rothenpieler and Dressler, 1993; Herzlinger et al, 1994) and factors which may promote transdifferentiation in the kidney (wnt-4, Pax-8; Stark et al, 1994; Plachov et al, 1990).

## **6.2 Potential Contributors to Finite Penetration Length of Differentiation Signal**

We postulated a wide array of potential contributors to the spatial heterogeneity observed in the hepatocyte phenotype in co-cultures. Of the many possibilities, we discounted the effect of three potential contributors: inadequate delivery of oxygen or other nutrients to center of hepatocyte islands, a primary homotypic effect wherein lack of hepatocyte neighbors in island periphery induced up-regulation of functions, and heterogeneous signaling from fibroblasts attached to the top surface of hepatocytes.

We determined that the role of primary hepatocyte homotypic interactions in induction of spatial heterogeneity of hepatocyte phenotype was not significant. Specifically, we found that when hepatocytes were cultured alone, no spatial variation in intracellular albumin was observed as a result of variations in homotypic interaction. Figure 5.1 shows that hepatocytes in small islands exhibited intense, uniform staining similar to staining (A,C,E,G) patterns of hepatocytes both in the periphery and center of larger islands followed by a spatially uniform decline in liver-specific function at day 6 (B,D,F, H). In contrast, micropatterned co-cultures exhibited marked variations in hepatocyte phenotype where hepatocytes adjacent to the heterotypic interface expressed greater levels of albumin (Figure 5.2, day 6 (B,D,F,H)), indicating that spatial heterogeneity is not an artifact of homotypic interactions. However, the possibility that homotypic interactions modulate hepatocytes' responsiveness to a heterotypic signal must also be considered. Indeed, preliminary agitation experiments showed a deeper, though still incomplete, 'penetration' of the differentiation signal into the hepatocyte islands late in culture when compared to static controls, indicating that homotypic soluble products may affect the receptivity of hepatocytes to a differentiation signal (data not shown).

The adequacy of diffusive transport of oxygen and other transport was determined by comparison of static and agitated micropatterned co-cultures- in both cases, a similar pattern of induction was observed at day 4 (Figure 5.6), indicating convective mixing of media did not modify hepatocyte behavior. Finally, the contribution of overlying fibroblasts in the observed spatial heterogeneity was also determined to be minimal. Fibroblasts were noted to adhere to the top surface of spread hepatocytes at larger dimensions of hepatocyte islands with dual label vital dyes and fluorescent microscopy (data not shown); however, experiments performed to separate cell populations effectively prevented fibroblast attachment to the surface of hepatocytes under these conditions (Figure 5.4A). Therefore, we assessed the presence of spatial heterogeneity resulting from highly characterized initial conditions. After 8 days of contact between cell types, intracellular albumin immunostaining indicated the presence of peripheral staining and persistence of the heterogeneous hepatocyte response (Figure 5.5B). We concluded that spatial heterogeneity could not be attributed to variations in signals arising from overlying fibroblasts.

In contrast, other potential contributors to spatial heterogeneity were considered and may play a significant role. These include gap junctional communication, physical penetration of fibroblast processes, and diffusion of factors through 'tissue phase' as opposed to overlying 'liquid phase'. Homotypic gap junctions could serve to propagate the differentiation signal from the heterotypic interface inward. Indirect immunofluorescent staining (Connexin 32 antibody acquired from Dr. David Paul, Harvard Medical School) showed presence of gap junctions in co-cultures at day 6 (data not shown). In addition, microinjection with Lucifer Yellow suggested functionality of these junctions at day 7 (data not shown). These data agree with others who have reported presence of functional homotypic, but not heterotypic, gap junctions in mature co-cultures (Mesnil et al, 1987). Indeed, these cell junctions which allow passage of molecules of less than 1200 Daltons, could play an integral role in propagation of the signal from the heterotypic interface to subsequent hepatocytes (Lowenstein et al, 1979). One could postulate that the signal to differentiate would cease to propagate, thereby generating spatial heterogeneity in the hepatocyte phenotype, by a variety of mechanisms including: (1) lack of functional gap junctions in central hepatocytes (2) modulation of gap junctional gating in central hepatocytes or (3) finite diffusive distance of signal arising in outer ring of hepatocytes- i.e. second messengers like cAMP could escalate only in the cells in the periphery and this signal could continue to signal adjacent hepatocytes until the concentration of cAMP fell under a threshold for activation. Future experiments will assess the dependence of spatial

heterogeneity on gap junctions by correlation of both kinetic and spatial behavior of connexin 32 expression with intracellular albumin expression.

Similarly, the role of fibroblast processes in spatial heterogeneity may be addressed by specific staining of the fibroblast cytoskeleton (i.e. intermediate filament specific to mesenchymal cells such as vimentin) or electron microscopy. This cause of spatial heterogeneity would correlate well with the hypothesis that neural cell contact with hepatocytes is the cause of zonal heterogeneity in the liver acinus (Wolfle et al, 1981). Future studies are underway to investigate the importance of this parameter in spatial heterogeneity which we observed.

Another possible cause for the well-demarcated ring of intense albumin staining is diffusion of signaling molecules in the 'tissue phase' of the culture, i.e. enmeshed with cell cytosol and hydrated extracellular matrix of the confluent cell population. Molecules secreted at the basal surface of fibroblasts may not have access to the 'fluid phase' and be forced to diffuse through the cellular microenvironment with a greatly reduced diffusivity. Spatial heterogeneity would result from diffusion of signals to target hepatocytes at bioactive concentrations; therefore, distal hepatocytes would not be exposed to critical concentrations of signaling molecules. This mechanism for induction of spatial heterogeneity would correlate well with the results of Schrode et al (1990) who invoked similar principles to explain the localization of glutamine synthetase-positive pericentral hepatocytes in the periphery of hepatocyte islands co-cultured with liver epithelial (ductal) cells.

### **6.3 Limitations of Experimental Method**

While the combined use of microfabrication techniques coupled with traditional methods allowed us to gain some insight into the mechanisms by which hepatocytes and mesenchymal cells communicate, individual experiments had some inherent limitations. For example conditioned media experiments have long been criticized for the inability to assess the role of 'freely soluble' rapidly degraded or dilute biochemicals and the potential for transfer of cells as well as media to the target hepatocyte population. We performed separate experiments to assess the role of rapidly degraded or diluted biochemicals and examined target hepatocyte populations microscopically to ensure minimal fibroblast contamination. Similarly, separation of cell populations was utilized to assess the role of rapidly degraded, freely soluble signals; however, 'capping' of hepatocytes to prevent attachment of fibroblasts to the surface of hepatocytes generated a period of relative hypoxia for 1 hour in enclosed hepatocytes. We assessed potential artifacts arising from this insult by comparison to 'uncapped'

controls for presence of cell blebbing, viability, and patterns of immunostaining. Last, 'cell-associated' signal were assessed by use of agitation experiments. While we did not observe significant differences in patterns of immunostaining between static and agitated cultures, fluid convection generated shear stresses at the cell surface. We attempted to minimize shear stress by agitating at only 1 Hz; however, the role of shear on co-cultures will need to be addressed further, especially for perfused bioreactor applications. Despite the individual limitations of each experiment, our results interpreted as a whole continue to support the conclusion that 'freely soluble' fibroblast products do not induce hepatic functions.

Finally, we address the role of tissue reorganization on spatial heterogeneity in hepatocyte phenotype. Notably, reorganization of cultures (both hepatocytes alone and co-cultures) was observed in smaller pattern dimensions and was significantly diminished in large hepatocyte islands (greater than 490  $\mu\text{m}$ ). In these studies, pattern configuration at later time points was perturbed by morphogenesis in the tissue- i.e. observed patterns of staining were dictated not only by initial pattern configuration but also by the long-term conformation adopted by the culture. For example, 100  $\mu\text{m}$  islands did not display spatial heterogeneity in albumin staining, presumably because they reorganized to a pattern where all hepatocytes were proximal to the heterotypic interface. In contrast, 36  $\mu\text{m}$  islands reorganized to larger dimension 'cord-like' hepatic structures where some hepatocytes were a greater distance from the heterotypic interface, resulting in spatial heterogeneity of hepatocyte phenotype. Despite the existence of reorganization in these tissues, the fundamental pattern of spatial heterogeneity remained constant- hepatic structures larger than 100  $\mu\text{m}$  exhibited spatial heterogeneity in hepatocyte phenotype wherein hepatocytes far from the heterotypic interface exhibited low levels of intracellular albumin. Therefore, our conclusion that the potential causes of spatial heterogeneity include gap junctional communication, 'tissue phase' signal diffusion, and physical penetration of fibroblasts, remains well founded.

## 7. SUMMARY AND FUTURE WORK

This study combined conventional culture techniques with microfabricated co-cultures to examine mechanisms of cell communication. We determined that the primary signal for induction of liver function in hepatocytes in hepatocyte/fibroblast co-cultures is tightly fibroblast-associated. Possible mechanisms for the finite penetration of the differentiation signal include: gap junctional communication, 'tissue phase' diffusion of signaling

molecules, and/or physical penetration of fibroblast processes. With respect to design of a co-culture-based bioreactor, evidence that the signal is fibroblast-associated implies that fibroblasts and hepatocytes must have direct contact (i.e. occupy the same compartment in a bioreactor) to produce adequate levels of liver-specific function. Further examination of the molecular nature of the signal, such as the role of membrane-bound liver regulating protein (LRP), would also be valuable for complete replacement of fibroblasts with a few necessary biochemical signals. Furthermore, the lack of freely soluble factors suggests streamlining of future mechanistic studies wherein many spatial configurations may be studied in parallel—previously, each disc contained a single, repeating pattern due to the potential for humoral signals. These studies will allow the examination of candidate biochemical signals as well as spatial configurations which minimize the fraction of hepatocytes far from the heterotypic interface, creating the potential for further improvements in bulk tissue function. Finally, the well-demarcated zone of differentiated hepatocytes in the area of the heterotypic interface, suggests that the heterotypic interface may be the key determinant of the level of tissue function. In the next chapter, we will utilize this observation to try and develop optimization strategies that allow for maximal heterotypic interface while utilizing fewer total fibroblasts (i.e. ‘background’ fibroblasts) for applications in bioreactor design. Furthermore, we will evaluate the implications of this optimization on bioreactor function using theoretical modeling of fluid mechanics and mass transport in a prototypical bioreactor configuration.

## Chapter 6

# Optimization Of Hepatic Function In Co-Cultures

### 1. OVERVIEW

Clinical implementation of hepatocyte-based bioreactors has historically been limited by (1) stability of hepatic function necessitating expensive 'cartridge' replacements every few hours (Rozga et al, 1994), (2) limited ability to scale-up (Nyberg et al, 1993; Wu et al, 1995), (3) large reactor volume causing dilution of hepatocyte products (Takahashi et al, 1992) and (4) adequate cell source (for recent reviews see- Rozga et al, 1993; Sussman and Kelly, 1995; Jauregui et al, 1996). A novel co-culture based bioreactor should address each of these limitations. We have shown previously that co-cultivation of hepatocytes with 3T3-J2 fibroblasts yielded stable hepatic function on the order of weeks to months. Furthermore, microfabrication techniques such as those utilized here offer unique advantages for scale-up by replication of many, identical units as seen in the integrated circuit industry. Here, we address the optimization of co-cultures to minimize reactor volume and to maximize cell function (minimize necessary cell source).

While we have demonstrated the ability to modulate stable, liver-specific functions through variation in initial cellular microenvironment with micropatterning techniques, we have utilized an excess of fibroblasts thus far. We have previously shown the prevalence of differentiated hepatic function at the heterotypic interface, and amassed significant evidence that the signal for hepatocyte differentiation is associated with the fibroblast-surface. These results indicate the potential for reduction of the surface area dedicated to fibroblasts by elimination of 'background' fibroblasts while



preserving the heterotypic interface. Indeed, the *in vivo* ratio of stromal:parenchymal cells of approximately 0.5 is an order-of-magnitude lower than the 3T3:hepatocyte ratio utilized in our previous studies (Naughton, 1995). In this chapter, we describe efforts to minimize fibroblast number without compromising hepatic function. We attempt to 'optimize' hepatic function per unit area by preservation of the heterotypic interface using micropatterning techniques and polymer elastomer surface masking (methods described in detail in Chapter 2). In addition, while we previously determined the importance of cellular microenvironment in determining levels of hepatic function, we have not yet addressed the role of the cellular microenvironment in the kinetics of up-regulation of liver-specific functions. The use of microfabrication in modulating these kinetics has the potential to create bioreactors which could be utilized soon after seeding- increasing flexibility of clinical implementation and reducing cost. Another biological parameter which affects the design and clinical utility of a device is the source of primary hepatocytes. Maximizing hepatocyte function would serve to reduce the required cell mass for a reactor (and therefore the cost) as well as offering important flexibility in the reactor design. Here, we compare the functional output of co-cultures of hepatocytes with 3T3-2 fibroblasts with other well-accepted methods of stabilizing hepatocyte function *in vitro*. Finally, we utilize simple models of oxygen transport and fluid flow to generate design criteria for a multi-unit, co-culture based bioreactor.

## 2. **REDUCTION OF FIBROBLAST:HEPATOCTE RATIO WHILE PRESERVING HETEROTYPIC INTERFACE IN MICROPATTERNED CO-CULTURES**

Since our earlier experiments on hepatocyte phenotype in co-cultures suggested up-regulation of liver-specific functions at the heterotypic interface, we investigated novel spatial configurations which preserved the same heterotypic interface but allowed reduction of fibroblast number. Our approach is schematically represented in Figure 2.3. Identical number of hepatocytes and initial heterotypic interactions are present in all conditions; however, surface area dedicated to fibroblasts is reduced by reduction of center-to-center island spacing.

Micropatterned cultures for preservation of heterotypic interface were fabricated using 490  $\mu\text{m}$  diameter hepatocyte islands due to the long-term pattern stability in co-cultures of this size (see Chapter 2). Center-to-

center spacing was reduced in order to progressively reduce the area dedicated to fibroblast adhesion by twelve-fold. Figure 6.1 shows phase contrast micrographs of four different patterns of  $\sim 250,000$  hepatocytes alone with center-to-center spacing from  $1230 \mu\text{m}$  to  $930$ ,  $650$ , and then  $560 \mu\text{m}$ . Well-defined structures were achieved even at relatively high packing densities. Figure 6.2 demonstrates the preservation of heterotypic interface after addition of growth arrested fibroblasts in fibroblast:hepatocyte ratios of 6:1, 3:1, 1:1, and 0.5:1.

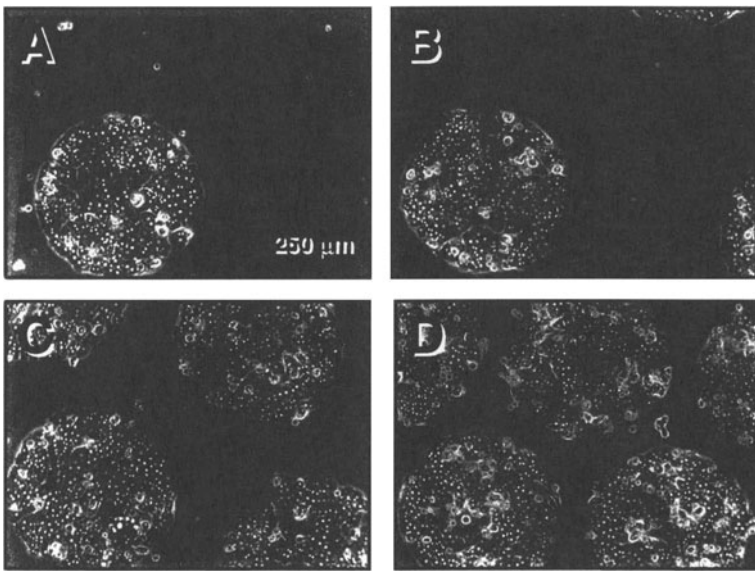


*Figure 6.1.* Phase Contrast Micrograph of Micropatterned Hepatocytes With Reduced Center-to-Center Spacing. Island Diameter,  $490 \mu\text{m}$ , Center-to-Center Spacing A)  $1230$ , B)  $930$ , C)  $650$ , and D)  $560 \mu\text{m}$ . Patterned surface area was also reduced in order to preserve similar hepatocyte numbers between conditions.

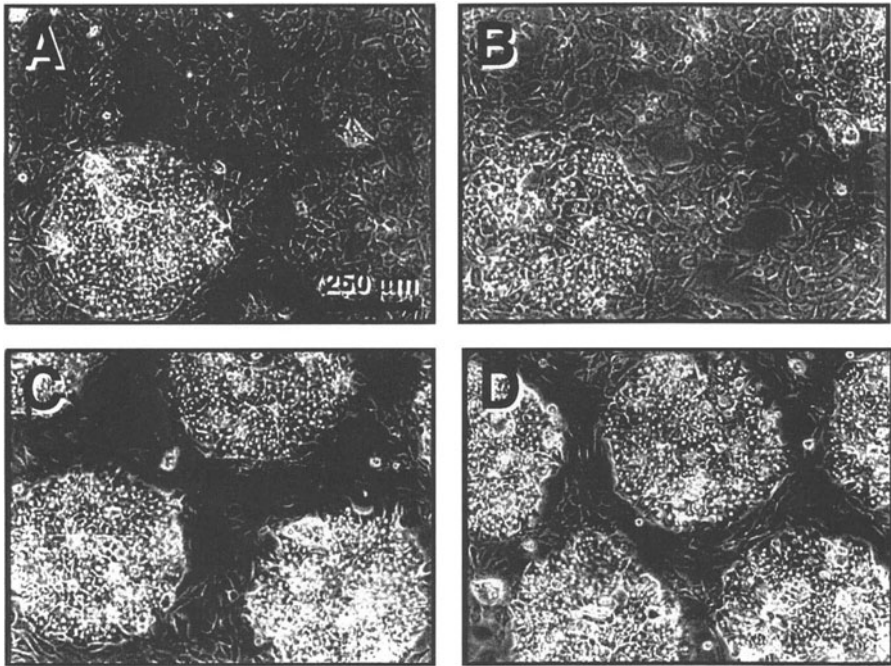


*Figure 6.2.* Phase Contrast Micrograph of Micropatterned Co-Culture with Reduced Spacing. Growth-arrested fibroblasts are seen between hepatocyte islands. Fibroblast:Hepatocyte Ratio varied from A)6:1, B)3:1, C)1:1, to D)0.5:1. Patterned surface area was also progressively reduced.

We probed the level of function of these micropatterned co-cultures by measurement of two liver-specific functions, albumin secretion as a marker of protein synthesis, and urea synthesis as a marker of metabolic function. Figure 6.3 shows that stable production of urea of 100-200  $\mu\text{g}/\text{day}$  was achieved by day 6 in all conditions. In general, reduction of fibroblast number caused a reduction of steady-state urea production; however, the effect was highly non-linear. Reduction of fibroblast number by twelve-fold resulted in approximately two-fold reduction in steady-state urea synthesis. Similarly, albumin synthesis for micropatterned co-cultures with preserved heterotypic interface is seen in Figure 6.4. Again, all cultures demonstrated induction of this liver-specific function, as evidenced by the increase in albumin secretion to 20-60  $\mu\text{g}/\text{day}$  over 11 days of culture. A similar trend in functional dependence on fibroblasts was observed wherein reduction of fibroblast:hepatocyte ratio by twelve-fold led to approximately two-fold reduction in albumin secretion. In comparison, micropatterned hepatocytes

in the absence of fibroblasts of 490  $\mu\text{m}$  diameter and center-to-center spacing of 1230  $\mu\text{m}$  produced negligible amounts of albumin (See Chapter 4). We concluded that reduction of fibroblast number in co-cultures with preservation of heterotypic interface resulted in some loss of liver-specific functions; however, even the lowest fibroblast:hepatocyte co-culture ratio of 0.5:1 resulted in a differentiated hepatocyte phenotype when compared to hepatocytes cultured alone. These data will be useful in optimization of liver-specific function per unit area for design of bioreactor specifications.

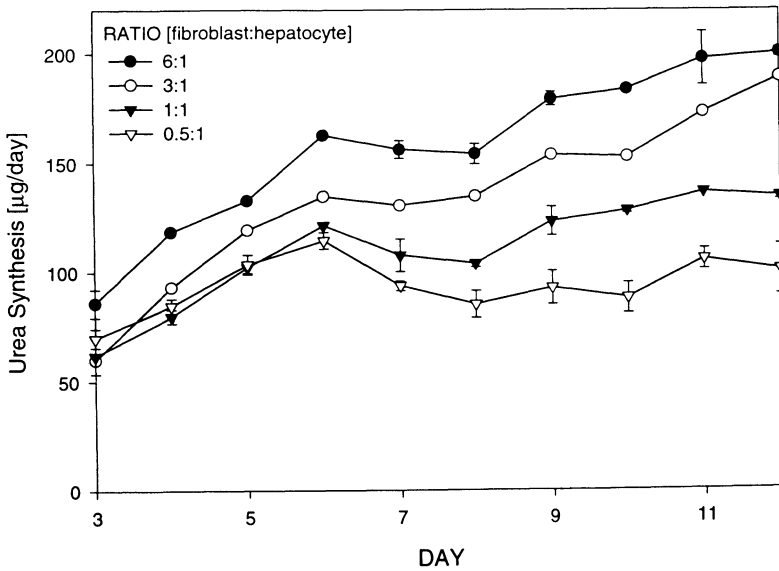


Figure 6.3. Urea Synthesis for Micropatterned Co-Cultures with Reduced Fibroblast:Hepatocyte Ratio and Similar Heterotypic Interface. Numbers of hepatocytes are approximately identical in all conditions.

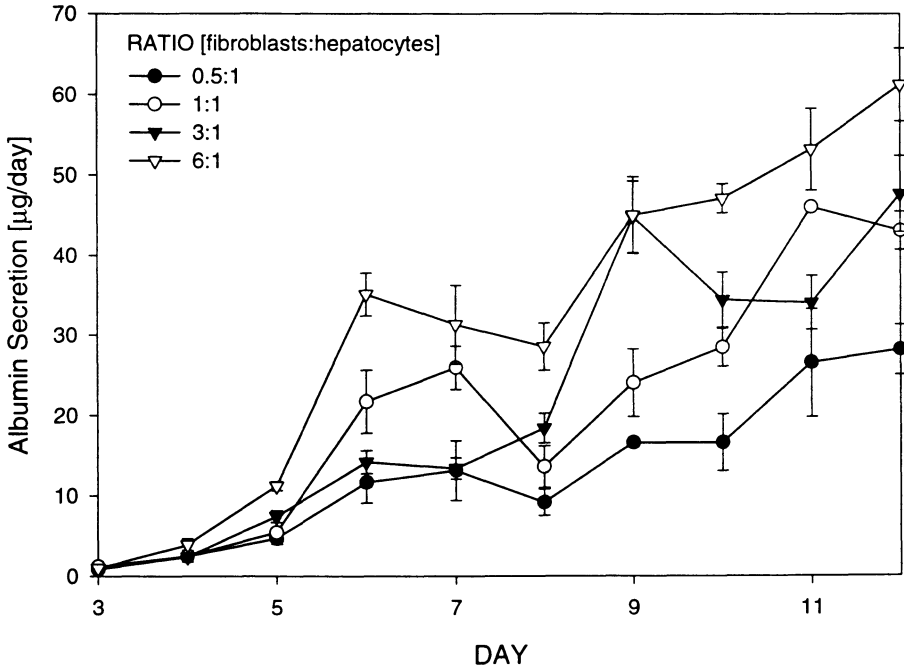


Figure 6.4. Albumin Secretion for Micropatterned Co-Cultures with Reduced Fibroblast:Hepatocyte Ratio and Similar Heterotypic Interface. Numbers of hepatocytes are approximately identical in all conditions.

### 3. REDUCTION OF FIBROBLAST:HEPATOCYTE RATIO WITHOUT CONTROL OF HETEROTYPIC INTERFACE IN CONVENTIONAL, RANDOMLY-DISTRIBUTED CO-CULTURES

In order to evaluate the value of preservation of the heterotypic interface in co-cultures, we performed similar experiments on reduction of fibroblast:hepatocyte ratio in conventional, randomly-distributed cultures. We examined urea synthesis and albumin secretion (Figures 6.5 and 6.6). Interestingly, fibroblast:hepatocyte ratios of greater than 2:1 (inclusive)

yielded a differentiated hepatocyte phenotype by 7 days as assessed by both these markers. Urea synthesis was found to plateau between 100 and 200  $\mu\text{g/day}$  and albumin secretion between approximately 30 and 80  $\mu\text{g/day}$ . In contrast, lower fibroblast:hepatocyte ratios yielded decline in liver-specific functions to background levels, similar to hepatocytes cultured alone. This apparent bifurcation occurred between 500,000 and 250,000 fibroblasts in a 20  $\text{cm}^2$  dish. Under these conventional culture conditions, reduction of fibroblasts below a threshold led to critically reduced heterotypic interaction and substantial loss of functional capacity of the resulting tissue.

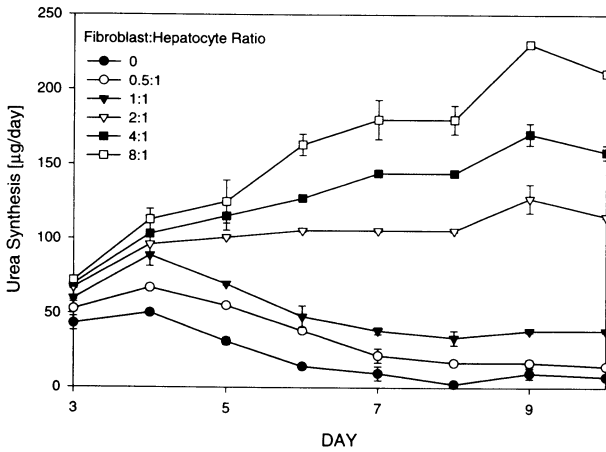


Figure 6.5. Urea Synthesis of Randomly-Distributed Co-Cultures with Reduced Fibroblast:Hepatocyte Ratio. Numbers of hepatocytes are approximately identical in all conditions.

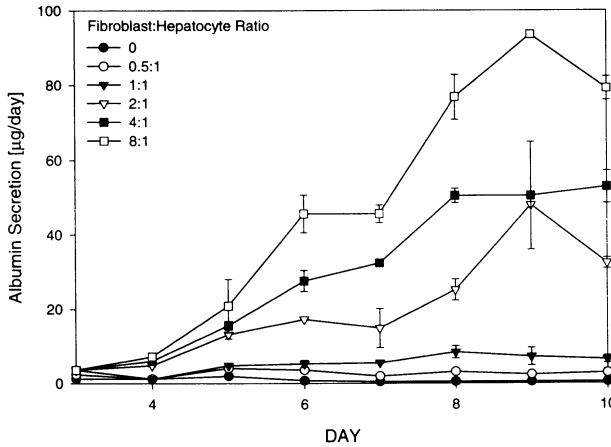


Figure 6.6. Albumin Secretion of Randomly-Distributed Co-Cultures with Reduced Fibroblast:Hepatocyte Ratio. Numbers of hepatocytes are approximately identical in all conditions.

#### 4. COMPARISON OF MICROPATTERNED AND RANDOMLY-DISTRIBUTED CO-CULTURES

Here, we explicitly compare micropatterned cultures with conventional culture to highlight the achievable improvements in kinetics of up-regulation and levels of function. Figures 6.7A and plot one representative ratio (fibroblast:hepatocyte ratio of 0.5:1) to emphasize the quantitative and qualitative differences in hepatic function. Albumin secretion increases dramatically in the micropatterned condition whereas the same cell populations in conventional, unpatterned culture do not produce significant levels of albumin. Similarly, urea synthesis remains stable for 11 days of co-culture in the micropatterned condition as compared to a steady decline in randomly distributed cultures of the same initial populations. Thus, we have modified the long-term hepatocyte phenotype by controlling initial cell-cell interactions. Furthermore, examination of these data from through a classical dose-response curve demonstrates a shift of the (approximately) sigmoidal dose-response curve, with a reduction in the  $K_m$  (fibroblast number necessary to elicit a half-maximal response) by four-fold (Figure 6.7C).

Finally, we examine the differences in kinetics of up-regulation of liver-specific functions between conventional co-culture and micropatterned

co-culture\*. Figure 6.7D shows that the increase in urea synthesis in certain micropatterned configurations (490  $\mu\text{m}$  islands) precedes that of the conventional, unpatterned controls by almost one week. Other micropatterns (17800  $\mu\text{m}$  islands), due to variations in initial cell-cell interactions, displayed lower, steady-state levels of urea synthesis. Interestingly, while randomly-distributed cultures produced low levels of urea initially (as in the larger micropatterns), they up-regulated levels of urea synthesis over the next week. These results indicated that micropatterned co-cultures have both kinetic and functional advantages over conventional cultures. We hypothesize that initial cell-cell interactions contribute significantly to these responses.

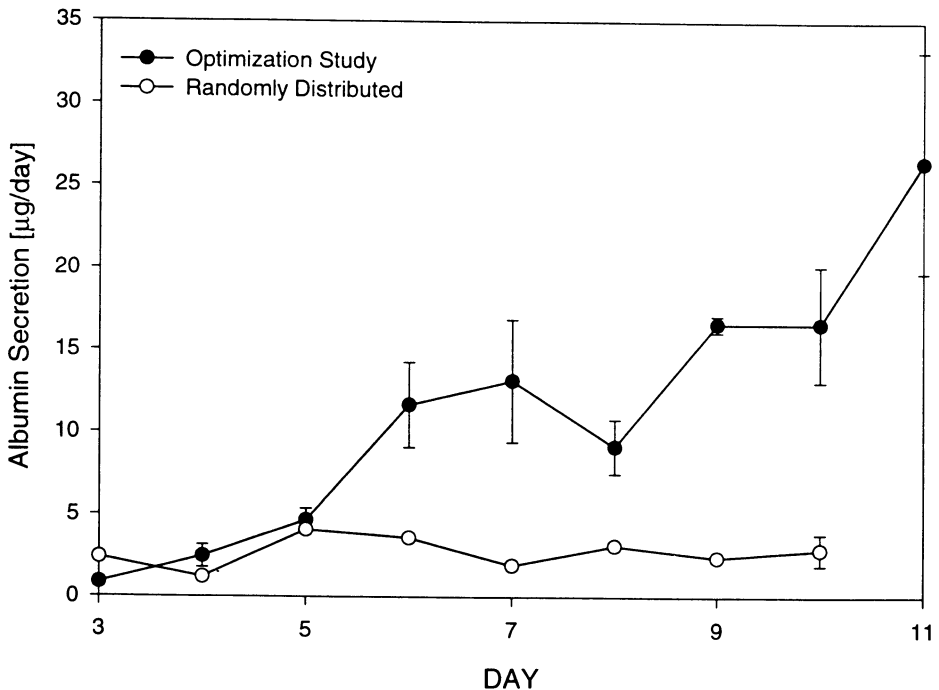


Figure 6.7. Comparison of Micropatterned Co-Cultures to Randomly-Distributed Co-Cultures. A. Pattern Of Induction Of Albumin Secretion Varies In Fibroblast:Hepatocyte Ratio Of 0.5:1.

\* These experiments were conducted with 750K fibroblasts (non growth-arrested) and ~250K hepatocytes in all 3 conditions



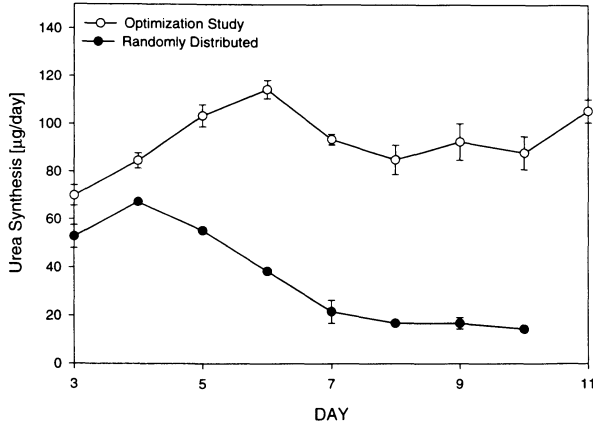


Figure 6.7B. Pattern Of Induction Of Urea Synthesis Varies In Fibroblast:Hepatocyte Ratio Of 0.5:1.

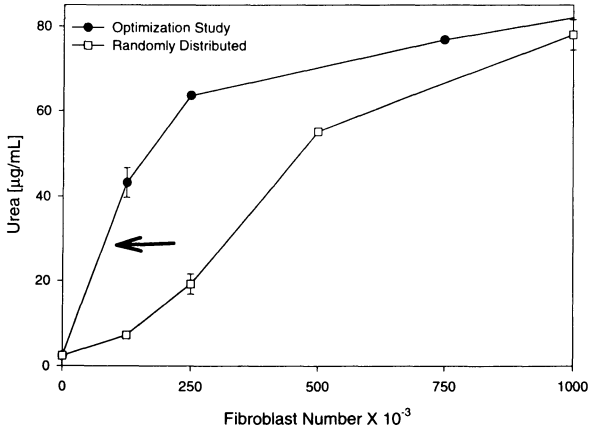


Figure 6.7C. Dose Response of Urea Synthesis as a Function of Fibroblast Number in Micropatterned versus Randomly-Distributed Cultures.  $K_m$  of micropatterned cultures  $\sim 1/4$  of  $K_m$  of randomly-distributed co-cultures.

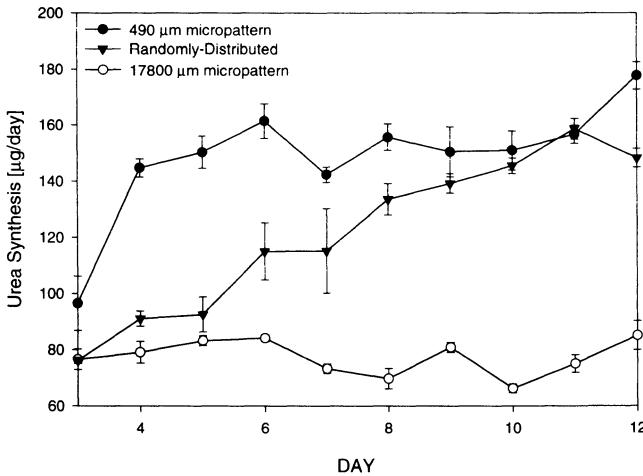


Figure 6.7D. Kinetics of Up-Regulation of Urea Synthesis

## 5. DISCUSSION

In this study we attempted to optimize tissue function of hepatic co-cultures for use in a bioreactor utilizing microfabrication techniques. Specifically, we investigated the potential for reduction of fibroblast number, and thereby surface area dedicated to mesenchymal cells, without deleterious effects on hepatic function. In addition, we examined whether the kinetics of up-regulation of liver-specific functions could be improved by manipulation of the initial cellular microenvironment. We compared our maximum achievable levels of function to other *in vitro* systems in order to assess the cell mass necessary for bioartificial liver applications. Finally, a simple fluid mechanics model is coupled to oxygen transport in a hypothetical device to estimate design criteria for a co-culture based bioreactor.

### 5.1 Optimization of Fibroblast:Hepatocyte Ratio

Evidence indicated that reduction of fibroblast number by an order of magnitude either, (1) had only a modest negative effect on hepatic functions or (2) diminished the hepatocellular function completely, depending on the cellular microenvironment. Conventional, randomly-distributed cultures were found to have a marked decline in both albumin secretion and urea synthesis with reduction of fibroblast:hepatocyte ratio (Figures 6.5, 6.6).

Approximate physiologic values for stromal:parenchymal ratio for the liver of 0.5 produced a de-differentiated hepatocyte phenotype as determined by morphology (detached, fibroblastic- data not shown), albumin secretion of less than 5  $\mu\text{g}/\text{day}$ , and urea synthesis of less than 20  $\mu\text{g}/\text{day}$  (Figure 6.7). In contrast, we argued that since our previous results indicated that a fibroblast-associated signal for hepatocyte differentiation originated at the heterotypic interface, preservation of the heterotypic interface while reducing 'background' fibroblasts could serve to preserve tissue function (Figures 6.1, 6.2). In fact, microfabricated and polymer-masked substrates with preserved heterotypic interface and reduction of fibroblast:hepatocyte ratio of 0.5 produced a relatively stable, well-differentiated, hepatic phenotype as assessed by morphology (cuboidal cells with distinct nuclei and distinct intercellular borders-data not shown), albumin secretion greater than 20  $\mu\text{g}/\text{day}$ , and urea synthesis greater than 100  $\mu\text{g}/\text{day}$  (Figure 6.7). Thus, use of microfabrication allowed the preservation of hepatic function with a twelve-fold reduction in fibroblast number causing only a two-fold reduction in liver-specific functions as compared to undetectable levels of hepatic markers in similar, randomly-distributed, conventional cultures (Figures 6.3, 6.4). The dramatic loss of function for randomly-distributed cultures is not surprising- seeding of small numbers of fibroblasts on a 20  $\text{cm}^2$  plate with approximately 2.5  $\text{cm}^2$  of hepatocyte coverage, would result in a low probability of extensive heterotypic contact. Poor function in randomly-distributed, low fibroblast number cultures, is also consistent with studies by Mesnil et al (1987) where hepatocytes were microscopically observed to lose viability in the absence of local mesenchymal contact.

The preservation of heterotypic interface while reducing fibroblast number, while successful in maintaining a differentiated hepatocyte phenotype, did not completely prevent a decline in liver-specific functions (Figures 6.3, 6.4). The two-fold loss of function implied that heterotypic interface is not the sole contributor to hepatic function. Potential causes for this decline in function include: modification of homotypic fibroblast signaling via cytokines or matrix, synergy of fibroblast-associated signal at heterotypic interface with some reduced concentration of a soluble fibroblast product, or some homotypic hepatocyte inhibition due to increase in local hepatocyte packing density. Cytokines known to have homotypic fibroblast signaling capability include interleukin-1 (Fini et al, 1994; Bergsteinsdottir et al, 1991), basic fibroblast growth factor (Baird and Klagsburn; 1991), and transforming growth factor- $\beta$  (Sporn and Roberts, 1990). Similarly, mesenchymal matrix products such as collagen I and fibronectin may play a role in homotypic signaling. These types of homotypic fibroblast signals could result in an altered composition of the heterotypic interface either by modification of fibroblast membrane-bound

proteins, locally secreted ECM, or variation in matrix or fibroblast-associated cytokines, which are presented to the hepatocyte surface. Cooperative signaling of at least two signals (i.e. membrane-bound protein and secreted factor) may also be important for hepatocyte differentiation. One significant example of this type of cell signaling is found in bone marrow stromal cell/hematopoietic cell interaction where the stromal cell product, stem cell factor, requires other growth factors for hematopoietic cell proliferation and differentiation (Handin et al, 1995). Finally, we speculate that increased packing of hepatocyte islands may have some down-regulatory effects on hepatocyte function. This type of 'long-range' inhibition could be due to local depletion of nutrients or local accumulation of metabolites or 'inhibitors'. A teleological explanation for this type of inhibition would be the cessation of up-regulated function after regenerative recovery from hepatic damage- hepatocyte density would increase and induce down-regulation in adjacent hepatocytes in order to preserve a constant level of overall liver function.

## **5.2 Kinetics of Up-Regulation of Hepatic Functions**

In order to further optimize tissue function for use in a bioreactor, we also investigated the kinetics of 'recovery' of liver-specific functions after initiation of co-culture. Typically, co-culture with mesenchymal cells induced hepatic functions on the order of 7-10 days (Figure 6.7D); however, in order to be able to utilize a bioreactor soon after cell seeding, we examined the utility of controlling initial cellular microenvironment in accelerating this up-regulation. We found that certain functions can be induced up to 1 week earlier by use of micropatterning. Specifically, a ~2-fold improvement in urea synthesis was noted early in culture in all three small hepatocyte island configurations (36, 100, 490  $\mu\text{m}$  -See Chapter 4). This level of urea synthesis reached a plateau by day 4 whereas randomly-distributed cultures steadily increased the amount of daily urea production until day 10. Subsequently, both cultures performed similarly. In contrast, large micropatterned island (17800  $\mu\text{m}$ ) had no improvement in initial levels of urea production, suggesting that cellular microenvironment played a role in modulating these kinetics.

The differences in kinetics observed between randomly-distributed cultures and smaller micropatterned co-cultures, have a number of potential causes. The most likely modulator of this response is the initial cell-cell interactions- indeed, randomly-distributed cultures reorganize over 7-10 days into cord-like structures (data not shown) and could be achieving more favorable cell-cell interactions as time progresses. In contrast, 490  $\mu\text{m}$  micropatterns and 17800  $\mu\text{m}$  micropatterns did not reorganize over time,

therefore a fixed cellular microenvironment led to relatively constant levels of urea synthesis with higher degree of heterotypic interaction (490  $\mu\text{m}$ ) leading to increased urea synthesis at the onset of co-cultures. While cell-cell interactions are a likely candidate for modulators of this response, the remodeling of the substrate by extracellular matrix deposition of both cell types must also be considered. Note that randomly-distributed cultures consisted of fibroblast adhesion on collagen I and serum-adsorbed proteins whereas micropatterned co-cultures consisted of fibroblasts on serum-adsorbed proteins alone. Fibroblasts in randomly-distributed cultures are likely to modify the extracellular matrix environment by secretion of local ECM. Matrix is well-known to modify cellular responses of all kinds, notably integrin expression in response to soluble growth factors (Xu and Clark, 1995). In addition, collagen I binding is integrin mediated (Hynes, 1992). Therefore, matrix deposition and/or cellular reorganization may play important roles in the kinetics of up-regulation. One experiment to examine the relative role of matrix versus cellular microenvironment would be use of micropatterning techniques to generate a randomly-distributed culture- this culture would have a diversity of initial cell-cell contacts but would preserve hepatocyte adhesion on collagen I and fibroblast adhesion on serum-adsorbed proteins. Cultures could be examined for urea synthesis to measure the kinetics of up-regulation and also stained with hepatocellular markers to track cellular reorganization.

Finally, we address the selectivity of this response (improved kinetics of up-regulation) to urea synthesis. Other liver-specific markers such as albumin did not display this behavior (data not shown). Indeed, the pattern of recovery for different markers of liver-specific function is known to vary in other in vitro hepatocyte systems (Dunn et al, 1991). We hypothesize that improved kinetics of albumin up-regulation are not observed in micropatterned co-cultures due to the extended recovery after isolation for this particular function; therefore, differences in level of hepatic function would not be clearly manifested until the requisite cellular machinery is intact. Dunn et al, 1992, hypothesized that albumin secretion is dependent on average polyribosomal size and showed that polyribosomal assembly requires approximately 1 week to recover from hepatocyte isolation. In addition, this and other protein secretion pathways require intact packaging and vesicular trafficking pathways, which may also recover over this time frame. In contrast, small biochemicals like urea can be easily synthesized from amino acids in the presence of the necessary enzymes without polyribosomal translation, packaging, or vesicular trafficking. The pattern of up-regulation which other functions (such as detoxification via P450 enzymes) display will need to be empirically determined.

### **5.3 Comparison of Observed Hepatic Function to In Vivo and In Vitro Values**

In order to estimate the parenchymal cell mass necessary to assemble a bioreactor, we compared maximum achievable levels of function in our micropatterned co-cultures to in vivo values and other in vitro methods for achieving differentiated hepatic functions (Figure 6.8). Co-cultures of hepatocytes with NIH 3T3-J2 fibroblasts produced far more albumin than all other cultures. In particular, randomly-distributed cultures produced 4 to 8-fold more albumin per hour than co-cultures with other 3T3 subclones, rat liver epithelial cells, and rat dermal fibroblasts, as well as hepatocytes cultured alone between layers of collagen I gel (sandwich) or on top of matrigel (Guguen-Guillouzo et al, 1983; Morin et al, 1988; Dunn et al, 1991; Moghe et al, 1996). Micropatterned co-cultures varied in the kinetics and absolute level of protein production- smaller patterns achieved high levels of function 1 week prior to randomly-distributed cultures, whereas large islands performed only as well as other culture techniques described above. Another marker of hepatic function, urea synthesis showed up-regulation in our co-cultures when compared to sandwich cultures by 8-fold (data not shown). Clearly, in order to replace the wide array of liver functions necessary for survival, other markers of hepatic function (such as P450 detoxification) should be characterized in our co-culture system. Preliminary evidence indicated that P450IA1 also showed 8-fold increased activity in co-cultures with 3T3-J2 fibroblasts as compared to another in vitro method of stabilizing liver-specific functions, sandwich culture (data not shown).

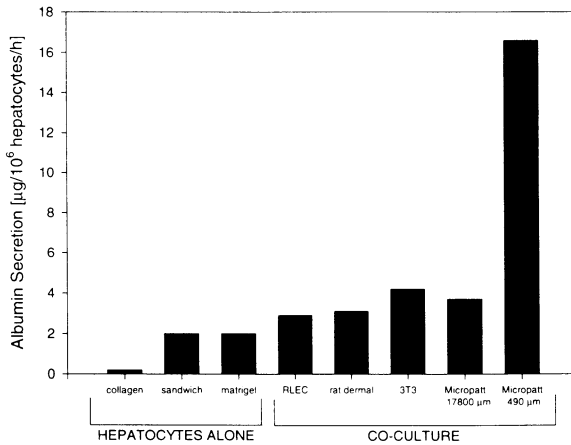


Figure 6.8. Comparison of Albumin Secretion in Hepatic Tissues In Vitro. Albumin secretion per  $1 \times 10^6$  cells was approximated from experimental data and available literature.

The human liver in vivo, consisting of  $150\text{-}250 \times 10^9$  hepatocytes (Rozga et al, 1993), produces approximately 12 g of albumin daily, or approximately  $2\text{-}3.3 \mu\text{g}/10^6$  hepatocytes/h (Harfenist and Murray, 1993). Therefore, our microfabricated co-cultures were superior ( $\sim 8$ -fold) to this, steady-state, physiologic synthesis of plasma proteins. Similarly, the human liver excretes approximately 16.5 g of nitrogen daily with 80-90% of nitrogen excretion in the form of urea<sup>†</sup> or  $5\text{-}8 \mu\text{g}/10^6$  hepatocytes/h (Rodwell et al, 1993). Our microfabricated cultures were also superior ( $\sim 5$ -fold) to the steady-state, physiologic excretion of urea. The specific mechanism for such dramatic improved function in co-cultures with this particular subclone of murine NIH 3T3 fibroblasts is unknown; however, these data indicate that a genetic approach such as subtractive hybridization with another 3T3 clone (i.e. 3T3 A31) could generate a relatively small list of candidate factors. The superior performance of murine stromal cells in co-culture to other cell types is not unprecedented- for example, a murine bone marrow stromal cell product, stem cell factor (SCF), shows 80% homology to human SCF, however while murine SCF is active on human cells, human SCF is 800-fold less active on mouse cells (Martin et al, 1990).

<sup>†</sup> molecular weight of urea=60; 28 from nitrogen, 32 non-nitrogen, therefore 47% of urea by weight is nitrogen

## 5.4 Design Criteria for Co-Culture-Based Bioreactor

The data presented above can be utilized to estimate the cell mass necessary to create a bioartificial liver to support a rat in liver failure. The fraction of liver mass necessary for survival has been estimated between 2-12% of the liver (Demetriou et al, 1988; Asonuma et al, 1992). This value has become widely accepted as the cell mass necessary for a temporary bioartificial liver support system. Because, our co-cultures will necessitate 4 to 8-fold fewer isolated cells than other culture techniques, we may be able to replace liver function with 0.3 - 3% of the hepatocytes in the liver. Assuming approximately 600 million hepatocytes per rat, this corresponds to 1.8 -18 million hepatocytes in microfabricated co-culture with 3T3-J2 cells in a device. We chose an intermediate value of 10 million hepatocytes for a hypothetical bioreactor.

A schematic of a hypothetical bioreactor is seen in Figure 6.9. In order to mimic the acinar structure of the liver and take advantage of the replicative advantages of microfabrication, we chose repeating subunits of 250,000 hepatocytes, approximating the number of hepatocytes in a single lobular unit in vivo. Thus, 40 lobular units of micropatterned co-cultures will be perfused with patient blood or plasma.



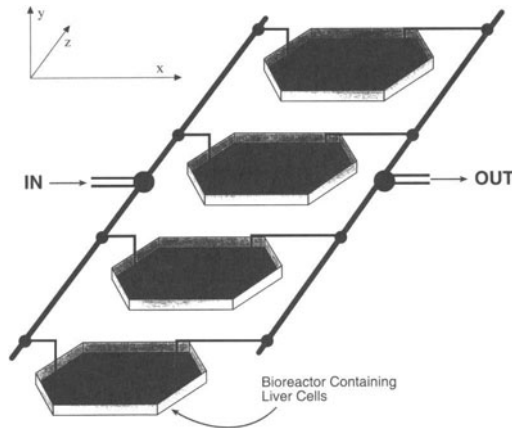


Figure 6.9. Schematic of Hypothetical Bioreactor. Multi-unit bioreactor with common inlet and outlet.

From our optimization data, we determined that the maximum function per unit area is obtained in co-cultures of 1:1 ratio (Table 6.1). Further reduction of fibroblast number resulted in a decline in hepatocyte function, therefore increased hepatocyte number would be required to achieve the same level of function. As a result, we chose the experimentally determined value of 5.65 cm<sup>2</sup> for the basal surface area of a single unit, with a 1:1 ratio of fibroblasts:hepatocyte, 250,000 cells of each type. In order to generate design criteria for the fabrication of such a device, the oxygen concentration profile, viscous pressure drop, shear stress, and dead volume were estimated.

Table 6.1. Effect of Reduced Fibroblast Number on Bioreactor Design

Area[cm <sup>2</sup> ]	Urea Synthesis [μg/day]	Urea Synthesis/Area [μg/day/cm <sup>2</sup> ]	Hepatocytes/Area [cells/cm <sup>2</sup> ]
20	200 ± 2.1	10	14,500
11.4	188 ± 3.4	16.4	25,400
5.7	134 ± 5.0	23.6	51,300
4.2	100 ± 11.5	23.8	69,100

In order to appropriately interface the bioreactor with the animal, we matched the plasma flow rate of 0.3-0.5 mL/min to the device flow rate (Stefanovich et al, 1996). Each of 40 units would therefore experience a volume flow rate of 12.5 to 20 X 10<sup>-5</sup> mL/s. The liver, predominantly composed of hepatocytes, consumes 20-33% of the body's oxygen at basal conditions (Campra and Reynolds, 1988). Due to the potential loss in cell

viability as a result of oxygen limitations in vitro, a previously described model of oxygen transport in perfused channels was modified to estimate the required inlet oxygen tension, and maximum achievable channel length given these flow rates (Bhatia, 1993).

Briefly, the fluid velocity profile was approximated as fully developed, laminar plug flow traveling at the mean fluid velocity with negligible axial diffusion of oxygen. Figure 6.9 illustrates a typical microchannel where ‘axial’ is defined along the length (L) of the channel and ‘radial’ is defined along the height (h) of the channel. Hepatocytes were modeled as an array of cells which account for a constant oxygen uptake rate at the cell surface, and the oxygen transport in the liquid flowing along the channel was modeled as a combination of axial convection and radial diffusion. The dimensionless transport equation describing the oxygen distribution is as follows:

$$\frac{\partial \hat{c}}{\partial \hat{x}} = \frac{\partial^2 \hat{c}}{\partial \hat{y}^2} \tag{6.1}$$

where  $\hat{c}$  is the dimensionless oxygen concentration,  $\hat{x}$  is the dimensionless axial coordinate and  $\hat{y}$  is the dimensionless radial coordinate. In order to utilize the analytical solution associated with a symmetrical oxygen concentration profile, the boundary conditions were approximated as follows:

$$\frac{\partial \hat{c}}{\partial \hat{y}} = 0 \quad \text{at} \quad \hat{y} = 0 \tag{6.2}$$

$$\hat{c} = 0 \quad \text{at} \quad \hat{x} = 0 \tag{6.3}$$

$$\frac{\partial \hat{c}}{\partial \hat{y}} = -\frac{V_m \rho D_h}{D c_i} = R \quad \text{at} \quad \hat{y} = \frac{(h/2)}{D_h} \tag{6.4}$$

$$\hat{c} = \frac{c - c_i}{c_i} \quad \text{and} \quad \hat{u} = \frac{u}{u_m} \tag{6.4}$$

where  $V_m$  is the oxygen uptake rate,  $\rho$  is the cell density,  $D_h$  is the hydraulic diameter,  $D$  is the diffusivity of oxygen in liquid, and  $c_i$  is the inlet oxygen concentration. Equation (6.2) describes a symmetrical gradient about the center of the channel (further discussion of this approximation will follow), Equation (6.3) describes an inlet oxygen concentration at the channel entrance, and Equation (6.4) describes a constant oxygen flux,  $R$ , at the cell surface (a simplification of the Michaelis-Menten model of oxygen uptake rate). The dimensionless variables are defined as follows:  $\hat{x} = x/D_h Pe$  and  $\hat{y} = y/D_h$ , where  $x$  is non-dimensionalized with respect to hydraulic diameter ( $D_h$ ) and Peclet number ( $Pe$ ). The inclusion of the dimensionless  $Pe$  number,

a measure of the relative magnitude of convective and diffusive effects, allows one to neglect axial diffusion for large Pe numbers.  $y$  is non-dimensionalized solely with respect to hydraulic diameter because no radial convective term exists in the axial mass transfer equation. In addition, oxygen concentration and fluid velocity are non-dimensionalized as follows:

$$\hat{c} = \frac{c - c_i}{c_i} \quad \text{and} \quad \hat{u} = \frac{u}{u_m} \quad (6.5)$$

where oxygen concentration is non-dimensionalized such that its inlet value is 0. Velocity,  $u$ , was normalized with respect to mean velocity,  $u_m$ . Finally, Peclet number and hydraulic diameter are defined below:

$$Pe = Re * Sc = \frac{u_m D_h}{D} \quad D_h = \frac{4A}{P} = \frac{2wh}{w+h} \quad (6.6)$$

$A$  is the cross-sectional channel area,  $P$  is the channel perimeter,  $w$  is the channel width,  $h$  is the channel height,  $Re (= D_h u_m / \nu)$  is the Reynolds number and  $Sc (= \nu / D)$  is the Schmidt number where  $\nu$  is the kinematic viscosity. The analytical solution of Equations (6.1) to (6.4) is described elsewhere (Carslaw et al., 1960; Bhatia et al, 1993). Constants used in the solution of Equations (6.1) to (6.4) are summarized in Table 6.2.

Table 6.2. Constants Used in Solution of Transport Equations

	DESCRIPTION	VALUE
D	diffusivity of O <sub>2</sub> in media	$2 \times 10^{-5}$ cm/s (Yarmush et al, 1992)
K	solubility of O <sub>2</sub> in liquid	1.19 nmol/ ml/ mm Hg (Yarmush et al, 1992)
Sc	Schmidt number	350
$\mu$	viscosity of media at 37°C	0.007 g/cm/s (van Kooten et al, 1992)
$\rho$	cell density	250,000 hepatocytes/5.65 cm <sup>2</sup>
$V_m$	oxygen uptake rate	0.22 - 0.36 nmol/s/10 <sup>6</sup> cells (Rotem et al, 1992)

The solution of this set of equations yields a dependence of flow rate on sustainable cell surface area. This is depicted graphically in Figure 6.10-varying flow rates correspond to various achievable channel lengths (with a fixed channel width, height, and inlet oxygen tension). The dashed line represents minimal acceptable oxygen level of 5 mmHg. Decreased channel width would allow proportionally greater achievable channel length (data not

shown); thus, a fixed surface area of cells can be sustained by a given inlet oxygen tension.

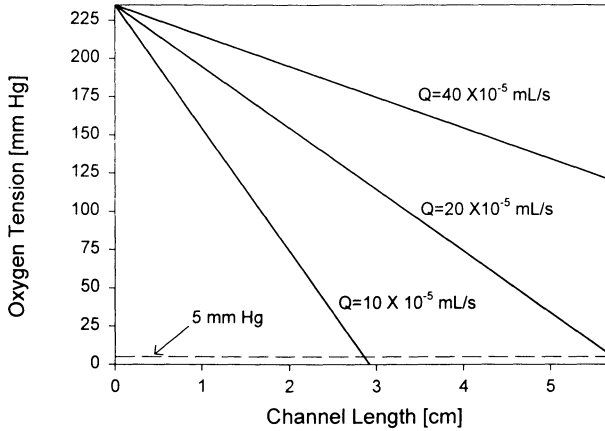


Figure 6.10. Effect of Flow Rate on Oxygen Concentration along Channel Length. Profile of oxygen concentration at cell surface with fixed inlet oxygen tensions and varying flow rate. Dashed line indicates minimal acceptable oxygen level.

Figure 6.11 depicts the theoretical cell surface area which can be sustained at various inlet oxygen tensions and flow rates. Utilizing the above range of device flow rates, it was determined that plasma must be oxygenated with at least 30% oxygen prior to perfusion in order to sustain the experimentally determined co-culture surface area of 5.65 cm<sup>2</sup> (250,000 hepatocytes and 250,000 fibroblasts).

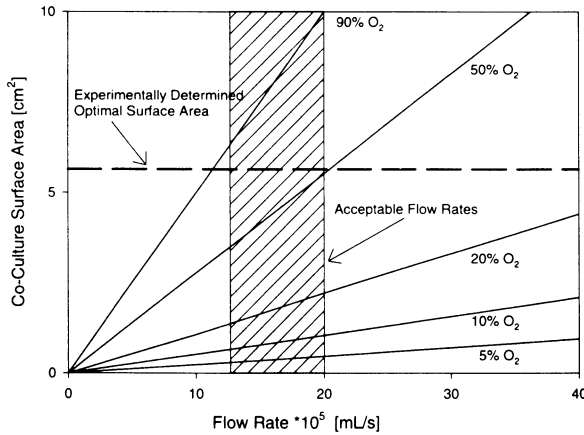


Figure 6.11. Effect of Oxygen Tension on Flow Rate versus Cell Surface Area. Achievable viable cell surface area as a function of flow rate and inlet oxygen tension.

Use of this mathematical model in estimating design criteria for a hypothetical bioreactor, required a number of approximations. This model assumed a symmetrical oxygen concentration profile with oxygen uptake at both the top and bottom of the channel (Equations 6.2 and 6.4). A more accurate model would utilize a concentration gradient of zero at the channel top, a non-dimensionalized inlet concentration of zero, and a concentration gradient of  $R$  only along the channel bottom with a computational solution. Therefore, in this study, we overestimated oxygen uptake by approximately two-fold (due to the lack of oxygen uptake of cells on the top surface of the channel). This overestimation was corrected by doubling the achievable channel length reported by the model. A further approximation made in this study was the negligible oxygen uptake of fibroblasts relative to hepatocytes (ref\*) and an average, uniform hepatocyte oxygen uptake rate over the entire bottom surface of the channel. The latter assumption is validated by the inability to sustain local gradients in oxygen tension due to the dominance of convective transport in the axial direction.

Our problem formulation also assumed plug flow along the channel at the mean velocity. At small channel heights, the aspect ratio  $\varepsilon$  ( $= h/w$ ) is less than 1 and the plug flow approximation has been experimentally verified in the  $z$ -direction (Brody et al, 1996). However, in the  $y$ -direction (i.e. in the direction of channel height), a parabolic profile exists. This parabolic flow profile could generate either parabolic or plug transport where plug transport refers to diffusive averaging of solute concentration across the face of the channel. If the characteristic transport time for diffusion of solutes across the face of the channel  $\tau_D$  ( $= h^2/D$ ) is less than the characteristic transit time

due to convection  $\tau_c (= h/u_{\max})$ , a plug transport profile will be generated. Manipulation of these equations with mean velocity equal to two-thirds of maximum velocity (for rectangular cross-section flow), we obtain  $Q/w < 1.33 \times 10^{-5}$  will yield plug transport. Therefore, one could design the channel dimensions to ensure plug transport profiles for certain applications (i.e. preservation of boundaries of administered solute bolus). Indeed, these issues may become more significant for larger proteins with lower diffusivities (and therefore larger  $\tau_D$ ) and consequently more parabolic transport profiles.

In addition to oxygen transport, we also modeled the fluid shear stress at the cell surface as well as viscous energy losses leading to a pressure drop along the length of the channel. Fully developed, rectangular channel, laminar flow is well described by Darcy's law (Bensimon et al, 1986) where the Navier-Stokes equation is solved for the classic Hele-Shaw geometry with an aspect ratio of  $\varepsilon = h/w$  (Brody et al, 1996). At low Reynolds numbers, the entrance length for fully developed flow is  $\sim 0.5D_h$ , and is indeed negligible (Duncan et al, 1970). This model yields expressions for viscous pressure drop,  $\Delta P$ , along a channel of length,  $L$ , and shear stress,  $\tau$ , at the cell surface, with a flow rate of  $Q$ :  $\Delta P = 12\mu QL/wh^3$  and  $\tau = 6\mu Q/wh^2$ .

Figure 6.12 graphically depicts the dependence of pressure drop and shear stress on channel height for a fixed channel width and length, and fixed flow rate. Channel heights of less than  $10 \mu\text{m}$  generated unacceptable shear stresses (greater than  $10 \text{ dynes/cm}^2$ - Truskey and Pirone, 1990) and, channel heights of less than  $10 \mu\text{m}$  also generated a viscous pressure drop greater than that observed in vivo across the liver ( $10 \text{ mm Hg}$ ) (Figure 6.12). Due to the extraction of these design parameters from the liver in vivo, the similarity of channel heights generated by pressure drop constraints and shear stress constraints with in vivo capillary dimensions is reasonable. The dead volume of the device was designed to be minimal- much of the volume is typically attributed to the interconnecting fluidics, nevertheless we attempted to maintain the dead volume of the sum of individual units under  $1 \text{ mL}$  so that the remaining fluidics could encompass as much as  $1\text{-}2 \text{ mL}$  and still be less than the animal blood volume ( $\sim 7 \text{ mL}$ ). Thus, a channel height of  $\sim 45 \mu\text{m}$  was chosen.

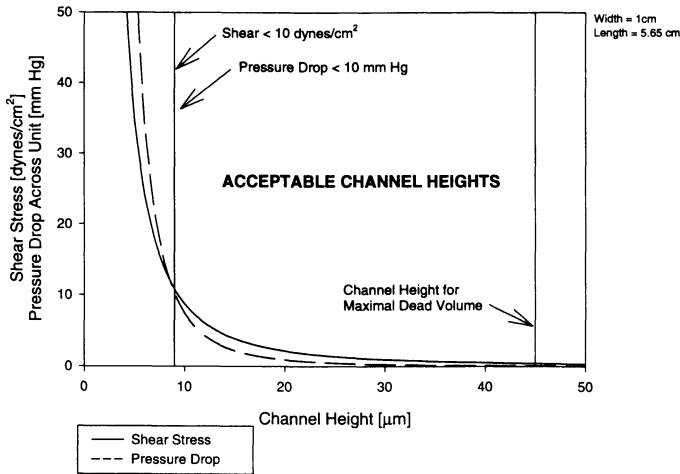


Figure 6.12. Effect of Channel Height on Shear Stress and Pressure Drop. Tolerable fluid shear stress and in vivo pressure head were utilized to estimate the lower bound on channel height given a fixed width and length. Acceptable reactor dead volume was utilized to estimate the upper bound on channel height.

This design is relatively insensitive to the aspect ratio of width:height; here, we chose 1:5.65 in order to minimize the expansion angle of the fluid flow from a tubular input, although one could design a bioreactor with a 'slit' input to eliminate fluid disturbances at the inlet. These dimensions create a Reynolds number of 0.05 ( $\ll 1$ , proportion of inertial to viscous fluid flows) and Peclet number of 20 ( $\gg 1$ , proportion of convective to diffusive oxygen transport), indicating laminar flow with convection of oxygen dominating over diffusion in the direction of flow. Finally, we consider the seeding of such a hypothetical device with hepatocytes. In a preassembled device, seeding of hepatocytes under stagnant conditions will deplete the oxygen very rapidly. Hepatocyte attachment and spreading is known to be highly oxygen-dependent; cell surface oxygen tension of less than 1 mm Hg has been found to impair hepatocyte attachment by 60% and cell spreading by 63% (Rotem et al, 1994). Therefore, we propose pre-equilibration of the hepatocyte suspension with high oxygen content gas (90%). However, given the dimensions proposed above (45  $\mu\text{m}$  height, 1 cm width, 5.65 cm length), the oxygen will still be completely depleted in approximately 3.5 min. One potential solution would be to utilize an increased chamber volume initially (i.e. a large spacer creating a height of  $\sim 450 \mu\text{m}$ ) which could be collapsed after hepatocyte attachment. This would allow for approximately 35 min of normoxic hepatic environment.

Alternatively, one could maintain a channel height of 45  $\mu\text{m}$  throughout the hepatocyte seeding by experimentally investigate alternative seeding protocols (i.e. periodic flow).

### 5.5 Comparison of Hypothetical Microfabricated Bioreactor to Existing Technologies

In order to compare our hypothetical, co-culture bioreactor to existing technologies, we estimated the requirements for replacement of rat liver function using both microfabricated, co-culture and hepatocyte only, hollow-fiber devices. Using albumin production as a marker of liver function, a co-culture based device was compared to another primary hepatocyte bioreactor (Wu et al, 1995). This device utilizes hepatocyte spheroids, previously reported to promote differentiated hepatic functions in vitro, entrapped within a collagen matrix and immobilized in the luminal compartment of a hollow-fiber cartridge. This configuration allows for long-term stability of liver-specific functions; however, since the bioreactor is perfused through the extraluminal space, transport between the fluid stream and the entrapped hepatocytes occurs through the wall of the hollow-fiber, the collagen hydrogel, and the spheroids themselves. A hypothetical, microfabricated co-culture device had many comparable operating parameters to the spheroidal hollow-fiber device (Table 6.3) with some notable exceptions: the typical diffusion path for solutes, the required hepatocyte number, and the uniformity of cell distribution differ significantly. Due to the up-regulation of hepatic function due to co-cultivation with mesenchymal cells and uniform accessibility to hepatocytes, our device would require  $\sim 28$ -fold fewer hepatocytes. In addition, transport of soluble molecules to and from the hepatocyte cell surface occurs over 10-fold smaller distance (and since diffusion time scales with the square of length, 100-fold shorter diffusion times). Furthermore, our design facilitates efficient utilization of all hepatocytes through uniform exposure to the soluble phase whereas spheroidal cultures and hollow-fiber devices, in general, are susceptible to variable viability,<sup>⊗</sup> functionality, and transport.

<sup>⊗</sup> Our calculations with 0.216 nmol  $\text{O}_2/10^6$  hepatocytes/s indicate 36% viability in these devices, based on reported oxygen uptake.



Table 6.3. Comparison of a hypothetical microfabricated liver reactor to a spheroid-based, hollow-fiber reactor for replacement of rat liver function.

	Microfabricated (this study)	Spheroids in Hollow-Fiber* (Wu et al, 1995)
no. cells	$10 \times 10^6$	$280 \times 10^6$
Albumin secretion	160 $\mu\text{g/h}$	160 $\mu\text{g/h}$
no. units	40 modules	200 fibers
Transport surface area	226 $\text{cm}^2$	727 $\text{cm}^2$
Perfusion length	6 cm	10 cm
Diffusion length	50 $\mu\text{m}$	500 $\mu\text{m}$
cell density	$\sim 1 \times 10^7$ cells/mL (uniform)	$\sim 1 \times 10^7$ cells/mL (non-uniform)

\*Assuming 10% of rat liver (60 million hepatocytes) at in vivo albumin secretion levels of approximately 120-180  $\mu\text{g}$  albumin/h. Each spheroid cartridge contains 140 million hepatocytes. Based on reported secretion rates, 2 cartridges would be required to achieve 160  $\mu\text{g/h}$ . Fiber number and transport surface area are calculated from 10 mL internal luminal volume and inner fiber diameter of 1.1 mm. Cell density is estimated from the approximation that extraluminal and intraluminal volume are of the same order of magnitude in typical hollow-fiber configurations.

## 6. SUMMARY

In this study we utilized microfabrication techniques to determine the utility of co-cultures in the design of a bioartificial liver. We determined that by preserving the heterotypic interface, the fibroblast:hepatocyte ratio could be greatly reduced without much effect on hepatic function. This data was utilized to determine the optimum ratio for a hypothetical device. Furthermore, control over initial cell-cell interactions using micropatterning was found to significantly improve the kinetics of cellular recovery from isolation. In addition, co-culture of primary rat hepatocytes with murine NIH 3T3-J2's was found to produce marked increases in liver-specific functions over other models for in vitro differentiation of hepatocytes (other co-cultures, matrix manipulation) as well as in vivo values, suggesting that fewer hepatocytes may be necessary for sustenance of an animal than previously described. We utilized the above data and models of oxygen transport and fluid flow in a hypothetical device, to generate specific design criteria for a multi-unit bioreactor where each unit mimics a liver lobule in vivo. Finally, we demonstrated the favorable comparison between our proposed co-culture based device with another well-established BAL. Thus, given the data on hepatic function and specific design criteria presented here,

we are well poised to take the essential next step- the design and fabrication of a multi-unit, co-culture-based, micromachined bioreactor to test in animal models of liver failure.

## Chapter 7

### Conclusions and Outlook

#### 1. SUMMARY

The development of functional substitutes for normal organs requires a fundamental understanding of the cellular cues that control tissue function. In particular, the cellular microenvironment is perturbed by neighboring cells as well as by local cell-substrate and cell-matrix interactions. While the effects of cell-substrate and cell-matrix interactions on function have been the focus of many studies, systematic control over cell-cell interactions as a component of this microenvironment has not been previously achieved.

A generic, versatile technique was developed for controlling cell-cell interactions between two cell populations based on photolithography, silane-mediated immobilization of extracellular matrix, and manipulation of serum content of media. The properties of this system were extensively characterized and its versatility and robustness were demonstrated. Cell-cell interactions were found to be more homogeneous than in conventional cultures and controllable over a wide range of interactions.

Modulation of initial homotypic and heterotypic cell-cell interactions were found to have dramatic effects on tissue function. In particular, two to three-fold variations in steady-state levels of representative cellular functions were achieved from identical numbers of cells. Furthermore, our results indicated that the use of microfabrication to control cell-cell interactions and cell-substrate

interactions for each cell type independently, may allow modulation over the kinetics of functional up-regulation as well. Thus, the level of long-term tissue function and kinetics of its response can be engineered through use of microfabrication to control initial cell-cell interactions.

We focused specifically on hepatic tissue engineering due to the clinical significance of liver failure and due to the widely reported benefits of 'co-culture' in this area. Co-cultivation of primary rat hepatocytes with mesenchymal cells (NIH 3T3-J2 fibroblasts) induced a marked increase in markers of liver-specific function. Micropatterning of these cultures allowed the examination of both the functional output of the tissue as well as the spatial distribution of liver-specific markers. This opportunity led to the novel finding that hepatocytes can not communicate throughout a confluent hepatocyte island- contradicting existing reports. The signal for differentiation seemed to arise at the heterotypic interface and penetrate a finite distance on the order of 100-400  $\mu\text{m}$ . This limited signal propagation was presumed to account for functional differences observed in bulk tissue function wherein large hepatocyte islands functioned poorly. A series of mechanistic studies were performed to characterize the mesenchymal cell product responsible for induction of liver-specific functions. While these experiments pointed to a cell-associated product (i.e. cell membrane-bound protein, or cell or matrix-bound secreted product), indicating that direct contact between cell populations would be necessary for practical applications, the precise molecular nature of this signal is yet undetermined.

In order to utilize co-cultivation of hepatocytes with 3T3-J2 fibroblasts to achieve stable, liver-specific functions in a bioartificial liver, hepatic functions were optimized. Microfabrication and elastomeric polymer masking were used to reduce the number of fibroblasts necessary for induction of hepatic functions. We were able to reduce the number of fibroblasts by twelve-fold with only mild effects on function, and were able to estimate a useful fibroblast:hepatocyte ratio for bioreactor applications of 1:1. Since co-culture with this particular 3T3 subclone was found to be superior to all other methods of achieving stable, liver-specific functions in vitro, we estimated the potential for use of 4 to 8-fold less isolated hepatocytes than previously reported. Finally, due to the ease with which microfabricated units can be replicated, we conceived of a hypothetical bioreactor based on the repeating pattern of the liver lobule in vivo. Experimental data combined with models of oxygen transport and viscous energy losses were utilized to determine design

criteria for such a multi-unit, co-culture based, bioartificial liver. In particular, this analysis generated specifications for individual chamber dimensions, device flow rate, optimal ratio of hepatocyte:fibroblasts, and required level of plasma oxygenation to sustain hepatocyte viability.

## 2. FUTURE DIRECTIONS

The control over cellular microenvironment has much to offer the area of tissue engineering as well as the study of developmental biology and the pathophysiology of certain human diseases. The techniques demonstrated here will have both fundamental and practical implications. From the basic science perspective, these tools will be useful in probing further the mechanisms by which cell populations interact, understanding the cues which control tissue remodeling and morphogenesis, and the influence of cell-cell interactions on the physiology and pathophysiology of tissue repair, regeneration, and transformation. These tools can be expanded to incorporate microscale control over the tissue topology by use of well-defined three-dimensional structures and to include genetically engineered cell interactions by use of gene therapy on one or both cell types.

The ability to modulate tissue function by control over local cell-cell interactions will have applications in many other organ systems. In particular, quantitative analysis of the role of cell interactions between endothelial cells and the smooth muscle of the vascular wall could provide insight into the area of general vascular physiology as well as the pathogenesis of atherosclerosis or neointimal hyperplasia associated with implanted vascular grafts. In the area of hematopoiesis, bone marrow stroma and various mesenchymal cell lines have been shown to play a fundamental role in the long-term proliferation and differentiation of isolated bone marrow *in vitro*. While some of the ligand/receptor interactions have been characterized at the molecular level, the use of stromal cells for *in vitro* sustenance of bone marrow is still poorly understood and could benefit from control over the cellular microenvironment. In the area of artificial skin equivalents, fibroblast-populated dermal equivalents have been shown to support proliferation, stratification, and differentiation of keratinocytes to form an intact epidermis. In this area, it may be possible to modulate the rate of this response and/or the characteristics of the resulting skin equivalent by modifying the degree of heterotypic cell-cell interaction. Finally, the control of

epithelial/mesenchymal interactions could be utilized to quantitatively probe the *in vivo* processes of embryogenesis and malignant transformations *in vitro*.

The potential for control over cell-cell interactions in hepatic tissue engineering will have implications both in the development of a bioartificial liver and from a scientific perspective. Due to the diversity of hepatocellular functions, further characterization of co-cultured 'tissues' will be necessary. The most imperative of these are the detoxification pathways of the liver- cytochrome P450 enzymes, glutathione-S-transferases, and UDP-glucuronyltransferases. In addition, the examination of other promising cell types, may lead to further improvements in function. In particular, Ito cells (fat-storing) cells have direct contact with hepatocytes *in vivo* and have been shown to form functional gap junctions *in vitro*. Their far-reaching, stellate morphology could induce liver function over a large area of hepatocytes- as such, they offer a compelling substitution for other, more compacted cell types. Similarly, the role of Kupffer cells in suppression of various hepatic functions has been studied in randomly-distributed co-cultures. Quantitative control over these interactions using microfabrication may provide additional insight into the mechanisms by which these cell types communicate to modulate the acute phase response.

The precise mechanism by which NIH 3T3-J2 fibroblasts induced liver-specific functions in our isolated hepatocytes whereas other related clones such as NIH 3T3-A31 have comparatively little effect, has remained elusive. The availability of two closely related murine stromal cell lines could provide the basis for a subtractive hybridization analysis of candidate factors. The molecular identification of the signal implicated in this response could have far-reaching implications. In addition, this could allow replacement of stromal cell support in reconstructed tissues with a limited number of biochemicals which would allow control over hepatocyte gene expression *in vitro*, significantly advancing the field of hepatic tissue engineering.

The development of a prototypic multi-unit, microfabricated, co-culture based bioreactor for animal experimentation will also be facilitated by the experimental and theoretical data presented here. An adequate, inexpensive cell source for primary hepatocytes will be necessary for sufficient cell mass to support a patient. Some recent studies have shown ~15-fold expansion of hepatocytes *in vitro* by variation of media composition and matrix interactions. If biochemical analysis of the resulting cell

populations confirms adequate liver-specific functions in these 'hepatocytes', the manipulation of media composition in vitro could provide a much-needed solution to this problem. Alternatively, large animal sources of hepatocytes, such as porcine, could be explored. These isolated hepatocytes will require empirical characterization for the effects of co-culture on their differentiation program.

Design criteria for a hypothetical, multi-unit, microfabricated, co-culture based bioreactor, were identified for oxygenation, flow rates, chamber dimensions, and cell densities in each unit of this multi-unit device. Further use of microfabrication techniques will allow the assembly of many, parallel units perfused by 'microfluidic' systems being developed elsewhere. As a result, we are well poised to construct a prototypic device and begin experimentation in animal models of liver failure. In contrast to the re-engineering frequently required in classical approaches to scale-up (from pilot plant to production plant or from animal model to human model), microfabrication offers the further advantage that scale-up can be accomplished by replication of many parallel units. This would eliminate the need for lengthy and costly redesign of bioreactors for scale-up to large animal and human applications. Thus, this 'brute force' approach to temporary replacement of liver function holds much promise for the eventual construction of a clinical device.

## References

- B. Arkles, J. R. Steinmetz, J. Zazycny, and P. Mehta, "Factors contributing to the stability of alkoxyxilanes in aqueous solution," in *Silicon Compounds, Register and Review*, R. Anderson, G.L. Larson and C. Smith (eds.), Hüls America, NJ, 65-73, (1991) .
- K. Asunoma, J.C. Gilbert, J.E. Stein, T. Takeda, and J.P. Vacanti, "Quantitation of transplanted hepatic mass necessary to cure the gunn rat model of hyperbilirubinemia," *Journal of Pediatric Surgery* **27**:298-301, (1992).
- G. Baffet, P. Loyer, D. Glaise, A. Corly, P. Etienne, and C. Guguen-Guillouzo, "Distinct effects of cell-cell communication and corticosteroids on the synthesis and distribution of cytokeratins in cultured rat hepatocytes," *Journal of Cell Science* **99**:609-615, (1991).
- H. Baier and F. Bonhoeffer, "Axon guidance by gradients of a target-derived component," *Science* **25**:472-475, (1992).
- A. Baird and P. Bohlen, "Fibroblast growth factors," in *Peptide Growth Factors and Their Receptors I*, Sporn and Roberts (eds.), Springer-Verlag, NY, (1990).
- L.R. Banner and P.H. Patterson, Major changes in the expression of the mRNAs for cholinergic differentiation factor/leukemia inhibitory factor and its receptor after injury to adult peripheral nerves and ganglia. *Proceedings of National Academy of Sciences* **91**:7109, (1994).
- H. Baumann, G.T. Jahreis, D.N. Sauder, and A. Koj, "Human keratinocytes and monocytes release factors which regulate the synthesis of major acute phase plasma proteins in hepatic cells from man, rat and mouse," *Journal of Biological Chemistry* **259**:7331, (1984).



- H. Baumann and G.G. Wong, "Hepatocyte-stimulating factor III shares structural and functional identity with leukemia-inhibitory factor," *Journal of Immunology* **143**:1163, (1989).
- R. Bellamkonda and P. Aebischer, "Review: Tissue engineering in the nervous system," *Biotechnology and Bioengineering* **43**:543-554, (1994).
- Bergsteinsdottir, A. Kingston, R. Mirsky, K.R. Jessen., "Rat schwann cells produce interleukin-1" *Journal of Neuroimmunology* **34**:15, (1991).
- J. Bernuau and J-P. Benhamou, "Fulminant and subfulminant failure, in *Oxford Textbook of Clinical Hepatology*, N. McIntyre, J-P Benhamou, J. Bircher, M. Rizzetto, and J. Rodes (eds.), Oxford University Press, London, England, (1991).
- F. Berthiaume, P.V. Moghe, M. Toner, and M.L. Yarmush, "Effect of extracellular matrix topology on cell structure, function, and physiological responsiveness: hepatocytes cultured in a sandwich configuration," *FASEB J* **10**:1471-1484, (1996).
- S.N. Bhatia "Development of a potential bioartificial liver: selective adhesion of hepatocytes" Master of Science Thesis, Massachusetts Institute of Technology, (1993).
- S.N. Bhatia, M. Toner, R.G. Tompkins, and M.L. Yarmush, "Selective adhesion of hepatocytes on patterned surfaces," *Annals of the New York Academy of Sciences*, **745**:187-209 (1994).
- S.N. Bhatia, M.L. Yarmush, and M. Toner, "Controlling homotypic vs heterotypic interactions by micropatterning: co-cultures of hepatocytes and 3T3 fibroblasts," *Journal of Biomedical Materials Research*, **34**(2):189-199, (1997).
- D.M. Bissel, D.M. Arenson, J.J. Maher, and F.J. Roll, "Support of cultured hepatocytes by a laminin-rich gel: Evidence for a functionally significant subendothelial matrix in normal rat liver," *Journal of Clinical Investigation* **79**:801-812, (1987).
- H. Brenner and L.J. Gaydos, "The constrained brownian movement of spherical particles in cylindrical pores of comparable radius: models of the diffusive and convective transport of solute molecules in membranes and porous media," *Journal of Colloid Interface Science* **58**:312-356, (1977).
- S. Britland, E. Perez-Arnaud, P. Clark, B. McGinn, P. Connolly, and G. Moores, "Micropatterning proteins and synthetic peptides on solid supports: a novel application for microelectronics fabrication technology," *Biotechnology Progress* **8**:155-160 (1992).
- J.V. Boykin and J.A. Molnar, "Burn scar and skin equivalents," in *Wound Healing*, I.K. Cohen et al (eds.), Saunders, Philadelphia, (1992).
- J.M. Calvert, "Coplanar molecular assemblies of amino- and perfluorinated alkylsilanes: Characterization and geometric definition of mammalian cell adhesion and growth," *Journal of American Chemical Society* **114**:8435-8442 (1992).
- J.M. Caron, "Induction of albumin gene transcription in hepatocytes by extracellular matrix proteins," *Molecular Cell Biology* **10**:1239-1243, (1990).
- S.B. Carter, "Principles of cell motility: the direction of cell movement and cancer invasion," *Nature* **20E**:1183-1187, (1965).
- T.M.S. Chang, "Hemoperfusion in 1981," in *Hemoperfusion*, Bononini and Chang (eds.), Karger, (1981).
- M. Chedid, J.S. Rubin, K.G. Csaky, and S.A. Aaronson, "Regulation of keratinocyte growth factor gene expression by interleukin 1," *Journal of Biological Chemistry* **269**:10753, (1994).
- P. Clark, P. Connolly, and G.R. Moores, "Cell guidance by micropatterned adhesiveness in vitro," *Journal of Cell Science* **103**:287-292, (1992).

- P. Clark, S. Britland, and P. Connolly, "Growth cone guidance and neuron morphology on micropatterned laminin," *Journal of Cell Science*, **105**:203-212 (1993).
- M.G. Clemens, M. Bauer, C. Gingalewski, E. Miescher, and J. Zhang. "Editorial Review: Hepatic intercellular communication in shock and inflammation," *Shock* **2**(1):1-9, (1994).
- B. Clement, C. Guguen-Guillouzo, J-P Campon, D. Glaise, M. Bourel, and A. Guillouzo, "Long-term co-cultures of adult human hepatocytes with rat liver epithelial cells: modulation of albumin secretion and accumulation of extracellular material," *Hepatology* **4**(3):373-380, (1984).
- B. Clement, C. Guguen-Guillouzo, J. Grimaud, M. Bissel, and A. Guillouzo, "Effect of hydrocortisone on deposition of types I and IV collagen in primary culture of rat hepatocytes," *Cellular and Molecular Biology* **34**(5):449-460, (1988).
- B. Clement, C. Guguen-Guillouzo, J. Campion, D. Glaise, M. Bourel, and A. Guillouzo. "Long-term co-cultures of adult human hepatocytes with rat liver epithelial cells: modulation of albumin secretion and accumulation of extracellular matrix material," *Hepatology* **4**(3):373-380, (1994).
- C. Coers and A.L. Woolf, (eds.), *The Innervation of Muscle*, C.C. Thomas, Springfield, Illinois, (1959).
- J.M. Corey, B.C. Wheeler, G.J. Brewer, "Compliance of hippocampal neurons to patterned substrate networks," *Journal of Neuroscience Research*, **30**:300-307 (1991).
- A. Corlu, B. Kneip, C. Lhadi, G. Leray, D. Glaise, G. Baffet, D. Bourel, and C. Guguen-Guillouzo, "A plasma membrane protein is involved in cell contact-mediated regulation of tissue-specific genes in adult hepatocytes," *Journal of Cell Biology* **115**(2):505-515, (1991).
- A. Corlu, G.P. Ilyin, N.Gerard, B. Kneip, M. Rissel, B. Jegou, and C. Guguen-Guillouzo, "Tissue distribution of liver regulating protein," *American Journal of Pathology* **145**(3):715-727, (1994).
- R. Cotran, V. Kumar, and S. Robbins, "Diseases of Muscle," in *Robbins Pathologic Basis of Disease*, R. Cotran, V. Kumar, and S. Robbins (eds.), WB Saunders, PA, (1989).
- Darnell, H. Lodish, and D. Baltimore, "The extracellular matrix serves many functions," in *Molecular Cell Biology*, J. Darnell, H. Lodish, and D. Baltimore (eds.), 904-5, W.H. Freeman and Company, New York, (1990).
- P.F. Davies, "Biology of disease: vascular cell interactions with special reference to the pathogenesis of atherosclerosis," *Laboratory Investigation*, **55**:5-24 (1986).
- E.T. den Braber, J.E. de Ruijter, H.T.J. Smits, L.A. Ginsel, A.F. von Recum, and J.A. Jansen, "Effect of parallel surface microgrooves and surface energy on cell growth," *Journal of Biomedical Materials Research*, **29**:511-518 (1995).
- F.M. De La Vega and T. Mendoza-Figueroa, "Dimethyl sulfoxide enhances lipid synthesis and secretion by long-term cultures of adult rat hepatocytes," *Biochimie* **73**:621-624 (1991).
- A.A. Demetriou, A. Reisner, J. Sanchez, S.M. Levenson, and A.D. Mocioni, and J.R. Chowdury, "Transplantation of microcarrier-attached hepatocytes into 90% partially hepatectomized rats," *Hepatology* **8**:1006-1009, (1988).
- T. A. Desai, W.H. Chu, J.K. Chu, G.M. Beattie, A. Hayek, and M. Ferrar, "Microfabricated immunisolating biocapsules" *Biotechnology and Bioengineering* **57**(1):118-120 (1998).
- M. Deyme, A. Baszkin, J.E. Proust, E. Perez, and M.M. Boissonnade, "Collagen at interfaces I. *In situ* collagen adsorption at solution/air and solution/polymer interfaces," *Journal Biomedical Materials Research*, **20**:951-962 (1986).

- J. Dich, C. Vind, and N. Grunnet, "Long-term culture of hepatocytes: effect of hormones on enzyme activities and metabolic capacity," *Hepatology* **8**:39-45, (1988).
- C.A. Dinarello, "Interleukin-1 and interleukin-1 antagonism," *Blood* **77**:1627, (1991).
- M.T. Donato, M.J. Gómez-Lechón, and J.V. Castell, "Drug metabolizing enzymes in rat hepatocytes co-cultured with cell lines," *In Vitro Cell and Developmental Biology*, **26**:1057-1062, (1990).
- M.T. Donato, J.V. Castell, and M.J. Gomez-Lechon, "Cytochrome P450 activities in pure and co-cultured rat hepatocytes: effects of model inducers," *In Vitro Cell and Developmental Biology* **30A**(12):825-832, (1994).
- N.M. Le Douarin, "An experimental analysis of liver development," *Medical Biology*, **53**:427-455 (1975).
- J.C.Y. Dunn, M.L. Yarmush, H.G. Koebe, and R.G. Tompkins, "Hepatocyte function and extracellular matrix geometry: Long-term culture in a sandwich configuration," *FASEB J*, **3**:174-177 (1989).
- J.C.Y. Dunn, R.G. Tompkins, and M.L. Yarmush, "Long-term in vitro function of adult hepatocytes in a collagen sandwich configuration," *Biotechnology Progress*, **7**:237-245 (1991).
- J.C.Y. Dunn, R.G. Tompkins, and M.L. Yarmush, "Hepatocytes in collagen sandwich: evidence for transcriptional and translational protein," *Journal of Cell Biology* **116**(4):1043-1053, (1992).
- J.C.Y. Dunn, J.S. Friedberg, R.G. Tompkins, and M.L. Yarmush, "Hepatocytes from rat liver perfusions: physicochemical effects on polyribosome size," *ASAIO Transactions* **38**(4): 841-845, (1992).
- J.C.Y. Dunn, "Long-term culture of differentiated hepatocyte in a collagen sandwich configuration," Doctoral Dissertation, Massachusetts Institute of Technology, (1992).
- P. Eklblom, "Developmentally regulated conversion of mesenchyme to epithelium," *FASEB J* **3**:2141-2150, (1989).
- P. Eklblom, M. Eklblom, L. Fecker, G. Klein, H. Zhang, Y. Kadoya, M-L Chu, U Mayer, and R. Timpl, "Role of mesenchymal nidogen for epithelial morphogenesis in vitro," *Development* **120**:2003-2014, (1994).
- M.F. Fillinger, S.E. O'Connor, R.J. Wagner, and J.L. Cronenvett, "The effect of endothelial cell coculture on smooth muscle cell proliferation," *Journal of Vascular Surgery*, **17**:1058-1068 (1993).
- M.E. Fini, K.J. Strissel, M.T. Girard, J.W. Mays, W.B. Rinehart, "Interleukin 1 alpha mediates collagenase synthesis," *Journal of Biological Chemistry* **269**:11291, (1994).
- J.M. Fraslin, B. Kneip, S. Vaultont, d. Glaise, A. Muunich, and C. Guguen-Guillouzo, "Dependence of hepatocyte-specific gene expression on cell-cell interactions in primary culture," *EMBO J* **4**(10):2487-2491, (1985).
- M. Fujita, D.C. Spray, H. Choi, J.C. Saez, L.C. Rosenberg, E.L. Hertzberg, and L.M. Reid, "Glycosaminoglycans and proteoglycans induce gap junction expression and restore transcription of tissue-specific mRNAs in primary liver cultures," *Hepatology* **7**:S1-S9, (1987).
- R. Gebhardt and D. Mecke, "Heterogeneous distribution of glutamine synthetase among rat liver parenchymal cell in situ in primary culture," *EMBO J* **2**:567-570, (1983).
- J.H. Georger, D.A. Stenger, A.S. Rudolph, J.J. Hickman, C.S. Dulcey, and T.L. Fare, "Coplanar patterns of self-assembled monolayres for selective cell adhesion and outgrowth," *Thin Solid Films* **210/211**:716-719, (1992).

- J.C. Gerlach, N. Schnoy, J. Encke, M.D. Smith, C. Muller, and P. Neuhaus, "Improved hepatocyte in vitro maintenance in a culture model with woven multicompartment capillary systems: electron microscopy studies," *Hepatology* **22** (1995).
- S.F. Gilbert, in *Developmental Biology*, Sinauer Associates, Sunderland, MA, 1991.
- I.D. Goldberg and E.M. Rosen (eds.), in *Epithelial-Mesenchymal Interactions in Cancer*, Birkhauser, Verlag, Basel, (1995).
- F. Goulet, C. Normand, and O. Morin, "Cellular interactions promote tissue-specific function, biomatrix deposition and junctional communication of primary cultured hepatocytes," *Hepatology*, **8**(5):1010-1018 (1988).
- C. Guguen-Guillouzo, B. Clement, G. Baffet, C. Beaumont, E. Morel-Chany, D. Glaise, and A. Guillouzo, "Maintenance and reversibility of active albumin secretion by adult rat hepatocytes co-cultured with another liver epithelial cell type," *Experimental Cell Research*, **143**:47-54 (1983).
- C. Guguen-Guillouzo, "Role of homotypic and heterotypic cell interactions in expression of specific functions by cultured hepatocytes," in *Isolated and cultured Hepatocytes* A.Guillouzo and C. Guguen-Guillouzo (eds.), John Libbery Eurotext, INSERM:259-284, (1986).
- R.W. Gundersen, "Response of sensory neurites and growth cones to patterned substrata of laminin and fibronectin in vitro," *Developmental Biology*, **121**:423-431 (1987).
- J.A. Hammarback, S.L. Palm, L.T. Furcht, and P.C. Letourneau, "Guidance of neurite outgrowth by pathways of substratum-adsorbed laminin," *Journal of Neuroscience Research* **13**:213-220, (1985).
- J.A. Hammarback, J.B. McCarthy, S.L. Palm, L.T. Furcht, and P.C. Letourneau, "Growth cone guidance by substrate-bound laminin pathways is correlated with neuron-to-pathway adhesivity," *Developmental Biology* **126**:29-39 (1988).
- J.A. Hammarback, and P.C. Letourneau, "Neurite extension across regions of low cell-substratum adhesivity: implications for the guidepost hypothesis of axonal pathfinding," *Developmental Biology* **117**:655-671, (1986).
- R.I. Handin, S.E. Lux, and T.P. Stossel, in *Blood: Principles and Practice of Hematology*, R.I. Handin, S.E. Lux, and T.P. Stossel (eds.), JB Lippincott Co, Philadelphia, (1995).
- E.J. Harfenist and R.K. Murray, "Plasma proteins, immunoglobulins, and blood coagulation," in, *Harpers Biochemistry*, R.K. Murray, D.K. Granner, P.A. Mayer, and V.W. Rodwell (eds.), Appleton and Lange, CT, (1993).
- A. Harris, "Behavior of cultured cells on substrata of variable adhesiveness," *Experimental Cell Research* **77**:285-297, (1973).
- R.G. Harrison, "The cultivation of tissues in extraneous media as a method of morphogenetic study," *Anatomic Records* **6**:181-193, (1912).
- E.D. Hay, and A. Zuk, "Transformations between epithelium and mesenchyme: normal, pathological, and experimentally induced," *American Journal of Kidney Diseases* **26**(4):678-690, (1995).
- K.E. Healy, B. Lom, and P.E. Hockberger, "Spatial distribution of mammalian cells dictated by material surface chemistry," *Biotechnology and Bioengineering* **43**:792-800, (1994).
- D. Herzlinger, J. Qiao, D. Cohen, N. Ramakrishna, and A.M.C. Brown, "Induction of kidney epithelial morphogenesis by cells expressing wnt-1," *Developmental Biology* **166**:815-818, (1994).
- T. Hirano, "Interleukin 6" in *The Cytokine Handbook*, Academic Press, NY, (1994).

- E. Houssaint, "Differentiation of the mouse hepatic primordium.I. an analysis of tissue interactions in hepatocyte differentiation," *Cell Differentiation* **9**:269-279, (1990).
- R.O. Hynes, "Integrins: versatility, modulation, and signaling in adhesion," *Cell* **69**:11-25, (1992).
- G.W. Ireland, P. Dopping-Hepenstal, P. Jordan, and C. O'Neill, "Effect of patterned surfaces of adhesive islands on the shape, cytoskeleton, adhesion and behavior of swiss mouse 3T3 fibroblasts," *Journal of Cell Science Supplement* **8**:19-33, (1987).
- H.C. Isom, T. Secott, I. Georgoff, C. Woodworth, and J. Mumaw, "Maintenance of differentiated rat hepatocytes in primary culture," *Proceedings of National Academy of Sciences* **82**:3252-3256, (1985).
- A.L. Jones and E. Mills In: Weiss L, Greys RO, eds. *Histology*, 4<sup>th</sup> edition, New York, McGraw-Hill:702-703, (1977).
- H.O. Jauregui, N.R. Chowdury, and J.R. Chowdury, "Use of mammalian liver cells for artificial liver support," *Cell Transplantation* **5**(3):353-367, (1996).
- N. Kaplowitz In: *Liver and biliary diseases*, Baltimore, MD, William & Wilkins, (1992).
- M. Kan, J.S. Huang, P.E. Mansson, H. Yasumitsu, B.Carr, W.L. McKeehan, "Heparin-binding growth factor type 1 (acidic fibroblast growth factor): a potential biphasic autocrine and paracrine regulator of hepatocyte regeneration," *Proceedings of National Academy of Sciences* **86**:7432, (1989).
- K. Kato, S. Saunders, H. Nguyen, and M. Bernfield, "Loss of cell surface syndecan-1 causes epithelia to transform into anchorage-independent mesenchyme-like cells," *Molecular Biology of the Cell* **6**:559-576, (1995).
- E.B. Keeffe, "Selection of patients for liver transplantation," in *Transplantation of the Liver*, W.C. Maddrey, and M.F. Sorrell, Appleton and Lange, Norwalk, CT, (1995).
- D. Kleinfeld, K.H. Kahler, and P.E. Hockberger, "Controlled outgrowth of dissociated neurons on patterned substrates," *Journal of Neuroscience*, **8**(11):4098-4120 (1988).
- R.J. Klebe, "Cytoscribing: A method for micropositioning cells and the construction of two- and three-dimensional synthetic tissues," *Experimental Cell Research* **179**:362-373, (1988).
- N. Koide, K. Sakguchi, Y. Koide, K. Asano, M. Kawaguchi, H. Matsushima, T. Takenami, T. Shinji, M. Mor, and T. Tsuji. "Formation of multicellular spheroids composed of adult rat hepatocytes in dishes with positively charged surfaces and under other nonadherent environments," *Experimental Cell Research* **186**:227-235, (1990).
- M. Koike, M. Matsushita, K. Taguchi, and J. Uchino, "Function of culturing monolayer hepatocytes by collagen gel coating and coculture with nonparenchymal cells," *Artificial Organs* **20**(2):186-192, (1996).
- W. Kuri-Harcuch and T. Mendoza-Figueroa, "Cultivation of adult rat hepatocytes on 3T3 cells: expression of various liver differentiated functions," *Differentiation*, **41**:148-157 (1989).
- R. Langenbach, L. Malick, A. Tompa, C. Kuszynski, H. Freed, E. Huberman, "Maintenance of adult rat hepatocytes on c3H/10T1/2 cells," *Cancer Research*, **39**:3509-3514 (1979).
- R. Langer and J.P. Vacanti. "Tissue Engineering," *Science* **260**:920-924, (1993).
- M.B. Lawrence, L.V. McIntire, and S.G. Eskin, "Effect of flow on polymorphonuclear leukocyte/endothelial cell adhesion," *Blood*, **70**:1284-1290 (1987).
- M.B. Lawrence, C.W. Smith, S.G. Eskin, and L.V. McIntire, "Effect on venous shear stress on CD18-mediated neutrophil adhesion to cultured endothelium," *Blood*, **75**: 227-237 (1990).

- E. LeCluyse, K. Audus, and J.H. Hochman, "Formation of extensive canalicular networks by rat hepatocytes cultured in collagen-sandwich configuration," *American Physiological Society*, (1994).
- J.S. Lee, M. Kaibara, M. Iwaki, J. Sasabe, Y. Suzuki, and M. Kusakabe, "Selective adhesion and proliferation of cells on ion-implanted polymer domains," *Biomaterials*, **14**: 12 (1993).
- J. Lee, R.G. Tompkins, and M.L. Yarmush, "The importance of proline on long-term hepatocyte function in a collagen sandwich configuration: regulation of protein secretion," *Biotechnology and Bioengineering* **40**:298-305, (1992).
- J. Lee, J.R. Morgan, R.G. Tompkins, and M.L. Yarmush, "Proline-mediated enhancement of hepatocyte function in a collagen gel sandwich culture configuration," *FASEB J*, **7** (1993).
- P.C. Letourneau, "Cell-to-Substratum adhesion and guidance of axonal elongation," *Developmental Biology* **44**:92-101, (1975).
- O. Loreal, F. Levavasseur, C. Fromaget, D. Gros, A. Guillouzo, and B. Clement, "Cooperation of ito cells and hepatocytes in the deposition of an extracellular matrix in vitro," *American Journal of Pathology* **143**(2): 538-544, 1993.
- B. Lom, K.E. Healy, and P.E. Hockberger, "A versatile technique for patterning biomolecules onto glass coverslips," *Journal of Neuroscience Methods*, **50**:385-397 (1993).
- W.R. Lowenstein, "Junctional intercellular communication and the control of growth," *Biochemica Biophysica et Acta* **560**:1-65, (1979).
- F.H. Martin, S.V. Suggs, K.E. Langley, H.S. Lu, J. Ting, K.H. Okino, C.F. Morris, I.K. McNiece, F.W. Jacobsen, and E.A. Mendiaz, "Primary structure and functional expression of rat and human stem cell factor DNAs," *Cell* **63**:203, 1990.
- T. Matsuda, K. Inoue, and T. Sugawara, "Development of micropatterning technology for cultured cells," *ASAI Transactions*, **36**: M559-M562 (1990).
- T. Matsuda, T. Sugawara, and K. Inoue, "Two-dimensional cell manipulation technology," *ASAI Journal*, **38**:M243-M247 (1992).
- R. Matsuo, M. Ukida, Y. Nishikawa, N. Omori, and T. Tsuji, "The role of Kupffer cells in complement in D-galactosamine/lipopolysaccharide-induced hepatic injury of rats," *Acta Med Okayama* **46**(5):345-354, (1992).
- A. Mereau, L. Grey, C. Piquet-Pellorce, J.K. Heath, "Characterization of a binding protein for leukemia inhibitory factor localized in extracellular matrix," *Journal of Cell Biology* **122**:713, (1993).
- M. Mesnil, J. Frasin, C. Piccoli, H. Yamasaki, and C. Guguen-Guillouzo, "Cell contact but not junctional communication (dye coupling) with biliary epithelial cells is required for hepatocytes to maintain differentiated functions," *Experimental Cell Research* **173**:524-533, (1987).
- G.K. Michalopoulos, H.D. Cianciulli, A.R. Novotny, A.D. Kligerman, S.C. Strom, and R.L. Jirtle, "Liver regeneration studies with rat hepatocytes in primary culture," *Cancer Research* **42**:4673, (1982).
- G.K. Michalopoulos, and M.C. DeFrances, "Liver Regeneration," *Science* **276**:60-66, (1997).
- S. Miyamoto, A. Ohashi, J. Kimura, S. Tobe, and T. Akaike, "A novel approach for toxicity sensing using hepatocytes on a collagen-patterned plate," *Sensors and Actuators B*, **13-14**:196-199 (1993).
- P.V. Moghe, F. Berthiaume, R.M. Ezzell, M. Toner, R.G. Tompkins, and M.L. Yarmush, "Role of extracellular matrix composition and configuration in maintenance of hepatocyte polarity and function," *Biomaterials* **17**:373-385, (1996).

- P.V. Moghe, R.M. Ezzell, M. Toner, R.G. Tompkins, and M.L. Yarmush, "Role of beta1 integrin distribution in morphology and function of collagen-sandwiched hepatocytes," *Tissue Engineering* **3**:1-16, (1997).
- O. Morin, F. Goulet, and C. Normand, (eds.), in *Liver sinusoidal endothelial cells: isolation, purification, characterization and interaction with hepatocytes*, Springer International (1988).
- O. Morin and C. Normand, "Long-term maintenance of hepatocyte functional activity in co-culture: Requirements for sinusoidal endothelial cells and dexamethasone," *Journal of Cellular Physiology*, **129**:103-110 (1986).
- T. Nakamura, Y. Tomitaka, and A. Ichihara, "Density dependent growth control of adult rat hepatocytes in co-culture," *Journal of Biochemistry* **94**:1029-1035, (1983).
- B.A. Naughton, "The importance of stromal cells," in *Biomedical Engineering Handbook*, JD Bronzino (ed.), CRC Press, (1995).
- B.A. Naughton, J.S. Roman, B. Sibanda, J.P. Weintraub, and V. Kamali. "Stereotypic culture systems for liver and bone marrow: evidence for the development of functional tissue in vitro and following implantation in vivo," *Biotechnology and Bioengineering* **43**:810-825, (1994).
- J.M. Nitsche, "Pore diffusion of nonspherical brownian particles," *Ind. Eng. Chem. Res.* **34**: 3606-3620, (1995).
- R. Nusse and H.E. Varmus, "Wnt genes," *Cell* **69**:1073-1087, (1992).
- S.L. Nyberg, M.V. Peshwa, W.D. Payne, W-S. Hu, and F.B. Cerra, "Evolution of the bioartificial liver: the need for randomized clinical trials," *American Journal of Surgery* **166**: 512-521, (1993).
- C. Oakley and D.M. Brunette, "Topographic compensation: Guidance and directed locomotion of fibroblasts on grooved micromachined substrata in the absence of microtubules," *Cell Motility and the Cytoskeleton*, **31**:45-58 (1995).
- M.J. Olson, M.A. Mancini, M. A. Venkatachalam, and A.K. Roy, "Hepatocyte cytodifferentiation and cell-to-cell communication" in *Cell Intercommunication*, W.C. De Mello (ed.), CRC Press, Inc., Boca Raton, Florida (1990).
- C. O'Neill, P. Jordan, P. Riddle, and G. Ireland, "Narrow linear strips of adhesive substratum are powerful inducers of both growth and total focal contact area," *Journal of Cell Science* **95**:577-586, (1990).
- V.M. Paralkar, S. Vukicevic, A.H. Reddi, "Transforming growth factor beta type 1 binds to collagen IV of basement membrane matrix: implications for development," *Developmental Biology* **143**:303-308, (1991).
- E.R. Peterson, and S.M. Crain. "Regeneration and innervation in cultures of adult mammalian skeletal muscle coupled with fetal rodent spinal cord," *Experimental Neurology* **36**:136-159 (1972).
- D. Plachov, K. Chowdury, C. Walther, D Simon, J-L Guenet, and P Gruss, "Pax-8 a murine paired a box gene expressed in the developing excretory system and thyroid gland," *Development* **110**:643-651, (1990).
- H. Popper, C.S. Davidson, C.M. Leevy, and F. Schaffner. "The social impact of liver disease." *New England Journal of Medicine* **281**:1455, (1969).
- G. Ramadori, J.D. Sipe, C.A. Dinarello, S.B. Mizel, and H.R. Colten, "Pretranslational modulation of acute phase hepatic protein synthesis by murine recombinant interleukin 1 (IL-1) and purified human IL-1," *Journal of Experimental Medicine* **162**:930, (1985).
- J.P. Ranieri, R. Bellamkonda, J. Jacob, T.G. Vargo, J.A. Gardella, and P. Aebischer, "Selective neuronal cell attachment to a covalently patterned monoamine on

- fluorinated ethylene propylene films," *Journal of Biomedical Materials Research* **27**:917-925 (1993).
- J.P. Ranieri, R. Bellamkonda, E. J. Bekos, J.A. Gardella, H.J. Mathieu, L. Ruiz, and P. Aebischer, "Spatial control of neuronal cell attachment and differentiation on covalently patterned laminin oligopeptide substrates," *International Journal of Developmental Neuroscience* **12**(8):725-735, (1994).
- P.D. Rathgen et al, *Cell* **62**:1105, (1990).
- A.R. Rincon-Sanchez, A. Hernandez, M. de Lourdes Lopez, T. Mendoza-Figueroa, "Synthesis and secretion of lipids by long-term cultures of female rat hepatocytes," *131-138*, (1993).
- V.W. Rodwell, "Catabolism of proteins and amino acid nitrogen," in *Harpers Biochemistry*, R.K. Murray, D.K. Granner, P.A. Mayer, and V.W. Rodwell (eds.), Appleton and Lange, CT, (1993).
- S.Rohr, D.M. Schöllly, and A.G. Kléber, "Patterned growth of neonatal rat heart cells in culture, Morphological and electrophysiological characterization," *Circulation Research*, **68**:114-130 (1991).
- M. Rojkind, P.M. Novikoff, P. Greenwel, J. Rubin, L. Rojas-Valencia, A. Campos de Carvalho, R. Stocker, D. Spray, E.L. Hertzberg, and A.W. Wolkof. "Characterization and functional studies on rat liver fat-storing cell line and freshly isolated hepatocyte coculture system," *American Journal of Pathology* **146**(6): 1995.
- E.M. Rosen, A. Joseph, L. Jin, S. Rockwell, J.A. Elias, J. Knesel, J. Wines, J. McClellan, M.J. Kluger, I.D. Goldberg, and R. Zitnik, "Regulation of scatter factor production via a soluble inducing factor," *Journal of Cell Biology* **127**:225-234, (1994).
- A. Rotem, M. Toner, R.G. Tompkins, and M. L. Yarmush, "Oxygen uptake rates in cultured rat hepatocytes," *Biotechnology and Bioengineering* **40**:1286-1291, (1992).
- A. Rotem, M. Toner, S. Bhatia, B.D. Foy, R.G. Tompkins, and M.L. Yarmush, "Oxygen is a factor determining in vitro tissue assembly: effects on attachment and spreading of hepatocytes," *Biotechnology and Bioengineering* **43**:654-660, (1994).
- U.W. Rothenpieler and G. R. Dressler, "Pax-2 is required for mesenchyme to epithelium conversion during kidney development," *Development* **119**:711-720, (1993).
- J. Rozga, F. Williams, M.S. Ro, D. Neuzil, T.D. Giorgio, G. Backfisch, A.D. Moscioni, R. Hakim, and A.A. Demetriou, "Development of a bioartificial liver:properties and function of a hollow-fiber module inoculated with liver cells," *Hepatology* **17**:258-265, (1993).
- J. Rozga, E. Morsiani, E. LePage, A.D. Moscioni, T. Giorgio, and A.A. Demetriou, "Isolated hepatocytes in a bioartificial liver: a single group view and experience," *Biotechnology and Bioengineering* **43**:645-653, (1994).
- J.Rozga, L. Podesta, E. LePage, E. Morsiani, A. Moscioni, A. Hoffman, L. Sher, F. Villamil, G. Woolf, M. McGrath, L. Kong, H. Rosen, T. Lanman, J. Vierling, L. Makowka, and A.A. Demetriou, "A bioartificial liver to treat severe acute liver failure," *Annals of Surgery* **219**(5):538-546 (1994).
- J.S. Rubin, H. Osada, P.W. Finch, W.G. Taylor, S. Rudikoff, S.A. Aaronson, "Purification and characterization of a newly identified growth factor specific for epithelial cells," *Proceedings of National Academy of Sciences* **86**:802, (1989).
- T.W. Sadler, *Langman's Medical Embryology*, Williams & Wilkins, Baltimore, (1990).
- W. Schrode, D. Mecke, and R. Gebhardt, "Induction of glutamine synthetase in periportal hepaocytes by cocultivation with a liver epithelial cell line," *European Journal of Cell Biology* **53**:35-41, (1991).
- P.O. Seglen, "Preparation of isolated rat liver cells," *Methods in Biology*, **13**:29-83, (1976).



- S. Shimaoka, T. Nakamura, A. Ichihara, "Stimulation of growth of primary cultured adult rat hepatocytes without growth factors by coculture with nonparenchymal liver cells," *Experimental Cell Research*, **172**:228-242 (1987).
- D.B.A Silk, and R. Williams. "Experiences in the treatment of fulminant hepatic failure by conservative therapy, charcoal hemoperfusion and polyacrylonitrile hemodialysis," *International Journal of Artificial Organs* **1**:29 (1978).
- R. Singhvi, G. Stephanopoulos, D.I.C. Wang, "Review: Effects of substratum morphology on cell physiology," *Biotechnology and Bioengineering*, **43**:764-771 (1994a).
- R. Singhvi, A. Kumar, G.P. Lopez, G.N. Stephanopoulos, D.I.C. Wang, G.M. Whitesides, D.E. Ingber, "Engineering cell shape and function," *Science*, **264**:696-698 (1994b).
- J.M.W. Slack, "Theoretical Embryology," in *From Egg to Embryo, Developmental and Cell Biology Series*, Cambridge University Press, (1991).
- M.B. Sporn and A.B. Roberts, "The transforming growth factor-betas" in *Peptide Growth Factors and Their Receptors I*, Sporn and Roberts, (eds.), Springer-Verlag, NY, (1990).
- A. Soekamo, B. Lom, and P.E. Hockberger, "Pathfinding by neuroblastoma cells in culture is directed by preferential adhesion to positively charged surfaces," in *NeuroImage* (1993).
- E. Sonnenberg, D. Meyer, K.M. Weidner, and C. Birchmeier, "Scatter factor/hepatocyte growth factor and its receptor, the c-met tyrosine kinase, can mediate a signal exchange between mesenchyme and epithelia during mouse development," *Journal of Cell Biology* **123**:223-235, (1993).
- M.B. Sporn and A.B. Roberts, "The transforming growth factor-betas" in *Peptide Growth Factors and Their Receptors I*, Sporn and Roberts (eds.), Springer-Verlag, NY, (1990).
- K. Stark, S. Vainio, G. Vassilera, and A. McMahon, "Epithelial transformation of metanephric mesenchyme in the developin kidney regulated by wnt-4," *Nature* **372**:679-683, (1994).
- P. Stefanovich, H.W.T. Matthew, M. Toner, R.G. Tompkins, and M.L. Yarmush, "Extracorporeal plasma perfusion of cultured hepatocytes: effect of intermittent perfusion on hepatocyte function and morphology," *Journal of Surgical Research* **66**:57-63, (1996).
- M. Steinberg. "Reconstruction of tissue in dissociated cells," *Science* **141**:401-408, (1963).
- A.J. Strain, G. McGuinness, J.S. Rubin, S.A. Aaronson, "Keratinocyte growth factor and fibroblast growth factor action on DNA synthesis in rat and human hepatocytes: modulation by heparin," *Experimental Cell Research* **210**:253, (1994).
- D.A. Stenger, J.H. Georger, C.S. Dulcey, J.J. Hickman, A.S. Rudolph, T.B. Nielsen, S.M. McCort, and J.M. Calvert, "Coplanar molecular assemblies of amino- and pefluorinated alkylsilanes: characterization and geoetric definition of mammalian cell adhesion and growth," *Journal of the American Chemical Society* **114**:8345-8442, (1992).
- M. Stoker and M. Perryman, "An epithelial scatter factor released by embryo fibroblasts," *Journal of Cell Science* **77**:209-223, (1985).
- M. Stoker, E. Gherardi, M. Perryman, and J. Gray, "Scatter factor is a fibroblast-derived modulator of epithelial cell motility," *Nature* **327**:238-242, (1987).
- N.L. Sussman, MiG. Chong, T. Koussayer, D. He, T. Shang, H.H. Whisennand, and J. Kelly, "Reversal of fulminant hepatic failure using an extrcorporeal liver assist device," *Hepatology* **16**:60-65, (1992).

- N.L. Sussman and J.H. Kelly, "The Artificial Liver," *Scientific American: Science and Medicine* May:68-77, (1995).
- N.L. Sussman and J.H. Kelly, "Temporary hepatic support systems: the then and the maybe," in *Transplantation of the Liver*, W.C. Maddrey and M.F. Sorrell (eds.), Appleton and Lange, Norwalk, CT, (1995).
- K. Taguchi, M. Matsushita, M. Takahashi, and J. Uchino, "Development of a bioartificial liver with sandwiched-cultured hepatocytes between two collagen gel layers," *Artificial Organs* **20(2)**:178-185, (1996).
- M. Traiser, B. Diener, D. Utesch, and F. Oesch, "The gap junctional intercellular communication is no prerequisite for the stabilization of xenobiotic metabolizing enzyme activities in primary rat liver parenchymal cells in vitro," *In Vitro Toxicology*:266-273, (1995).
- Trentin JJ, "Hemopoietic microenvironment, historical perspectives, status, and projections," in *Handbook of the hemopoietic microenvironment*, Tavassoli M, (ed), Hermana Press, NJ, (1989).
- C. Trey, D.G. Burns, and S.J. Saunders. "Treatment of hepatic coma by exchange blood transfusion," *New England Journal of Medicine* **274**:473, (1966).
- G.A. Truskey and J.S. Pirone, "The effect of fluid shear stress upon cell adhesion to fibronectin-treated surfaces," *Journal of Biomedical Materials Research* **24**:1333-1353, (1990).
- T.Tsukui, K. Kikuchi, A. Mabuchi, T. Sudo, T. Sakamoto, G. Asano, K. Yokomuro, "Production of interleukin-1 by primary cultured parenchymal liver cells (hepatocytes)," *Experimental Cell Research* **210**:172, (1994).
- D. Utesch, E. Molitor, K-L Platt, and F. Oesch, "Differential stabilization of cytochrome p-450 isoenzymes in primary cultures of adult rat liver parenchymal cells," *In Vitro Cell and Developmental Biology* **27A**:858-863, (1991).
- R.F. Valentini, T.G. Vargo, J.A. Gardello, and P. Aebischer, "Patterned neuronal attachment and outgrowth on surface modified, electrically charged fluoropolymer substrates," *Journal of Biomaterials Science Polymer Edition* **5(1/2)**:13-36, (1993).
- C.R. Vanderberg, and E.D. Hay, "Embryonic corneal fibroblasts transfected with E-cadherin cDNA undergo mesenchymal-epithelial transformation," *Molecular Biology of the Cell* **3**:5a, (1992).
- Y. Vanderberghe, L. Tee, V. Rogiers, and G. Yeoh, "Transcriptional- and post-transcriptional-dependent regulation of glutathione S-transferase expression in rat hepatocytes as a function of culture conditions," *FEBS* **313(2)**:155-159, (1992).
- S. Vukicevik, H.K. Kleinman, F.P. Luyten, A.B. Roberts, N.S. Roche, and H. Reddi, "Identification of multiple active growth factors in basement membrane matrigel suggests caution in interpretation of cellular activity related to extracellular matrix components," *Experimental Cell Research* **202**:1-8, (1992).
- M. Watabe, A. Nagafuchi, S. Tsukita, and M. Takeichi, "Induction of polarized cell-cell association and retardation of growth by activation of the E-cadherin-catenin adhesion system in a dispersed carcinoma line," *Journal of Cell Biology* **127**:247-256, (1994).
- D.H. Wolfe, H. Hartmann, and K. Jungermann, "Induction of phosphoenolpyruvate carboxykinase by sympathetic agents in primary culture of adult rat hepatocytes," *Biochemica Biophysica Research Communications* **98**:1084-1090, (1981).
- F. Wu, M. Peshwa, F. Cerra, W. Hu, "Entrapment of hepatocyte spheroids in a hollow fiber bioreactor as a potential bioartificial liver," *Tissue Engineering* **1(1)**:29-40, (1995).
- J. Xu and R.A.F. Clark, "Extracellular matrix alters PDGF regulation of fibroblast integrins," *Journal of Cell Biology* **132(1&2)**:239-249, (1996).

M. Yamazaki, M. Tsuchida, K. Kobayashi, T. Takezawa, and Y. Mori, "A novel method to prepare size-regulated spheroids composed of human dermal fibroblasts," *Biotechnology and Bioengineering* **44**:38-44, (1994).

KM Zsebo, D.A. Williams, and E.N. Geissler, "Stem Cell Factor is encoded at the S1 locus of the mouse and is the ligand for the c-kit tyrosine kinase receptor," *Cell* **63**:175, (1990).

S.D. Zucker and J. L. Gollan, "Physiology of the Liver," in *Bockus Gastroenterology*, W.S. Haubrich and F. Schaffner (eds.), WB Saunders, Philadelphia, (1995).

# Glossary

## ABBREVIATIONS

AFM- Atomic Force Microscopy  
AS- 3-[(2-aminoethyl) amino] propyltrimethoxysilane  
BAL- Bioartificial Liver  
ECM- Extracellular Matrix  
PDMS- Polydimethyl Siloxane

## SYMBOLS

A- cross-sectional channel area  
c- oxygen concentration  
D- Diffusivity  
 $D_h$ - hydraulic diameter  
h- channel height  
k- solubility of oxygen in liquid  
 $\rho$ - cell density  
P- channel perimeter  
Pe- Peclet number  
Q- volumetric flow rate  
R- oxygen flux at cell surface  
Re- Reynolds number  
Sc- Schmidt number  
 $\tau$ - shear stress  
u- fluid velocity  
 $V_m$ - maximal oxygen uptake rate  
 $\nu$ - kinematic viscosity

w- channel width

x- axial coordinate (corresponding to channel length)

y- radial coordinate (corresponding to channel height)

z- radial coordinate (corresponding to channel width)

## **DEFINITIONS**

differentiated- in the context of our study, we use the term ‘differentiated’ to signify characteristics of a cell which are normally exhibited by the adult hepatocyte in vivo including: morphology, polarity, and liver-specific gene expression.

microenvironment- we use this term to describe the environment in the vicinity of a cell ( i.e. within a few microns) as distinguished from the overall environmental influences which are generally held constant throughout a tissue (i.e. temperature)

spatial heterogeneity- we use this term to describe spatial differences in gene expression manifested in cells of the same type in the same culture.

# Index

## 3

- 3T3 culture, 32
- 3T3 fibroblasts, 29, 50, 56, 110, 130, 134

## A

- agitation of co-cultures, 85
- albumin assay, 36
- albumin, intracellular, 37
- autofluorescence, 33, 46

## B

- bile duct function, 37
- bile duct staining, 68
- bioartificial liver, v, vi, 7, 8, 11, 19, 78, 105, 111, 120, 124, 126, 130, 136, 137, 139
- biomolecules, 9, 22, 23, 24, 26, 29, 30, 44, 45, 54, 55, 56, 135
- bioreactor, 8, 27, 29, 41, 78, 86, 93, 94, 95, 96, 99, 105, 107, 109, 111, 112, 116, 118, 119, 120, 124, 126, 127, 139

## C

- cellular microenvironment, 69, 71, 95

- characterization of Substrates, 45
- co-culture effect, 11
  - DNA synthesis, 14, 15, 17, 138
  - gap junctions, 5, 13, 14, 15, 17, 18, 19, 91, 92, 126
  - kinetics, 107
  - mechanisms, 16
  - tight junctions, 13
- conditioned media, 38
- cytokines, 106

## D

- design of bioreactor, 111
- DNA assay, 36

## E

- extracellular matrix, 9, 16

## G

- growth-arresting cells, 32

## H

- hepatocyte culture, 31
- heterotypic interaction, 52, 53

heterotypic interface, 17, 26, 41, 43, 57, 60, 61, 62, 65, 67, 68, 69, 70, 71, 72, 73, 74, 77, 78, 79, 86, 90, 91, 93, 94, 95, 96, 98, 100, 106, 120, 124

hollow-fiber, 7, 8, 119, 120, 137

homotypic interaction 13, 14, 26, 51, 54, 56, 60, 65, 69, 72, 73, 74, 78, 79, 90, 91, 106, 123, 130, 133

## I

image analysis, 34

immunofluorescence, 34

immunostaining, 60, 65, 67, 71, 72, 87, 91, 93

intracellular albumin, 14, 41, 60, 65, 67, 69, 71, 72, 79, 85, 87, 88, 90, 91, 92, 93

## L

liver

- biliary ductal cells, 11, 18, 88
- endothelial cells, 4, 5, 11, 12, 13, 16, 17, 56, 125, 132, 134, 136
- Ito cells, 4, 5, 12, 17, 18, 19, 126
- Kupffer cells, 4, 5, 11, 12, 126, 135
- lobule, 4
- normal function, 2
- sinusoid, 2, 5
- structure, 2

liver development, 10

liver regulating protein (LRP), 18, 88, 94, 131

## M

mechanism of hepatocyte/3T3-J2 interaction, 77

mesenchymal, 19, 25, 50, 78, 92, 105, 106, 107, 119, 124, 125, 132, 139

methodology, 29

microenvironments, 26, 53, 60, 69

microfabrication, 1, 5, 7, 24, 25, 26, 30, 41, 49, 55, 74, 78, 86, 92, 95, 96, 105, 106, 111, 120, 123, 126, 127

micropatterning review, 21

## O

optimization, 41, 95

oxygen tension, 113, 114, 115, 116, 118

## P

parenchymal, 11, 12, 14, 19, 32, 59, 96, 106, 109, 132, 139

PDMS, polydimethyl siloxane, 42

profilometry, 33, 46

## R

randomly- distributed co-cultures, 43, 102

rat liver epithelial cells, 12, 13, 71, 72, 109, 131

## S

separation of cell types, 39

silanes, 22, 23, 24

surface area, 8, 35, 41, 43, 60, 61, 62, 71, 95, 96, 97, 98, 105, 112, 114, 115, 116, 120

surface characterization, 33

surface modification, 31

## T

tissue engineering, v, vi, 1, 7, 25, 74, 124, 125, 126

## U

urea assay, 35

## V

viability, 11, 18, 19, 32, 87, 93, 106, 113, 119, 125

**Z**

zonal heterogeneity, 77, 92